QTL MAPPING OF POST-PROCESSING COLOR RETENTION AND OTHER TRAITS IN TWO BLACK BEAN POPULATIONS

By

Nolan M. Bornowski

A THESIS

Submitted to
Michigan State University
in partial fulfillment of the requirements
for the degree of

Plant Breeding, Genetics and Biotechnology – Crop and Soil Sciences – Master of Science

2018

ABSTRACT

QTL MAPPING OF POST-PROCESSING COLOR RETENTION
AND OTHER TRAITS IN TWO BLACK BEAN POPULATIONS

By

Nolan M. Bornowski

When black beans are processed for consumption, they can lose their dark coloration due to the leaching of water-soluble pigments called anthocyanins. After hydrothermal processing, beans are commonly a faded brown color instead of the dark black color typical of the dry seed. The aim of this research was to develop mapping populations with different genetic sources of color retention in order to identify regions of the dry bean genome associated with canning quality traits. To this end, two half-sibling black bean recombinant inbred line (RIL) populations segregating for post-processing color retention were developed. These RIL populations were phenotyped for canning quality over two years and genotyped using the BARCBean6k_3 BeadChip. A novel phenotyping method using digital image analysis was shown to outperform current methods of quantitative color measurement. QTL for post-processing color retention were detected on six chromosomes, with QTL on Pv03, Pv08, and Pv11 being the most notable for their co-localization with QTL for quantitative measurements of color. In particular, QTL associated with color retention on Pv11 mapped to a very small physical interval and were consistent across years, populations, and phenotyping methodologies. Color retention QTL on Pv08 and Pv11 are good candidates for development of molecular markers that may be used in marker assisted selection (MAS) or early-generation screening to improve post-processing color retention in black beans.

This thesis is dedicated to Aaron Charles Rodgers.

ACKNOWLEDGEMENTS

First, I want to thank Dr. James Kelly for sharing his knowledge of plant breeding and his passion for dry bean research. I also want to thank my fellow graduate students for providing a great environment in which to learn, live, and love. In addition, thanks go out to my family members, who are incredible advocates of science education. Finally, I want to thank Amber Bassett for her emotional support, scientific discussion, and delicious cooking.

TABLE OF CONTENTS

LIST OF TABLES

LIST OF FIGURES

CHAPTER 1: LITERATURE REVIEW

INTRODUCTION

Dry edible beans (*Phaseolus vulgaris* L.) provide an economical, nutritious food source for millions of people around the world and exhibit a wide diversity of seed sizes, colors, shapes, and agronomic traits. For US consumers, dry beans are commonly consumed as already-prepared canned products. Dry beans belonging to the black bean market class are unique in that they exhibit significant loss of color during the canning process, which is attributed to leaching of the anthocyanin pigments that give black beans their characteristic coloration. Color loss during processing may result in a faded brown product that is undesirable to many consumers. Post-processing color retention and other quality traits are important when breeding black bean varieties. This breeding process requires significant time, resource, and labor inputs to develop new lines and evaluate them for quality traits. In order to further improve post-processing color retention of black beans, more information is needed concerning the genetic mechanisms underlying this trait. This genetic mapping study will identify genomic regions associated with black bean color retention that breeders and researchers can use to meet consumer standards.

DRY BEAN PRODUCTION

In the United States, dry beans are categorized into commercial classes based on seed characteristics. Commercially-produced beans are generally grown under non-irrigated conditions in the north central region of the US, with North Dakota, Michigan, Minnesota, and Nebraska accounting for approximately 70 percent of the country's production (USDA- NASS, 2016). US-grown dry beans are mostly purchased by domestic consumers, but approximately 30 percent is

exported annually to countries like Mexico, Canada, the United Kingdom, and Italy, among others (Parr et al., 2018; USDA- NASS, 2018)

Michigan has been an important dry bean producer since the early 1900's when the nation's first dry bean breeding program was founded at Michigan State College, now Michigan State University. Subsequent research efforts generated improved varieties for growers within and beyond Michigan's borders. Michigan is currently responsible for nearly 20 percent of national dry bean production and is the leading producer of small red, cranberry, and black beans (USDA-NASS, 2016). Black beans are especially important to Michigan, where approximately half of US black beans are produced annually [Figure 1].

DRY BEAN CONSUMPTION TRENDS

US consumption of *Phaseolus vulgaris* dry edible beans has fluctuated around 6 pounds per capita for several decades. Market class preference among consumers is relatively stable except for navy beans, which have gradually declined in popularity over the years [Figure 2]. Pinto beans, on the other hand, remain the most consumed market class, largely due their presence in both home, institutional, and commercial dishes such as soups, salads, and refried beans (Lucier et al., 2000). While other market classes have plateaued or declined, black bean consumption has been increasing exponentially since the 1980s [Figure 3], providing an economic justification for quality improvement in processed black beans. Likewise, other grain legumes such as chickpeas (*Cicer arietinum*), also known as garbanzo beans, have rapidly increased in popularity. The rapid rise in chickpea consumption has prompted growers in north central states to increase planting acreage, mostly by replacing wheat (Bonds, 2017).

Since both dry beans and chickpeas undergo similar processing prior to consumption, they share a similar market space and dietary function. Of the dry bean market classes, black bean consumption is increasing at a similar rate as chickpea consumption and may play a deciding role in the future of the dry bean industry by competing with other pulse crops for consumer demand. Unlike other dry bean market classes, black beans are uniquely susceptible to undesirable color leaching during processing. Genetic improvements in post-processing color retention and other quality traits of processed black beans will provide an opportunity for black beans to maintain their place in future markets.

HEALTH BENEFITS

Cooked dry beans are an excellent source of protein, fiber, and other minerals (Hornick and Weiss, 2011), but black bean pigments are thought to bestow additional health benefits. These pigments belong to a class of flavonoids called anthocyanins that localize to the seed coat of black beans (Takeoka et al., 1997; Beninger and Hosfield, 2003). Anthocyanins are considered as antioxidants that prevent reactive oxygen species (ROS) from causing damage to cell membranes (Miguel, 2011). Antioxidant-rich foods are associated with lowered risk of cardiovascular disease and cancer (Arts and Hollman, 2005; Wang and Stoner, 2008). While black beans can vary in amount of total phenolic compounds, they generally contain more phenolic compounds than other market classes (Luthria and Pastor-Corrales, 2006; Marles et al., 2010). Studies by Oomah et al. (2005) and Akond et al. (2011) found that beans with high anthocyanins and total phenolic compounds exhibited high antioxidant activity *in vitro*. Unfortunately, flavonoid antioxidant activity is greatly reduced after processing (Xu and Chang, 2009). In fact, Lotito and Frei (2006) conclude that *in vivo* antioxidant activity is not due to flavonoids, but urate production attributed

to glucose consumption. However, flavonoids represent only a fraction of the nutraceutical potential of dry beans.

Compared to cereal grains, dry beans are an excellent source of resistant starch (Murphy et al., 2008) and fiber (USDA- Agricultural Research Service, 2018), which result in a low glycemic index. A low glycemic index signifies that a food's carbohydrates are digested and metabolized more slowly. Among other claims, foods with low glycemic indices have been shown to help manage diabetes (Brand-Miller et al., 2003), lower "bad" LDL cholesterol (Goff et al., 2013), and improve children's academic performance (Micha et al., 2010). In addition, rodents fed milled samples of canned beans reduced their cancer incidence and tumor numbers (Thompson et al., 2009), though there is scant evidence of anti-cancer properties in human models (Messina, 2014). Although the health effects of black bean anthocyanins may be overstated, black beans (and dry beans in general) still provide an affordable source of other nutritional benefits to consumers. In fact, Foyer et al. (2016) states, 'the current lack of coordinated focus on grain legumes has compromised human health, nutritional security and sustainable food production.' Therefore, increasing consumption of dry beans and other legumes could have a large positive impact on global public health.

FLAVONOID BIOSYNTHESIS

Dry bean seed colors and patterns result from various pigments located within the seed coat. These pigments belong to a class of polyphenolic compounds called flavonoids. Flavonoids are secondary plant metabolites containing two phenyl groups commonly linked by a 3-carbon oxygenated heterocycle (Bravo, 1998). Within the flavonoids, several classes can be characterized according to modifications of the 3-ring flavone backbone: flavanones, flavones, isoflavones,

flavan-4-ols, dihydroflavonones, and flavonols. Flavonoid biosynthesis [Supplemental Figure 1] is initiated by two Co-enzyme A (CoA) conjugates derived from separate pathways: 4-Coumaroyl-CoA (also known as p-Coumaroyl-CoA or 4-Hydroxycinnamoyl-CoA) from the phenylpropanoid pathway and 3 units of malonyl-CoA that have been carboxylated from aceytl-CoA used in the Krebs Cycle. These molecules serve as substrates for (naringenin) chalcone synthase (CHS) to produce naringenin chalcone (tetrahydroxychalcone) in the first committed step of flavonoid biosynthesis (Martens et al., 2010). The yellow-colored naringenin chalcone is then converted into the flavanone naringenin either by a chalcone isomerase (CHI) or spontaneous cyclization at room temperature (Cheng et al., 2018). Spontaneous cyclization of chalcones to flavanones (e.g. naringenin chalcone to naringenin) occurs at a much slower rate (Bednar and Hadcock, 1988), yet may produce sufficient quantities of flavanone substrate for use in downstream pigment biosynthesis (Heller and Forkmann, 1988).

Flavanones are involved in many branches of flavonoid biosynthesis. They can form isoflavones via isoflavone synthase (IFS, synonym 2HIS), flavones via flavone synthases (FSI and FSII), flavan-4-ols via dihydroflavonol 4-reductase (DFR), or flavanonols via flavanone 3-hydroxylase (F3H, synonym FHT) (Lepiniec et al., 2006). It should be noted that both flavanonols and their flavanone precursors can undergo B-ring hydroxylation by the enzymes flavonoid 3′-hydroxylase (F3′H) and flavonoid 3′,5′-hydroxylase (F3′5′H) resulting in the compounds diverging into different pathways. Flavononols, also referred to as 3-OH-flavanones or dihydroflavonols, can be catalyzed either by flavonol synthase (FLS) to produce flavonols (3-hydroxyflavones) or DFR to produce flavan-3,4 -diols (leucoanthocyanins). These flavan-3,4 -diols can be catalyzed either by anthocyanidin reductase, ANS (also known as leucocyanidin dioxygenase, LDOX) into 3-OH-anthocyanidins or by leucoanthocyanin reductase (LAR) into flavan-3-ols (also called

flavanols). Flavan-3-ols like catechin and epicatechin are condensed into oligomers known as condensed tannins, or proanthocyanidins. Proanthocyanidins are colorless, but can be oxidized by polyphenol oxidase (PPO) to become yellow-brown, or, as their name suggests, can become anthocyanidins via acid hydrolysis. Anthocyanidins are the aglycone form of anthocyanins. Once glycosylated (commonly via 3-O-glycosylation), the anthocyanin compound increases in polarity, which allows it to be transferred and stored in the vacuole, where it functions as a pigment visible in the seed coat (Corradini et al., 2011). These pigments are responsible for the coloration of dry bean seeds. The dark coloring of black beans is attributed to anthocyanins like delphinidin 3-glucoside, petunidin 3-glucoside, and malvidin 3-glucoside (Takeoka et al., 1997; Beninger and Hosfield, 2003).

In dry beans, some of the genes encoding flavonoid biosynthesis enzymes have been characterized and mapped. According to Feenstra (1960), Hosfield (2001), and Bassett (2007), loci P, C, R, J, D, G, B, V, and Rk all contribute to seed coat color and often interact epistatically. Efforts by McClean et al. (2002) and Reinprecht et al. (2013) have generated markers and genomic positions for these loci and have associated color loci with flavonoid pathway enzymes in dry bean and soybean (*Glycine max*). These loci controlling flavonoid biosynthesis are fundamental to the characteristic dark coloration of black bean seeds. However, it is unknown whether these loci controlling flavonoid production also have a role in post-processing color retention of black beans.

PHASEOLUS MOLECULAR TOOLS

Dry bean breeders have been using molecular tools for many years to indirectly select for disease resistance traits. Using a recombinant inbred population of a cross between BAT93, a Mesoamerican breeding line, and Jalo EEP558, an Andean landrace, a low-density linkage map

was created (Nodari et al., 1993a). This map utilized early generation markers like isozymes, restricted fragment length polymorphisms (RFLPs), and random amplified polymorphisms (RAPDs) and was integrated with other contemporary linkage maps (Freyre et al., 1998). RAPD markers were later refined into sequence characterized amplified region (SCAR) markers, which were successfully used in marker assisted selection of major disease resistance loci (Miklas et al., 2000). In order to improve genome coverage further, microsatellite markers detecting length polymorphisms in simple sequence repeats (SSRs) were developed and aligned to the genomic map (Blair et al., 2003; Grisi et al., 2007).

Despite the ease of using PCR-based markers, low genomic coverage prevented higher-resolution mapping. This obstacle was addressed by single nucleotide polymorphism (SNP) marker discovery resulting from the BeanCAP (Common Bean Coordinated Agricultural Project) initiative (Hyten et al., 2010). In addition to marker development, the BeanCAP also funded nutritional research and student training across public universities and government sectors (http://www.beancap.org/). Another highly useful BeanCAP outcome was the selection of 5,398 polymorphic SNPs for development of the BARCBean6k_3 BeadChip (Song et al., 2015). SNPs selected for the BeadChip are distributed across all chromosomes and can be assigned physical positions according to the dry bean reference genome. The SNP chip can detect polymorphisms among and within market classes, aiding various genomic studies (Hoyos-Villegas et al., 2015; Zuiderveen et al., 2016).

Recently, genomes for G19833, an Andean landrace, and BAT93 have been assembled, revealing independent domestication events and extensive synteny with soybean (Schmutz et al., 2014; Vlasova et al., 2016). Assembly information for these genomes is publicly available online and will be useful in many future research projects. Sequencing costs have fallen since the

development of these reference genomes, improving access to sequence data for more targeted mapping and cloning experiments. First described by Elshire et al. (2011), genotyping by sequencing (GBS) can identify thousands of SNPs that may be used for linkage map construction or aligned to a reference genome if desired. Several GBS protocols have recently been published for dry beans with differing restriction enzymes and experimental objectives (Zou et al., 2014; Hart and Griffiths, 2015; Ariani et al., 2016; Schröder et al., 2016). Further adaptation of bioinformatics and sequencing technologies by the dry bean community will facilitate many genome-scale studies.

CANNING QUALITY TRAITS

Dry beans require hydrothermal processing to soften the cotyledons and inactivate anti-nutritional factors before being consumed (Van Der Poel, 1990; Martínez-Manrique et al., 2011). In a domestic setting, preparation may include a soaking step followed by heat treatment, either by boiling or pressure-cooking. However, for many consumers the convenience of canned beans is preferable to the long preparation time associated with soaking and cooking dry beans. As part of the industrial canning process, beans are cleaned, soaked in a salt solution, quickly heated ("blanched"), and then filled into cans where they are covered in brine or sauce before being heat-sterilized under pressure (Matella et al., 2013).

Similar to boiling, canning also causes physico-chemical changes in the beans that influence culinary quality parameters (Wassimi et al., 1990). Quality parameters like water absorption, texture, color, and appearance after canning vary among and within market classes due to both genetic and genotype by environment effects (Hosfield et al., 1984; Hosfield and Uebersax, 1990). Washed and drained weight of the canned beans is useful for determining the degree of

hydration during the canning process. Texture measurements of canned beans are based on the amount of force required to compress the cooked sample and serve as a proxy for mushiness or firmness of the beans. Color and appearance are typically subjective measurements of processed beans, where a panel of reviewers rate canned samples according to the degree of pigment leaching, seed coat integrity, and other visual characteristics. These measurements, collectively, indicate the quality of the canned product.

Quantitative Color Measurements

Color is commonly measured quantitatively according to CIELAB color space. CIELAB color space is based on the "color-opponent theory" of Ewald Hering (Busse and Bäumer-Schleinkofer, 1996), where perception of some colors excludes the perception of other colors. For example, humans cannot perceive a "blueish-yellow" color. The CIELAB color space was developed in 1976 by international collaboration as an improvement on previous color spaces such as CIEXYZ and HunterLAB (CIE, 2008) and is widely-used across disciplines. In CIELAB color space, a single color is partitioned into three components: L^*, a^*, and b^* [Supplemental Figure 2].

L^* measures darkness to lightness from 0 (black) to 100 (white); a^* measures the level of greenness to redness and ranges from negative values (green) to positive values (red); b^* measures the level of blueness to yellowness and ranges from negative values (blue) to positive values (yellow). Values of a^* and b^* near zero are a neutral grey. CIELAB measurements can be compared to other color spaces through transformation if desired (Hunter Laboratories, 1996). As opposed to the qualitative measurements provided by the reviewer panel, CIELAB values can provide quantitative measurements of canned bean color.

Breeding for Canning Quality Traits

The aforementioned quality traits are distinct from agronomic traits and must be selected independently. For example, the color of unprocessed black beans is independent of the color of the canned beans (Ghaderi et al., 1984). Unfortunately, because canning quality evaluation is performed in later generations when germplasm is mostly homozygous, many genotypes selected for favorable agronomic traits may be lacking in these quality traits.

Breeding dry beans for canning quality is a time-consuming endeavor, as breeders generally use a pedigree breeding method to develop desirable progeny. The process begins when parents are manually crossed in the greenhouse to produce F_1 progeny. F_1 plants (and all succeeding generations) are then allowed to naturally self-pollinate. F_2 plants are grown in the field and harvested as single plant selections until the F_4 generation. Plants are phenotypically selected for highly heritable traits like seed color, size, and shape and agronomic characteristics like growth habit, maturity, and lodging (Kelly and Cichy, 2013). To accelerate the process, early generations can be grown in greenhouses or warm-climate nurseries, but late-generation selection for more complex traits like yield and canning quality must be evaluated in the target environment.

After further selection based on yield, canning quality, agronomic traits, and disease resistance, elite lines are sent to western growers for seed increase in absence of disease pressure. Following several years of data analyses, a team of plant scientists, industry professionals, and administrators then decide if an elite line will be released as a variety (Kelly, 2010). Because canning quality evaluation is typically performed in the F_6 generation and beyond, selection is limited to later generations when most loci are fixed and sufficient seed is available for replicated field trials. Inbreeding and phenotyping are time- and resource-intensive processes that delay improvement of these traits. Phenotyping dry seed to predict canning quality traits has been

explored with varying results (Mendoza et al., 2014, 2017, 2018) [Supplemental Table 1]. Alternatively, identification of linked molecular markers associated with major loci influencing processing traits may allow marker assisted selection on early generation material, saving time, resources, and labor.

Canning Quality Research

Previous research suggests that canning quality traits like color retention are quantitatively inherited, meaning they are controlled by more than one locus. To locate these genomic regions and their effects on traits of interest, QTL (quantitative trait loci) mapping studies have been designed to associate genetic markers with phenotypic data (Collard et al., 2005). Mapping populations can be developed from RIL, F_2, backcross, or doubled haploid populations, provided the populations are segregating for the trait(s) of interest. Once phenotypic data is collected and populations are genotyped, QTL detection is possible when polymorphic molecular markers are associated with differences in the phenotypic data. Because reproductive self-compatibility of dry beans allows an individual near-homozygous line to be tested over multiple years, RIL mapping populations are commonly used in dry bean genetic mapping studies.

Significant genotype by environment interactions have been documented for canning quality traits in pinto (Ghaderi et al., 1984), navy (Walters et al., 1997), and black (Hosfield et al., 1984) bean market classes. In the Walters et al. (1997) study, navy bean parents with contrasting canned appearance were crossed to generate three RIL populations that were evaluated for canning traits. Small population sizes and use of RAPD markers available at the time limited marker-trait associations, but the authors estimated heritabilities for canned appearance “VIS” (0.59), texture “TXT” (0.64), and washed-drained weight “WDM” (0.67).

Posa-Macalincag et al. (2002) performed a QTL analysis on two kidney bean RIL populations derived from crosses between acceptable and excellent canning genotypes. The authors estimated narrow-sense heritability for canned appearance and degree of splitting to be approximately 0.84 and found high correlation between the two traits across environments (r = 0.91 to 0.97). The RAPD markers previously identified by (Walters et al., 1997) were not polymorphic in these populations, but others were associated with canned appearance and splitting, namely OP15.1150 on linkage group (LG) 1 (anchored to LG B8, now known as chromosome Pv08) and OG17.1300 on LG 2 (unanchored).

In black beans, Wright and Kelly (2011) used a RIL population to map agronomic and quality traits with SSR markers. Seven QTL were identified for post-processing color retention across 5 LGs. Appearance QTL mapped to Pv05 and Pv08, texture to Pv06 and Pv11, and washed-drained weight to Pv03 and Pv10, although few QTL were detected across multiple years. More recently, Cichy et al. (2014) developed a black bean RIL mapping population derived from crossing parents contrasting as shiny-seeded (*Asp*) and dull-seeded (*asp*). The RIL population was evaluated for canning traits and genotyped with SNP markers generated by DArT and DArTseq platforms (Diversity Arrays Technology, Yarralumla, Australia). SNP genotyping significantly increased the number of mapped markers (n=1449) and improved map resolution compared to previous studies. QTL for canned bean appearance, color retention, texture, and other quality traits were detected across the genome, with some traits exhibiting co-localization. Of note, QTL co-localized on Pv05 for anthocyanin content, *L**, *b**, and color retention; for *Asp*, water uptake, and texture on Pv07; and for *L**, *a**, *b**, color retention, and canned appearance on Pv11. While Posa-Macalincag et al. (2002) and Wright and Kelly, (2011) both identified a QTL for canned

appearance on Pv08, no APP QTL was detected on Pv08 in the RIL population of Cichy et al. (2014).

CONCLUSIONS

Black beans have dramatically increased in popularity over the past few years. They are healthful, affordable, and very convenient as a ready-to-eat canned product. However, after processing, black beans commonly become faded and lose their dark black coloring due to leaching of water-soluble anthocyanins. This color loss can be extreme and is undesirable to consumers. Post-processing color retention can be improved through traditional breeding, but despite previous studies, information remains lacking on the genetic mechanisms controlling this trait. This study utilizes two black bean RIL populations for QTL mapping of post-processing color retention. Genotypic data was collected using the BARCBean6k_3 SNP chip. Several methods of measuring canned bean color retention were evaluated to guide future phenotyping efforts. Identifying the genomic regions influencing color retention and other important traits will provide useful information to dry bean breeders and researchers seeking to create black bean varieties with improved canning quality. Quality gains will allow dry beans, and black beans in particular, to remain competitive in an evolving dietary landscape.

CHAPTER 2: QTL MAPPING OF POST-PROCESSING COLOR RETENTION AND OTHER TRAITS IN TWO BLACK BEAN POPULATIONS

ABSTRACT

When black beans are processed for consumption, they can lose their dark coloration due to the leaching of water-soluble pigments called anthocyanins. After hydrothermal processing, beans are commonly a faded brown color instead of the dark black color typical of the dry seed. Genotypes with superior post-processing color retention have been identified in the Michigan State University breeding program, providing an opportunity to study the genetics underlying this key trait. The aim of this research was to develop mapping populations with different genetic sources of color retention in order to identify regions of the dry bean genome associated with canning quality traits. To this end, two half-sibling black bean recombinant inbred line (RIL) populations segregating for post-processing color retention were developed. These RIL populations were phenotyped for canning quality over two years and genotyped using the BARCBean6k_3 BeadChip. Quantitative trait loci (QTL) governing color retention, other quality traits, and agronomic traits were identified and compared to previous studies. QTL for post-processing color retention were detected on six chromosomes, with QTL on Pv03, Pv08, and Pv11 being the most consistent across subjective and objective phenotyping methods. Color retention QTL on Pv03 were found at the proximal end of the chromosome near 2.2 Mb and explained a modest amount of phenotypic variation. The QTL on Pv08 had high LOD scores and explained a large amount of phenotypic variation, but mapped to a very large physical interval due to low marker coverage. Most encouraging, many QTL for color retention co-localized to a region near 52.5 Mb on Pv11. This relatively tight physical interval explained a large amount of phenotypic variation ($R^2 \approx 20\%$)

and had a large effect size on post-processing color retention across populations, years, and methods of measurement.

INTRODUCTION

Black bean consumption in the US is growing exponentially, with consumers preferring a dark black color in cooked and canned black beans. Black beans typically lose their coloration during soaking and/or thermal processing, which is attributed to leaching of the water-soluble anthocyanin pigments in the seed coat into the soaking or cooking water. Once fully cooked, black beans may have lost enough pigmentation that they turn a faded brown color that is undesirable to consumers. Michigan is the nation's top producer of black beans [Figure 1], so it is economically important to stay at the forefront of black bean research and improvements. Because of this regional connection to black beans, post-canning color retention is a major breeding priority for the dry bean breeding program at Michigan State University. Varieties released by the MSU dry bean breeding program need to meet classical agronomic parameters like yield, local adaptation, and disease resistance, but also need to meet quality standards. The black bean variety, Zorro, released by the program in 2009, is widely grown in Michigan and set higher standards for black bean color retention (Kelly et al., 2009). However, the latest MSU varietal release, Zenith, has even better agronomics and color retention than Zorro (Kelly et al., 2015). This study attempts to identify the genetic mechanisms contributing to the excellent color retention exhibited by Zenith and breeding line B12724 through biparental QTL mapping. Both genotypes were crossed to a common parent with poor post-processing color retention (breeding line B14311) to develop two half-sibling RIL mapping populations segregating for color retention. These populations were phenotyped for canning quality traits using traditional and novel methodologies and were

genotyped with the BARCBean6k_3 Illumina BeadChip (Song et al., 2015). QTL were detected for color retention, additional quality traits, and agronomic traits.

MATERIALS AND METHODS

Plant Materials

Parental Germplasm

The various biparental black bean RIL populations developed in this study were derived from crosses between several parental black bean genotypes with contrasting post-processing color retention. MSU advanced breeding lines B14302, B14303, and B14311 demonstrated high yields and acceptable agronomic traits when evaluated in yield trials, but showed similar, poor color retention [Table 1] following the breeding program's small-scale canning protocol (Hosfield and Uebersax, 1980). Lines B14302 and B14303 were siblings, both resulting from the cross B09197/B11334, while line B14311 is derived from the cross B11338/B10241 [Supplemental Figure 3]. The superior-canning parents in the RIL populations were the breeding line B12724 and the commercial variety, Zenith also known as breeding line B10244. These superior-canning parents also performed well in yield trials and maintained their dark black color during canning evaluations [Table 1]. Line B12724 is derived from the cross B09184/B09135 [Supplemental Figure 4], while Zenith is derived from the cross B04644/Zorro [Supplemental Figure 5]. Zorro was released in 2009 and is currently widely-grown in Michigan. The variety has upright architecture, resistance to anthracnose race 7, common bacterial blight, and avoidance to white

mold. (Kelly et al., 2009). Zenith, released in 2014, has higher yield, additional resistance to anthracnose race 73, and darker-colored canned seed compared to Zorro (Kelly et al., 2015).

Population Development

Parental genotypes were crossed in the greenhouse in the spring of 2015. Eighty-seven crosses were made in total and assigned individual cross numbers 15B261 through 15B347. F_1 seeds were planted at a distance of 20 cm (8 in) at the Saginaw Valley Research and Extension Center (SVREC) near Richville, MI on June 17, 2015. This planting distance was used to improve seed production and facilitate single plant selection at harvest. The soil at SVREC is classified as a Tappan-Londo loam with 0-3% slope. Standard agronomic practices were followed throughout the growing season. Individual F_1 plants were harvested separately. F_2 seed from each plant was collected, labeled with a unique accession number and weighed. 150 randomly-selected F_2 seeds from accession numbers 15A1005, 15A1011, 15A1031, 15A1045, 15A1076, and 15A1086 were planted in the greenhouse in October 2015. The resulting RIL populations were named according to the last two digits of the accession number (i.e. Population 5 was derived from 15A1005). $F_{2:3}$ seeds were harvested from individual plants, stored in coin envelopes, and planted in the greenhouse in February 2016. $F_{3:4}$ seeds were harvested from individual plants in May 2016, stored in coin envelopes, and assigned unique numbers for field planting.

2016 Field Season

$F_{3:4}$ seeds were planted at a distance of 20 cm (8 in) in separate rows at SVREC on June 3, 2016 to produce enough seed for canning evaluation and future field trials. Standard agronomic practices were followed throughout the growing season to manage weed, insect, and disease

pressure. Weather data for the 2016 field season can be found in Supplemental Figure 6A. No desiccants were applied prior to harvest. At harvest, each row of $F_{3:4}$ plants was hand-pulled and threshed separately. $F_{3:5}$ seed was collected, labeled, and all samples were opened and stored on an open-air drying rack before being measured for moisture content, weighed, and canned.

2017 Field Season

Remnant $F_{3:5}$ seed from the 2016 field season was used as a seed source for planting at SVREC on June 2nd 2017. Five RIL populations were planted as separate field experiments (7103 through 7107) with alpha lattice designs and included the parental genotypes, varietal checks Eclipse, Zorro, and Zenith, and selected MSU black bean breeding lines. RILs were planted in 4-row plots with 50 cm (20 in) row spacing and were manually end-trimmed to a length of 4.5 m. The RIL Populations 76 and 86 were selected for genetic study and planted in two replications, while the other RIL Populations 5, 11, 31, and 45 were entered into breeding program trials. At planting, the field was sporadically littered with straw residue due to the previous wheat crop being disk-ripped in the fall of 2016. Standard agronomic practices were followed throughout the growing season to manage weed, insect, and disease pressure. Weather data for the 2017 field season can be found in Supplemental Figure 6B. No desiccants were applied prior to harvest. At harvest maturity, the center two rows of each plot were harvested with a Wintersteiger Classic plot combine (Wintersteiger, Salt Lake City, UT). $F_{3:6}$ seed from each RIL plot was collected and labeled with a breeding line designation based on the identification numbers from the previous growing season. The samples were stored on an open-air drying rack before being measured for moisture content, weighed, and canned. Remnant RIL samples from both the greenhouse and field were stored at the MSU Agronomy Farm.

Phenotyping Canning Quality Traits

Canning quality traits were evaluated over two years. $F_{3:5}$ RILs grown at SVREC over the 2016 field season were evaluated in winter 2017, while $F_{3:6}$ RILs grown at SVREC over the 2017 field season where evaluated in winter 2018. Canning traits evaluated included: canned color rating (COL), canned appearance rating (APP), washed and drained weight (WDW), texture (TXT), and values of L^*, a^*, and b^* in CIELAB color space.

Sample Preparation

A subsample of field-harvested seed was hand-cleaned to remove off-types, split seeds, and debris. This subsample was stored and labeled with the RIL identity (unique breeding line number) and a three-digit can code used to identify canning samples. The samples were temporarily stored in a humidifying chamber to raise the moisture content to approximately 12-15%. Seeds were measured for % moisture in order to calculate the amount of seeds representing 90 grams of dry weight using the formula: $required\ mass\ of\ canning\ sample = 90\ g/(100\% - \%moisture)$. Weighed canning samples were placed in mesh bags labeled with the sample's corresponding three-digit can code and fastened with twist ties. Approximately 30 small mesh bags were then placed in a larger mesh bag to facilitate transportation and simultaneous blanching.

Canning Protocol

After the 2016 and 2017 growing seasons, RILs were canned according to a protocol devised by Bush Brothers & Co. (Knoxville, TN) that differs from the traditional MSU small-scale canning protocol developed by Hosfield and Uebersax (1980). The decision to use this new

canning protocol was based on anecdotal evidence that beans canned with the Bush Brothers & Co. protocol maintained better seed coat integrity. Due to time and space limitations, mapping populations from both years were canned on separate days. Large mesh bags containing the canning sample mesh bags were blanched by submerging for 90 seconds in a 0.03% granular anhydrous calcium chloride solution heated to 95 °C in a steam-heated stainless-steel kettle (Groen Mfg. Co, Chicago, IL). After blanching, beans were transferred from the small mesh bags into tin cans labeled with corresponding can code stickers on the bottom of the cans. Cans were then filled to the top with brine heated to 95 °C. Brine solution was comprised of 1.5% sugar, 1.25% sodium chloride, and 0.03% granular anhydrous calcium chloride. Filled cans were placed on a 5.6 m metal-tiled conveyor belt moving at approximately 2.15 cm/s through an exhaust box heated to 95 °C to facilitate water uptake and removal of air bubbles. Lids were placed on the cans and sealed using a Dixie Double Seamer (Dixie Canner Co, Athens, GA) and placed in a retort (Loveless Mfg. Co, Tulsa, OK). Cans were cooked in the retort at 120 °C and 15 psi for 30 minutes. After 30 minutes, cold water was pumped into the retort for 15 minutes to cool the cans. Cans were removed from the retort, towel-dried, and stacked in tubs until opened for canning quality evaluation.

Reviewer Evaluation

Cans were equilibrated for at least two weeks before being opened for canning quality evaluation. Over the equilibration period, beans become increasingly hydrated as they equilibrate with the canning liquids. On the day of the evaluation, cans were opened and both beans and brine were poured into individual food trays that were arranged on stainless-steel tables in the material handling wing of the MSU Agronomy farm. Reviewers included graduate students, faculty, and

members of the dry bean industry. Reviewers were trained to evaluate canned beans according to separate 1-5 scales for color and appearance, using reference printouts [Figure 4] and varietal checks to assign ratings to each sample. Color of the canned samples was rated on a 1-5 attribute intensity scale, where 1 represented a light brown color and 5 represented a dark black color. Appearance of the canned samples was rated on a 1-5 scale largely according to seed coat integrity, but could also account for the amount of extruded starch, amount of clumping, and brine opacity. Therefore, a '1' on the appearance score represented completely split beans, while a '5' represented intact beans with minimal clumping. Both color and appearance ratings were averaged across reviewers within year for each RIL. Statistical analysis of reviewer consistency was performed in SAS v9.4 (SAS Institute, Cary, NC).

Machine Phenotyping

Digital Imaging

Following evaluation by the panelists, quantitative measurements of canned color and texture were obtained. Beans were transferred to plastic colanders and rinsed under cool water to remove brine and extruded starch from the seed coats. Next, beans were evenly distributed on a black plastic plate so that the black plastic was not visible. Beans were then photographed in a custom-built photobox containing a mounted digital camera centered between two fluorescent tube lamps, as described by Mendoza et al. (2017). To minimize effects of internal and external lighting, the box interior was painted matte black and the loading side was covered with a black foam flap. The digital camera was a Canon model EOS Rebel T3i single-lens reflex camera (Canon, Melville, NY). Fluorescent T4 lamps 45 cm long were mounted 35 cm above the imaging stage at a 45-

degree angle and powered on at least 30 minutes before imaging. The camera was connected to a laptop (Latitude E5570 Series, Dell, Round Rock, TX) via USB, using the software EOS Utility version 2.1 (Canon) for remote shooting and setting configuration. Settings were: manual exposure, auto focusing, lens aperture of f = 5.6, shutter speed of 1/125, white balanced, and ISO 100. Images were saved according to can code identifiers in both .CR2 (raw) and .JPEG (large size, fine-quality) formats. A grey standard card with 18% reflectance (Kodak, Rochester, NY) and a Munsell color checker card (X-Rite, Grand Rapids, MI) were imaged before and after photographing canned beans.

Other Measurements

After digital imaging, samples were transferred to plastic boats and weighed to determine washed and drained weights (WDW). Washed and drained weight is a weight measurement of canned beans once they have been rinsed under water to remove brine and the rinse water has drained off. Because an equal amount of bean dry matter was added to each can, this measurement is a proxy of water uptake that has occurred during the canning process.

A Hunter Labscan XE spectrophotometer (Hunter Associates Laboratory Inc., Reston, VA) was used to measure CIE L^*, a^*, and b^* values of canning samples grown in 2017. L^* values measure darkness to lightness from 0 (black) to 100 (white); a^* values measure the level of greenness to redness and range from negative values (green) to positive values (red); b^* values measure the level of blueness to yellowness and range from negative values (blue) to positive values (yellow) [Supplemental Figure 2].

Texture (TXT) was measured as the peak force required to compress a 100 g subsample of canned beans. Measurements on the RILs from the 2016 season were recorded by a Kramer Shear

Press (Food Technology Corp., Sterling, VA) and interpreted by visually estimating the peak force reading on a printout. Measurements on the RILs from the 2017 season were recorded by a TA.XTplus100 texture analyzer (Texture Technologies Corp., Hamilton, MA). Raw measurements from the Kramer Shear Press required multiplication by a 1.36 conversion factor (http://arsftfbean.uprm.edu/bic/wp-content/uploads/2018/04/Bean_Processing.pdf) to obtain true texture measurements that were then comparable to those from the texture analyzer.

Digital images of the canned beans from both years were analyzed with ImageJ software (Schneider et al., 2012). An experimental macro was developed to measure CIELAB values from the digital images. As part of the macro, digital images of canned samples were loaded into the software and brightened by a constant gamma correction. Then, reflectance was minimized through noise reduction and images were partitioned into L^*, a^*, and b^* slices. The mean value of each slice was recorded to obtain L^*, a^*, and b^* values in CIELAB color space. Color values from the Hunter Labscan spectrophotometer are denoted as L^*H, a^*H, and b^*H, while color values from digital images processed in ImageJ are denoted as L^*I, a^*I, and b^*I.

Phenotyping Agronomic Traits

Agronomic traits were evaluated in replicated plots during the 2017 growing season at SVREC and included days to flowering, days to maturity, canopy height, lodging, foliar effects of common bacterial blight and ozone damage, and an overall desirability score. After harvest, seed yield (SY) was taken for each RIL as the mean across field replications and seed weight (SW) was recorded as the mass of 100 randomly-selected seeds from each RIL.

Days to flowering (DF) were visually estimated as the number of days after planting when 50% of a plot was flowering. Days to maturity (DM) were visually estimated as the number of

days after planting for a plot to reach harvest maturity (i.e. “dried down.”). Lodging (LDG) was rated on a per-plot basis using a 1-5 scale where ‘1’ indicated fully upright plants and ‘5’ indicated fallen-over plants or stem breakage. Nearly every RIL was given a lodging rating of ‘1’ so this trait was not included in QTL analysis. Canopy height (HT) was visually estimated in cm as an average distance from the soil surface to the top of the plants in a plot at harvest.

An agronomic desirability score (DS) from 1-7 was assigned to each plot based on perceived agronomic potential, where a score of ‘1’ indicated exceptionally poor field performance and a ‘7’ indicated excellent field performance. The DS is used by the MSU dry bean breeding and genetics program to guide breeding decisions and is based on a combination of factors that are important to breeding potential: height, architecture, adaptability, pod load, disease symptoms, and other subtle characteristics.

Dry beans affected by ozone stress will sometimes develop bronze or brown patterning on the leaves. In 2017, this foliar bronzing (BRZ) was rated on a 1-5 scale where ‘1’ signified no bronzing and ‘5’ signified severe bronzing throughout the plot.

Common bacterial blight (CBB) is a disease caused by the fungus *Xanthomonas axonopodis* pv. *phaseoli* (Xap). The disease can infect both leaves and pods, but CBB resistance in this study was measured by visually rating each 2017 field plot for foliar symptoms on a 1-5 severity scale. A CBB rating of ‘1’ signified no observable disease, while a rating of ‘5’ signified severe foliar lesions widespread throughout the plot.

Statistical Analysis

Canning Traits

RILs from both populations segregated for canning quality according to evaluations on samples grown in 2016 and 2017. For Population 76, canned $F_{3:5}$ RILs (n=147) grown at SVREC in 2016 were evaluated by 16 reviewers on February 9, 2017, while canned $F_{3:6}$ RILs (n=147) grown at SVREC in 2017 were evaluated by 10 reviewers on February 12, 2018. There were eight reviewers in common across both years of evaluation for Population 76. For Population 86, canned $F_{3:5}$ RILs (n=148) were evaluated by 14 reviewers on March 2, 2017, while canned $F_{3:6}$ RILs (n=147) were evaluated by 15 reviewers on February 14, 2018. There were 10 reviewers in common across both years of evaluation for Population 86.

SAS v9.4 (SAS Institute, Cary, NC) was used for statistical analysis of canning quality traits. Trait data was input as individual reviewer ratings across all RILs and years. Boxplots were generated to visually confirm normality and homogeneity of variance. Several statistical models were tested, and the best was selected according to the lowest Akaike information criterion value (AIC). The final full model was: $\gamma = \mu + RIL_i + Reviewer_j + Year_k + \varepsilon_{ijkl}$ where μ is the grand mean, RIL is a fixed effect, Reviewer is a random effect, Year is a random effect, and ε is the residual effect of the three-way interaction RIL*Reviewer*Year.

Both populations were phenotyped for post-processing color-retention, canning quality, and agronomic traits [Table 2; Table 3]. All color retention and canning quality traits were approximately normally distributed in both populations and across both years. For canned color rating, parental lines generally exhibited the most extreme phenotypes, though a few transgressive segregants were observed [Figure 5]. Most RILs exhibited average ratings for both color and

appearance ratings. CIELAB color components were similarly distributed across both populations [Figure 6; Figure 7]. Other canning quality traits like appearance rating, washed and drained weight, and texture were also approximately normal [Figure 8], although measurements of washed and drained weights and texture on Population 76 RILs were noticeably lower in 2016 than in 2017. Pearson correlation coefficients were calculated for all canning quality traits in both populations [Table 4].

Variance components for broad sense heritability estimates of color and appearance ratings were determined stepwise to minimize the confounding effect of Reviewer*Year interaction. First, the model was run with the Year effect excluded to derive least square means (LSmeans) incorporating a reviewer effect. LSmeans were then used in the model with the Reviewer effect excluded to derive LSmeans incorporating a year effect. This methodology is justified because reviewers did not give ratings to biological replicates in any one year and reviewers were not always consistent across years. Broad sense heritabilities for other canning quality traits were determined by using the full model. Variances were estimated using the type 3 sums of squares method and used to calculate broad sense heritabilities (H^2) on an entry mean basis according to Fehr (1991) [Figure 11].

Agronomic Traits

Although the focus of this research primarily concerned canning quality, RILs were evaluated for various agronomic traits during the 2017 field season [Table 2; Table 3]. Agronomic traits were generally normally distributed, although parental lines were similar or identical in several instances [Figure 10]. SAS v9.4 (SAS Institute, Cary, NC) was used to determine Pearson correlation coefficients for agronomic traits [Table 5].

Genotyping

RILs from Populations 76 and 86 were planted in the greenhouse in January 2017 from remnant 2016 $F_{3:5}$ seed. Six seeds per RIL were planted in a 20 cm (8 in) clay pot filled with potting soil. Young trifoliates from four plants per pot were pooled together to represent a RIL genotype. Tissue was collected in duplicate; four small trifoliates were pooled in labeled 1.5 ml tubes, while four larger trifoliates were pooled in labeled 15 ml tubes as backup. Tissue samples were submerged in liquid nitrogen immediately after harvesting and stored at -80 C. Samples in 1.5 ml tubes were lyophilized using a VirTis Wizard 2.0 lyophilizer (SP Scientific, Stone Ridge, NY). DNA was isolated with CTAB (hexadecyl-trimethyl-ammonium bromide) in April-May 2017 using a modified protocol of the MSU dry bean program, which is itself a modified protocol of Doyle and Doyle (1991). DNA was suspended in 1.5 ml tubes containing $T_{10}E_1$ buffer and RNase A and stored at -20 C. Thawed samples were pipet-mixed and quantified using a BioDrop μLite spectrophotometer (Denville Scientific, Holliston, MA). A series of dilutions and quantifications were performed on each sample to achieve a final volume of 120 μl at final concentrations of 100-120 ng/μl. 50 μl aliquots were loaded onto three 96-well plates, with parental genotypes included on each plate.

Because the population sizes were too large for every RIL to fit on three 96-well plates, specific RILs were excluded on the basis of creating more normal distributions of color, appearance, and texture traits from the 2017 canning evaluation on RILs grown in 2016. After exclusion, 140 RILs remained in Population 76 and 141 RILs remained in Population 86. Parental genotypes were included on each plate. The three plates were shipped to the USDA Beltsville Agricultural Research Center (BARC) in Beltsville, MD where they were genotyped for 5398 SNP markers from the BARCBean6k_3 BeadChip developed by Song et al. (2015).

Linkage Map Construction and QTL Mapping

Marker clustering was surveyed in GenomeStudio v2011.1 (Illumina Inc., San Diego, CA) and genotypic calls were exported in AB format. Markers were filtered to remove SNPs monomorphic for the parents and SNP IDs were assigned according to SNP location in the dry bean v2.1 reference genome (Goodstein et al., 2012; Schmutz et al., 2014). Locus files were created for each chromosome and imported into JoinMap 4.1 (Van Ooijen, 2011) for linkage map construction. Loci were filtered for segregation distortion and missing data. Questionable markers had chi-square values > 10 or 50% missing genotypic data, but were not always removed to improve marker coverage. The remaining markers were binned into linkage groups representing chromosomes using a LOD threshold. A LOD threshold of 3 was used for all linkage groups with the exception of two chromosomes from RIL Population 76: Pv01 was grouped at LOD 2 to allow inclusion of markers from the proximal arm, and Pv10 which was grouped at LOD 2 to maximize number of markers, though only 5 were ultimately informative. Linkage maps for all chromosomes were generated using the maximum likelihood mapping algorithm. Map order was optimized using simulated annealing with a chain length of 5000 and a burn-in of 50000. After the burn-in chain, 10 cycles of Monte Carlo Expectation Maximization (MC EM) with chain lengths of 5000 were performed to determine map distance over a period of 3 optimization rounds. After initial map construction, markers were examined according to the JoinMap parameters of plausible positions and nearest-neighbor stress and were removed if they had extreme values for these criteria relative to other markers on the linkage group. Linkage maps were then compared to physical maps with marker order and position based on the v2.1 reference genome. Linkage maps using the fixed marker order from the v2.1 reference genome were ultimately selected for QTL mapping.

The program Windows QTL Cartographer v2.5 (Wang et al., 2012) was used to analyze marker-trait associations. Preliminary single marker analysis and interval mapping were preformed to identify regions of interest. Composite interval mapping (CIM) with forward and backward regression, background markers (n = 5), a window size of 10 cM, and a LOD threshold of 3 was used to refine regions of interest. These regions were refined again using a window size of 5 cM and a LOD threshold determined on a per-trait basis from 1000 permutations at a significance level of $p = 0.05$. QTL and marker positions were imported to MapChart (Voorrips, 2002) for graphical visualization.

In total, Population 76 (B14311 x Zenith) included 656 SNP markers and 141 RILs, while Population 86 (B14311 x B12724) included 391 SNP markers and 140 RILs for linkage map construction and QTL mapping. However, both populations contained markers that mapped to identical genetic positions, which lowered the number of informative markers to 527 in Population 76 and 307 in Population 86. Attempts to integrate linkage maps constructed from the two RIL populations were unsuccessful.

Molecular Marker Analysis

Genomic regions significantly associated with QTL for post-processing color retention on Pv08 and Pv11 were further explored with insertion-deletion (InDel) markers. The InDel markers were developed by Moghaddam et al. (2014) at North Dakota State University (NDSU) and can be used across and within dry bean market classes. Marker names provide information regarding the university where they were developed (NDSU), type of marker (IND), chromosome number, and physical position in the dry bean v1 reference genome (e.g. NDSU_IND_11_47.0739 is located on chromosome Pv11 at 47.0739 Mb in the v1 genome). InDel markers were selected by

identifying BARCBean6k_3 SNPs that flanked the InDel markers' physical positions in the v1 genome and then referencing the SNPs' updated physical positions in the v2.1 genome. The PCR protocol of Moghaddam et al. (2014) was followed: 3 minutes at 95 °C for one cycle, 20 seconds at 95 °C, 30 seconds at 55 C, and 1 minute at 72 °C for 45 cycles, then 10 minutes at 72 °C for one cycle. PCR products were transferred to a 3% agarose gel containing 3% ethidium bromide that underwent gel electrophoresis in 1x TAE buffer. Bands were visualized under UV light and scored for each genotype.

RESULTS

Statistical Analysis

Comparing Methods of Quantitative Color Measurement

Both the Hunter Labscan XE spectrophotometer and ImageJ software were used to measure CIELAB color components of canned black beans. The spectrophotometer was only used on canning samples from 2017-grown RILs, but the ImageJ macro was applied to saved digital images collected from both years of canning evaluation. *L**, *a**, and *b** color values were different across methods, which was expected because of the post-processing involved in the ImageJ analysis. However, while the methods gave different values, they were mostly consistent relative to each other (e.g. a sample with a high Labscan-derived *L**H would typically have a high ImageJ-derived *L**I). Pearson correlation coefficients were generated for both methods to compare consistency across methods [Table 4]. *L**, *a**, and *b** color components measured by different methods were generally strongly positively correlated with each other ($r > 0.50$). Among the Hunter Labscan

values, *b**H was most correlated to visual color rating (r ≈ -0.82 to -0.93), followed by *L**H (r = -0.73 to -0.83) and then *a**H (r ≈ -0.73). This trend held true across populations. Among the two-year average ImageJ values, *b**I was most correlated to color rating (r ≈ -0.95), followed by *L**I (r ≈ -0.89), and then *a**I (r ≈ -0.81). This trend was also consistent across populations. Simple linear regression was used to compare accuracy of color components derived from both methods with actual canned color ratings [Figure 11]. Scatterplots of the regressions show that the ImageJ-derived color components had less variation and were more strongly correlated to visual color ratings. This was observed across populations.

Agronomic Traits

In both populations, the most strongly-correlated agronomic traits were desirability score (DS) and canopy height (HT), with correlation coefficients of r = 0.73 and 0.78 in Population 76 and Population 86, respectively. Interestingly, DS was also moderately correlated with yield (r = 0.46 to 0.53) and days to maturity (r = 0.32 to 0.40). Correlations between these traits make sense, since the MSU breeding program attempts to select high-yielding, more upright plant types that are adapted to the Michigan environment. These results affirm that gains from selection can be made based on innate knowledge of a crop and a skilled 'breeder's eye.'

Correlations between agronomic traits and canning quality traits were much weaker. In Population 86, visual appearance ratings of canned beans (APP) were moderately negatively correlated to height (r = -0.35), desirability score (r = -0.33), yield (r = -0.32), and days to maturity (r = -0.29), which exemplifies the difficulty in breeding high-performing varieties with acceptable canned bean appearance.

QTL Mapping of Post-Processing Color Retention

A complete list of QTL for post-processing color retention is located in Table 6. QTL graphs from Population 76 are located in Figure 12, and QTL graphs from Population 86 are located in Figure 13.

Color Ratings (COL)

QTL for visual color ratings of canned black beans (COL) were found on chromosomes Pv02, Pv03, Pv08, and Pv11 in Population 76 and on Pv03, Pv05, Pv08, Pv10, and Pv11 in Population 86 [Table 6]. The B14311 parent contributed a negative effect on color rating in all instances, except for a single QTL found on Pv10 in Population 86.

A QTL for color rating on Pv02 named COL2.1^{76} was detected by color ratings for 2017 seed (COL_2017) and the two-year average (COL_2YA) [Table 6]. The QTL was within a 54-74 cM interval, with a peak LOD located at near 63 cM. The region associated with 2017 color rating explained 6% of the phenotypic variation and influenced color rating by 0.16. The region associated with the two-year average color rating explained just 5% of the phenotypic variation and influenced color ratings by 0.13. Although below the significance threshold, the color ratings from RILs grown in 2016 formed a peak slightly upstream of the COL2.1^{76} (data not shown).

QTL were found on Pv03 that were unique to each population. In Population 76, a color rating QTL, COL3.1^{76}, was detected over a 26.4 to 32.8 cM interval using color ratings from 2016 (COL_2016) and the two-year average (COL_2YA). Both COL_2016 and COL_2YA explained about 6% of the total phenotypic variation and affected color ratings by 0.15. In Population 86, two COL QTL were detected on separate chromosome arms. A 2017 color rating QTL, COL3.1^{86}, mapped to the top of the chromosome from 0-1.5 cM (1.19-1.30 Mb), while a 2016 color rating

QTL, COL3.2[86], mapped to the distal end of the chromosome from 102.4-121.7 cM (47.28-50.39 Mb) [Table 6]. Both of these color QTL remained significant at permutation thresholds below LOD 3, explained approximately 4% of the phenotypic variation, and influenced color ratings by 0.16 and 0.13, respectively.

A QTL for color rating on RILs grown in 2017 was found on Pv05 in Population 86 only (COL5.1[86]). This peak had an interval of 167.5-170.7 cM and was flanked by markers ss715645449 and ss715645459 (38.92-38.84 Mb). A peak for the two-year average color rating was just below the significance threshold, but mapped to an adjacent interval from 170.9-171.6 cM.

QTL for color rating were shared across years and populations despite poor marker coverage on Pv08 [Table 6]. In Population 76, QTL COL8.1[76] was detected across all years of evaluation. Color ratings from 2016 seed (COL_2016) were significant across a large map interval from 16.8-62.3 cM and contained a peak at 41.55 cM that explained 16% of the phenotypic variation and altered color scores by 0.26. Color ratings from 2017 (COL_2016) and two-year average color ratings (COL_2YA) co-localized within this interval and a shared peak LOD position at 53.42 cM. Both COL_2016 and COL_2YA had peak LOD scores over 7 and affected color ratings by approximately 0.24 [Table 6]. In Population 86, QTL COL8.1[86] was detected across all years of evaluation (COL_2016, COL_2017, and COL_2YA). LOD scores were significant over a large mapping interval from 15.3-60.4 cM, ranged from 7 to 8, and were all closest to marker ss715647116 located at a physical position of 1.58 Mb. Each individual year explained 12-13% of the phenotypic variation and influenced color ratings by approximately 0.26.

Although both populations had few markers on Pv10, a QTL for color rating in 2017 was detected in Population 86 (COL10.1[86]). The QTL was contained within a 69.6-82.1 cM interval

and flanked by markers ss715645524 (42.22 Mb) and ss715645501 (43.29 Mb). LOD peaks for 2016 color rating and two-year average color rating were apparent in the same interval, but were below the significance threshold.

Similar to Pv08, Pv11 also contained color QTL identified in both populations [Table 6]. In Population 76, peak LOD scores reached 7.4 for 2016-grown RILs, 7.01 for the two-year average, and 4.8 for 2017-grown RILs. The 2016 region (COL_2016) mapped to a 144.3-149.6 cM interval, while the other two regions (COL_2017 and COL_2YA) spanned a 149.6-150.6 cM interval slightly downstream. The 2016 region was most significant, explained 14% of the phenotypic variation, changed color scores by 0.25, and was flanked by markers with physical positions from 52.16-52.65 Mb. Since these regions were significant over several years and occupied a similar interval, they were considered a single QTL named COL11.1^{76}. The yearly color ratings in Population 86 also co-localized and were also considered as one QTL named COL11.1^{86}. These regions (COL_2016, COL_2017, and COL_2YA) had higher LODs (>10), R^2 (0.19-0.22), and larger additive effects (0.31-0.32) than those detected in Population 76. COL11.1^{86} mapped to a 26.4-28.6 cM interval and was flanked by markers ss715648350 and ss715640405 that have physical positions of 52.47-52.84 Mb on Pv11.

*L**

Measurements of *L** describe darkness to lightness and range from 0 (pure black) to 100 (pure white). In this study, *L** refers to the color component itself, while *L**H and *L**I refer to *L** values measured by a Hunter Labscan and ImageJ software, respectively. QTL for *L** were detected on Pv02 and Pv03 for Population 76, Pv05 and Pv10 for Population 86, and in both populations on Pv08, Pv09, and Pv11. All detectable *L** value QTL in Population 86 were derived

from the ImageJ macro (*L**I). All *L** QTL but one increased *L** values when contributed by the B14311 parent.

A QTL on Pv02 (*L**2.1^{76}) was detected in 2017 by the ImageJ macro and had a peak LOD score of 4.66. It covered a 61.6-74.1 cM interval bound by flanking markers ss715648552 (13.27 Mb) and ss715651061 (17.24 Mb). Accounting for 9% of the total phenotypic variation, this QTL affected *L**I values by 0.43.

The 2017 *L**I QTL on Pv03 (*L**3.1^{76}) was barely above the significance threshold, but co-localized with noticeable peaks from other measurements of *L** that fell below the significance threshold. Although the map interval was large (26.4-32.8 cM), the physical interval of flanking markers was just 2.02-2.43 Mb. Only accounting for 5% of the phenotypic variation, this QTL lightened *L**I values by 0.33 when the allele was derived from the B14311 parent.

A 2017 *L**I QTL (*L**5.1^{86}) mapped to the interval 121.9-126.9 cM on Pv05 and was flanked by markers ss715647683 and ss715639578 (34.33-35.96 Mb). It had a LOD score of 3.8, explained 6% of the phenotypic variation, and influenced lightness by 0.40.

QTL for *L** were identified on Pv08 in both populations despite low marker coverage. In Population 76, all measurements of *L** were considered as a single QTL, *L**8.1^{76}. LOD scores from 2016 *L**I values were significant from 0-15.3 cM, while 2017 *L** values from both Hunter Labscan and ImageJ methods were significant from 17-62 cM and shared peaks near 52 cM. These shared peaks were flanked by markers ss715650193 and ss715648558 with physical positions at 5.86 and 7.15 Mb, respectively. In Population 86, QTL *L**8.1^{86} was detected by ImageJ analysis in both years over the map interval 15.8-40.1 cM, corresponding to a 1.58-6.27 Mb physical region. The 2017 peak (*L**I_2017) explained 17% of phenotypic variation and affected *L**I values by 0.67,

while the QTL peak in 2016 (*L**I_2016) explained 8% of the phenotypic variation and influenced *L**I values by 0.49.

Population-dependent *L**I QTL were detected on Pv09 [Table 6]. In Population 76, the *L**9.1^{76} QTL had a peak LOD score of 6.8 and spanned a map interval of 27.0-27.2 cM (10.30-10.32 Mb based on physical positions of flanking markers). This QTL accounted for 14% of the phenotypic variation and affected *L**I values by 0.53. Another QTL detected in Population 76, *L**9.2^{76}, was downstream of *L**9.1^{76}. It had a peak LOD of 3.1 near 40 cM and only explained 4.8% of the phenotypic variation. In Population 86, LOD scores for the *L**9.1^{86} QTL plateaued at 3.5 across the map interval 2.6-5.8 cM, corresponding to a physical interval of 27.58-29.1 Mb. QTL *L**9.1^{86} accounted for just 5.5% of the phenotypic variation and lowered *L**I values by 0.38, the only *L** value QTL where the B14311 allele that bestowed a darkening effect.

QTL *L**10.1^{86} was detected in Population 86 in 2016 on Pv10. The QTL reached a peak LOD of 3.98, explained 6.8% of the variation, and lightened *L**I values by 0.48. Both map and physical intervals were small (65.6-67.3 cM and 41.96-42.01 Mb, respectively).

Pv11 contained *L** QTL that were shared across populations. Peaks from Hunter Labscan-derived *L**H values were noticeably co-localizing to the same region, but only reached the significance threshold in Population 76 [Table 6]. In Population 76, the *L**11.1^{76} QTL was comprised of measurements from the Hunter Labscan (*L**H_2017) and ImageJ analysis (*L**I_2016, *L**I_2017). Both years of *L**I measurements mapped to a 149.6-150.6 interval (52.65-52.84 Mb) while the Hunter Labscan-derived *L**H QTL was nearby at 150.9-154 cM (52.84-52.87 Mb). In Population 86, the *L**11.1^{86} QTL mapped to a similar physical position as detected in Population 76. The *L**11.1^{86} QTL was comprised of ImageJ measurements from 2016 (*L**I_2016) and 2017 (*L**I_2017). The region associated with *L**I_2016 explained 18% of the phenotypic

variation, modified *L**I values by 0.68, and mapped to 22.9-30.8 cM (52.47-52.87 Mb). The region associated with *L**I_2017 explained 15% of the phenotypic variation, influenced *L**I values by 0.62, and mapped to 22.9-30.5 cM (52.47-52.84 Mb).

*a**

Measurements of *a** describe the level of greenness to redness and range from negative values (green) to positive values (red). In this study, *a** refers to the color component itself, while *a**H and *a**I refer to *a** values measured by a Hunter Labscan and ImageJ software, respectively. QTL for *a** values were found on Pv08 across all populations and included all detection methods and years [Table 6]. A single QTL was found on Pv10 in Population 86 where the B14311 allele had a negative effect on *a**. Observable peaks on Pv03 and Pv05 in Population 76 fell below the significance thresholds.

On Pv08, LOD scores for *a** values were significant over a large mapping interval containing few markers. In Population 76, QTL *a**8.1^{76} was comprised of *a** measurements from all years and methods. ImageJ-derived *a**I values in 2017 (*a**I_2017) had a peak LOD of 9.8 spanning 17.5-49.7 cM, and explaining 27% of the phenotypic variation, while the Hunter Labscan-derived *a**H values (*a**H_2017) explained 13% of the phenotypic variation in that same interval. Local LOD peaks for were detected downstream of the peak LOD. These localized peaks were from 49.7-50.4 cM (5.86-6.00 Mb). Two regions for 2016 *a**I values (*a**I_2016) mapped outside of the larger interval at intervals of 0-17.54 cM (0.484-1.54 Mb) and 55.3-83.9 cM (7.16-18.75 Mb), though only the upstream one was visualized in MapChart [Figure 12H]. Like Population 76, Population 86 *a** values co-localized to a very large mapping interval from 15.3-60.4 cM (1.57-53.68 Mb) that was considered a single QTL named *a**8.1^{86}. Peaks for all

measurements of Population 86 *a** values explained approximately 20% of the phenotypic variation and influenced *a** values by approximately 0.48.

A QTL for *a**I from RILs grown in 2017 was detected on Pv10 in Population 86. This QTL was named *a**10.1^{86} and spanned the map interval 69.7-82.1 cM, with flanking markers ss715645524 and ss715645501 located at physical positions 42.22-43.29 Mb. This QTL explained 8% of the phenotypic variation and was the only QTL where the B14311 allele decreased the *a**I value by 0.31. LOD peaks for other *a** values from 2016 ImageJ and 2017 Hunter Labscan measurements were apparent near this QTL, but were below the significance threshold.

*b**

The *b** value measures the level of blueness to yellowness and ranges from negative values (blue) to positive values (yellow). In this study, *b** refers to the color component itself, while *b**H and *b**I refer to *b** values measured by a Hunter Labscan and ImageJ software, respectively. Population 76 had QTL for *b** on Pv02, Pv03, Pv08, and Pv11, while Population 86 had QTL on Pv03, Pv08, and Pv11 [Table 6]. All alleles from the B14311 parent increased *b** values, signifying a more yellow coloration.

A *b**I QTL on Pv02 (*b**2.1^{76}) was detected by ImageJ software in 2017. It plateaued at 4.38 LOD, explained 9% of the phenotypic variation, and influenced the *b**I value by 0.41. Flanking markers occupied an interval from 54-74 cM (11.0-17.2 Mb).

Two *b** value QTL on Pv03 were detected in separate populations by the ImageJ software: *b**3.1^{76} in 2016, and *b**3.1^{86} in 2017. In Population 76, the *b**3.1^{76} QTL mapped to an interval of 3.4-14.7 cM, and a physical interval of 1.00-1.19 Mb. This QTL explained just 7% of the phenotypic variation and affected *b**I values by 0.41. In Population 86, the *b**3.1^{86} QTL barely

cleared the LOD permutation threshold of 2.7 and only explained 3.9% of the phenotypic variation. This QTL mapped to a larger mapping interval of 0-1.51 cM, but had a similar physical interval of 1.19-1.30 Mb.

A QTL for *b** on Pv08 was detected across populations using both methods and years. In Population 76, *b**8.1^{76} mapped to the interval 16.8-62.3 cM, (1.53-7.25 Mb). Individual measurements *b**I_2016, *b**I_2017, and *b**H_2017 explained a range of phenotypic variation from 7-16% and modified the *b** value by a range of 0.39 to 0.47. In Population 86, all measurements of *b** co-localized to a large map interval 15.3-40.1 cM in length and were designated as QTL *b**8.1^{86}. Markers flanking this QTL had physical positions of 1.57-6.27 Mb, which is within the physical interval identified in Population 76. The three measurements (*b**I_2016, *b**I_2017, and *b**H_2017) explained a range of phenotypic variation from 9-12.6%.

Pv11 also contained *b** QTL that were shared across populations and detected over methods and years. In Population 76, QTL *b**11.^{76} was comprised of individual measurements of *b** with very high peak LOD scores: 8.8 for *b**I_2016, 6.9 for *b**I_2017, and 5.3 for *b**H_2017. These regions explained 11-21% of the phenotypic variation and affected the *b** value by 0.38 to 0.45. All three peaks co-localized to 149.3 cM and were within a physical interval of 52.12-52.84 Mb. In Population 86, QTL *b**11.1^{86} was comprised of *b** measurements with even higher LOD scores (13.3-14.6), larger amount of phenotypic variation explained (26-27%), and greater influence on *b** values (0.62 to 0.81). Notably, the *b**11.^{86} QTL from Population 86 co-localized to an interval from 22.9-30.5 cM (52.47-52.84 Mb), which is within the physical interval of *b**11.1^{76} from Population 76.

QTL Mapping of Other Canning Quality Traits

A complete list of QTL for appearance, washed and drained weight, and texture is located in Table 7. QTL graphs from Population 76 are located in Figure 12, and QTL graphs from Population 86 are located in Figure 13.

Appearance Ratings (APP)

QTL for canned bean appearance (APP) were unique to populations; Population 76 had QTL on Pv02, Pv05, and Pv08, while Population 86 had QTL on Pv02, Pv03, Pv04, Pv06, and Pv10 [Table 7].

QTL on Pv02 were similar in their effects on appearance ratings, but were considered unique between populations because of large differences in their physical positions. The APP2.1^{76} QTL in Population 76 mapped to the interval 142.8-164.4 cM corresponding to the physical interval 37.81-44.97 Mb, while the APP2.1^{86} QTL in Population 86 mapped to the interval 0-1.83 cM corresponding to the physical interval 3.90-4.48 Mb. The QTL from Population 76 was detected in 2017 and explained 9% of the phenotypic variation with the B14311 allele lowering appearance ratings by 0.12. The QTL from Population 86 was detected in 2016 and explained 8.7% of the phenotypic variation with the B14311 allele lowering appearance ratings by 0.16.

In Population 86, Pv03 contained the APP3.1^{86} QTL that included regions significant for 2016 (APP_2016) and two-year average appearance (APP_2YA) ratings. Both regions had minor effects, explaining just 9.7 and 6.7% of the total phenotypic variation, and decreasing appearance scores by 0.16 and 0.11 from the B14311 allele, respectively. The APP3.1^{86} QTL mapped to a 1.5 cM interval at the top of the chromosome, which corresponded to a physical interval of 1.2-1.3 Mb.

Population 86 also had an APP QTL on Pv04, APP4.1[86]. The QTL had an R^2 of 7% and the B14311 allele improved appearance rating by 0.13. This QTL mapped to 51.1-52.1 cM and was flanked by markers ss715646227 and ss715646218 (2.75-2.89 Mb) [Table 7].

The APP5.1[76] QTL on Pv05 was detected in 2016 in Population 76. This QTL mapped to 40.6-57.1 cM, corresponding to a physical interval of just 4.47-4.75 Mb. It explained 8% of the total phenotypic variation and was responsible for lowering appearance rating by 0.12 when the allele was derived from B14311.

Population 86 also detected a barely-significant QTL on Pv06 in spite of low marker density. The APP6.1[86] QTL explained 6% of the phenotypic variation and improved appearance scores by 0.13 when the allele was donated by the B14311 parent. The QTL mapped to a small interval and was flanked by markers located at 20.9-21.7 cM (28.97-29.04 Mb).

One QTL from each year was detected on Pv08 in Population 76, where both QTL explained 7% of the phenotypic variation. The APP8.1[76] QTL detected in 2016 was located at 145.5-147.0 cM (60.97-61.30 Mb) and the B14311 allele improved APP by 0.12. The APP8.1[76] QTL was detected in 2017 and located at 49.7-50.4 cM (5.86-6.00 Mb) and the B12724 allele improved APP by 0.10.

In Population 86, the APP10.1[86] QTL was detected at the end of the chromosome Pv10 spanning a 69.65-90.23 cM interval (42.22-44.22 Mb). Two local peaks occurred within this interval, but they were considered as part of one QTL. Both local peaks had similar LOD scores, explained about 9% of the phenotypic variation and improved appearance by 0.13 when the allele was donated by the B14311 parent.

Texture (TXT)

QTL for texture (TXT) were identified on Pv02, Pv05, Pv09, and Pv10. Separate, minor effect texture QTL for 2016 were detected in each population.

A TXT QTL (TXT2.1^{76}) was detected on Pv02 in Population 76 and was located in the mapping interval from 81.8-88.9 cM (17.31-20.44 Mb). This QTL explained 8% of the phenotypic variation and increased texture by 2.64 kg when B14311 contributed the allele. In Population 86, a TXT QTL on Pv02 was located from 0-1.83 cM (3.90-4.48 Mb). It explained 6% of the variation and decreased texture by 2.25 kg when B14311 contributed the allele.

A QTL for texture on Pv05 was detected across years within Population 76 and named TXT5.1^{76}. Measurements from both 2016 (TXT_2016) and 2017 (TXT_2017) mapped near 138 cM and were very significant, having peak LOD scores of 7.0 in 2016 and 11.6 in 2017. The 2016 peak explained 14% of the phenotypic variation and influenced texture by 2.4 kg, while the 2017 peak explained 25% of the phenotypic variation and influenced texture by 2.5 kg. In both instances, the B14311 allele increased texture measurements. Both peaks were flanked by markers ss715649539 and ss715646996 which mapped to a 128.2-141.5 cM interval (27.70-36.79 Mb).

A TXT QTL (TXT9.1^{76}) was identified on Pv09 in Population 76 in 2017. This QTL contained two localized peaks at 27 and 33.5 cM with similar LOD scores and was considered as a single QTL spanning the interval 16.3-39.6 cM (7.87-13.55 Mb). This QTL explained 7.6% of the phenotypic variation and softened texture by 1.38 kg when the allele was donated by B14311.

The TXT10.1^{86} QTL at the distal end of Pv10 in Population 86 had a peak LOD greater than 11 and mapped the interval 82.06-90.23 cM (43.29-44.20 Mb) in 2016. This QTL explained over 26% of the phenotypic variation for that year and the B14311 allele decreased texture by 4.45

kg. A noticeable peak for texture measurements from 2017 co-localized to the exact same region, but its peak LOD of 3.17 was below its permutation threshold of 3.42.

Washed and Drained Weight (WDW)

QTL for the washed and drained weight trait (WDW) of canned beans were detected only in 2016 on chromosomes Pv02 and Pv08 [Table 7]. A peak from 2016 with a LOD of 3.15 was detected on Pv04 in Population 86, but it was below the 3.7 LOD permutation threshold. Although both populations shared a distinct peak for 2017 WDW near 46.2 Mb on Pv01, it was below the significance threshold.

The top of Pv02 contained WDW2.1[76] detected in 2016 in Population 86. It explained 11% of the phenotypic variation and increased WDW by 1.6 g when the allele was contributed by the B14311 parent. This QTL was positioned from 0-25.4 cM, which corresponded to a large physical interval of 3.90-30.15 Mb.

The only WDW QTL found in Population 76 was located at the end of Pv08 from 158.4-160.1 cM (62.27-62.75 Mb). This QTL was named WDW8.1[76] and had a sharp peak at 158.4 cM with a LOD of 4.4. The R^2 was 12%, and it decreased the washed and drained weight by 2.43 g when the allele was donated by the B14311 parent.

QTL Mapping of Agronomic Traits

Agronomic traits were not the primary focus of this research, but agronomic data was useful for identifying RILs that could potentially contribute to the MSU breeding program. Many of these traits are polygenic in nature and are thus affected by many loci, each with a small contribution to a trait phenotype. A complete list of QTL for agronomic traits is located in Table

8. QTL graphs from Population 76 are located in Figure 12, and QTL graphs from Population 86 are located in Figure 13.

Seed Yield (SY)

A single QTL for seed yield (SY) was identified on Pv08 for both populations; these QTL were considered distinct due to large differences in the physical positions of the flanking markers (60.07-60.56 Mb in Population 76, compared to 0.374-1.41 Mb in Population 86) [Table 8]. In Population 76, the SY8.1^{76} QTL had a peak LOD of 3.5 at 137.7 cM, explained 9% of the phenotypic variation, and lowered yield by 110 kg/ha when the B14311 allele was present. In Population 86, the SY8.1^{86} QTL had a peak LOD of 6.85 at 0.01 cM, explained 14.8% of the phenotypic variation, and lowered yield by 130 kg/ha when the B14311 allele was present.

Seed Weight (SW)

QTL for seed weight (SW) were detected on Pv03 and Pv04 in both populations, Pv05 in Population 86, and Pv07 and Pv08 in Population 76.

A SW QTL was identified in both populations within a similar physical interval on Pv03 [Table 8]. In Population 76, the SW3.1^{76} QTL had a peak LOD of 12.4 located within the interval 119.3-122.8 cM (11.47-11.82 Mb). It explained 23% of the phenotypic variation and the B14311 allele increased seed weight by 0.79 g. In Population 86, the SW3.1^{86} QTL had a peak LOD of 4.5 located within the interval 43.6-60.2 cM (3.82-12.30 Mb). This QTL explained 12% of the phenotypic variation and the B14311 allele increased seed weight by 0.42 g.

The SW4.1^{76} QTL was detected in Population 76 on Pv04 with an R^2 of 13% and an additive effect of 0.60 [Table 8]. Its peak LOD of 8.1 was located within the interval 10.3-20.6 cM

(0.16-1.90 Mb). In Population 86, two QTL were found, SW4.1^{86} at the proximal end of Pv04 (.73-1.2 cM) and SW4.2^{86} within the interval 51.1-63.9 cM. The SW4.1^{86} QTL near the top of Pv04 was between 2.2-2.33 Mb, had an R^2 of 8% and decreased seed weight by 0.34 g when the B14311 allele was present. The SW4.2^{86} QTL contained two local peaks, but was considered as a single QTL because the local peaks did not have a sufficiently large drop in LOD between them. This QTL spanned the physical interval 2.75-3.59 Mb, explained about 9.6% of the phenotypic variation and decreased seed weight by 0.38 g when the allele was contributed by the B14311 parent.

A SW QTL (SW5.1^{86}) was found on Pv05 in Population 86 that explained 9% of the phenotypic variation and increased seed weight by 0.36 when the B14311 allele was present. This QTL had a peak LOD of 4.1 that mapped between 126.9-133.3 cM (35.96-36.79 Mb).

A minor effect SW QTL (SW7.1^{76}) on Pv07 in Population 76 explained just 6% of the total phenotypic variation and affected seed weight by 0.5 g. It was located over a large map distance from 83.1-109.5 cM, but a relatively small physical distance from 4.25-4.39 Mb.

Another minor effect SW QTL from Population 76 was found on Pv08, named SW8.1^{76}. This QTL had a relatively high LOD score of 5.6 and mapped near the end of the chromosome from 151.1-158.4 cM (62.06-62.27 Mb). This QTL explained 8% of the phenotypic variation and decreased seed weight by 0.45 g when donated by the B14311 parent.

Days to Flowering (DF)

Despite a lack of phenotypic variation in days to flowering amongst the parents of both populations [Table 2; Table 3], days to flowering QTL were found in Population 76 on Pv07, Pv08, and Pv11 [Table 8].

A QTL on Pv07 (DF7.1[76]) contained two local peaks and reached the significance threshold with a LOD score of 3. Markers flanking the region had physical positions of 27.48-30.85 Mb. This QTL only explained 5% of the phenotypic variation and affected flowering by 0.25 days.

The DF8.1[76] QTL Pv08 had a highly-significant peak with a LOD score of 10. The QTL mapped to a tight mapping interval of 145.5-147.0 cM, corresponding to a physical interval of 60.97-61.30 Mb. This QTL explained 20% of the phenotypic variation and the B14311 allele delayed flowering by approximately half of a day.

Like the DF7.1[76] on Pv07, the DF11.1[76] QTL peak on Pv11 was barely significant with a LOD score of 2.99 from 143.7-144.0 cM. The DF11.1[76] QTL influenced days to flowering by 0.25, explained only 5% of the phenotypic variation, and mapped to the tight physical region from 51.95-51.96 Mb.

Days to Maturity (DM)

Days to maturity QTL were found on Pv02 in Population 76 and on Pv04 and Pv11 in Population 86 [Table 8].

The DM2.1[76] QTL on Pv02 was found in Population 76 from 110.1-113.2 cM (31.67-33.65 Mb). It had a peak LOD of 4.69, an R^2 of 11%, and the B14311 allele hastened maturity by 0.43 days.

A DM QTL with a tightly peaked LOD score of 4.29 was detected near the top of Pv04 from 0.73-1.2 cM (2.2-2.41 Mb). This QTL (DM4.1[86]) explained 11.6% of the phenotypic variation and hastened maturity by 0.39 days when the allele was contributed by B14311.

On Pv11, the DM11.1[86] QTL explained 8% of the phenotypic variation and delayed maturity by 0.35 days when the B14311 allele was present. It was located over a mapping interval of 0-10.8 cM, which corresponded to a modest physical interval of 49.59-51.12 Mb [Table 8].

Canopy Height (HT)

Several minor-effect QTL for canopy height were found above the significance threshold, but all were population-dependent. Population 76 had QTL on Pv02, Pv03, Pv07, and Pv11, with the B14311 parent generally increasing height, whereas Population 86 had QTL on Pv01, Pv04, and Pv08, with the B4311 parent decreasing height in all instances.

The Pv01 QTL (HT1.1[86]) was located over a large interval from 43.6-63.7 cM (1.29-2.85 Mb). It had an R^2 of 6.7% and affected height by 0.34 cm.

The HT2.1[76] QTL on Pv02 explained 10% of the phenotypic variation and was the only HT QTL in Population 76 where the B14311 allele decreased height by 0.45 cm. It was positioned over the large interval 95.3-110.1 cM, corresponding to 25.39-31.67 Mb.

QTL HT3.1[76] on Pv03 contained a peak that barely reached the significance threshold with a LOD score of 3.08. It explained just 6% of the phenotypic variation and was located from over the interval 92.4-108.8 cM (10.69-11.25 Mb).

The HT4.1[86] QTL on Pv04 had a LOD peak of 10.62 located at 50.86 cM. It explained 17% of the phenotypic variation and influenced height by approximately 0.5 cm. It mapped to an interval from 44.49-52.13 cM and the flanking markers had physical positions from 2.55-2.89 Mb.

On Pv07, the HT7.1[76] QTL had a peak LOD score of 3.07 that barely reached the significance threshold. It was located over 5.85-9.43 cM (0.65-0.91 Mb), only explained 5% of the phenotypic variation, and changed height by 0.34 cm.

The HT8.1[86] QTL on Pv08 had the highest peak LOD score of any HT QTL detected in this study at 12.79. This QTL explained 22% of the phenotypic variation and the B14311 parent lowered height by nearly 0.6 cm. It was located at the top of the chromosome from 0-12.88 cM, which corresponded to a physical interval of 0.374-1.50 Mb.

The HT11.1[76] QTL on Pv11 had a peak LOD of 4.6 at 144.34 cM. This peak lay within the interval 144.33-149.57 cM (52.16-52.65 Mb). It was responsible for 9% of the phenotypic variation and impacted height by 0.42 cm.

Desirability Score (DS)

Desirability score QTL were population-dependent; Population 76 had QTL on Pv04 and Pv08, while Population 86 had QTL on Pv02 and Pv09. In all cases, the B14311 parent contributed a negative additive effect.

A QTL on Pv02 named DS2.1[76] barely met its permutation threshold with a LOD score of 3.0. It was located from 50.6-51.1 cM (5.86-7.1 Mb), explained 7% of the phenotypic variation, and affected DS by 0.14.

Similarly, the DS4.1[86] QTL on Pv04 explained just 7% of the phenotypic variation and influenced the desirability by 0.13. This QTL was located on the interval 51.1-52.1 cM (2.75-2.89 Mb).

The strongest QTL for desirability score (DS8.1[86]) was detected at the proximal end of Pv08 from 0-12.9 cM, which corresponded to a physical interval of 0.37-1.5 Mb. This QTL had a peak LOD of 6.7, explained over 14% of the phenotypic variation, and affected the score by 0.19.

On Pv09, the DS9.1[76] QTL had a peak located at 14.9 cM with a LOD score of 4.92. It fell within the interval 14.9-15.8 cM, corresponding to a small 7.70-7.79 Mb physical region. This QTL explained 11% of the phenotypic variation and impacted desirability score by 0.18.

Ozone Bronzing (BRZ)

In Population 76, QTL for foliar bronzing were discovered on Pv06 and Pv08, while in Population 86, QTL for foliar bronzing were discovered on Pv05, Pv07, and Pv09. A noticeable, yet insignificant peak was also identified in Population 76 near the same physical region as the Pv07 BRZ QTL in Population 86.

The BRZ5.1[86] QTL on Pv05 plateaued at a LOD score of 3.2 over the map interval 174.7-188.5 cM, corresponding to a small physical interval of 39.24-39.34 Mb. This QTL explained about 7% of the phenotypic variation, and the B14311 allele reduced bronzing ratings by 0.19.

The BRZ6.1[76] QTL in Pv06 plateaued over a large map distance containing few markers (0.51-22.9 cM), although the physical positions of the flanking markers were located at a smaller interval from 12.21-13.75 Mb. The QTL explained just 6% of the phenotypic variation and bronzing ratings were reduced by 0.25 when the B14311 allele was present.

The BRZ7.1[86] QTL on Pv07 was the most significant QTL detected for this trait. It had a peak LOD of 6.6 at 46.1 cM, explained 17% of the phenotypic variation, and the B14311 allele reduced bronzing ratings by 0.3. This QTL was located within the map interval 46.1-49.8 cM and was flanked by markers ss715649276 and ss715646465 (3.99-4.17 Mb).

The BRZ8.1[76] QTL was detected near the end of Pv08 over the interval 144.8-158.4 cM, corresponding to a physical interval of 60.71-62.27 Mb. This QTL explained 10% of the phenotypic variation and the B14311 allele increased bronzing ratings by 0.31.

The BRZ9.1[86] QTL was located on Pv09 and was significant from 12.2-19.2 cM. This small map interval corresponded to a small physical interval of 31.40-33.35 Mb that was flanked by markers ss715646279 and ss715645629. The QTL explained about 7% of the phenotypic variation and the B14311 allele increased bronzing ratings by 0.18.

Molecular Marker Analysis

Parental lines were screened with seven InDel markers with v2.1 physical positions near COL QTL located on Pv08 [Figure 14A]. This region had low marker coverage, but high LOD scores. The markers spanned an approximate physical interval of 5.43 to 7.16 Mb in the v2.1 genome. InDel markers screened were: NDSU_IND_8_5.4417 (between 5.43-5.50 Mb), NDSU_IND_8_6.0169 (between 5.95-6.27 Mb), NDSU_IND_8_6.2923 (between 6.27-6.44 Mb), NDSU_IND_8_6.6519 (near 6.71 Mb), NDSU_IND_8_6.6880 (between 6.71-6.99 Mb), NDSU_IND_8_6.7497 (between 6.99-7.04 Mb), NDSU_IND_8_7.0078 (near 7.16 Mb). None of the markers showed a polymorphism between B14311 and both of the other parents. The B12724 product was polymorphic to products from B14311 and Zenith for marker NDSU_IND_8_6.2923. The product from Zenith was polymorphic to products from B14311 and B12724 for marker NDSU_IND_8_7.0078. Markers NDSU_IND_8_6.6880 and NDSU_IND_8_6.7497 were heterozygous amongst all parental lines.

Parental lines were also screened with six InDel markers with v2.1 physical positions near COL QTL located on the distal end of Pv11 [Figure 14B]. The markers spanned an approximate physical interval of 50.68 to 53.17 Mb in the v2.1 genome. InDel markers screened were: NDSU_IND_11_47.0739 (between 50.68-50.75 Mb), NDSU_IND_11_47.7708 (between 51.50-51.53 Mb), NDSU_IND_11_47.9412 (between 51.72-51.75 Mb), NDSU_IND_11_48.4937

(between 52.23-52.48 Mb), NDSU_IND_11_48.7818 (between 52.53-52.54 Mb), and NDSU_IND_11_49.5223 (between 52.96-53.17 Mb). The B14311 product was polymorphic to the other parents' products for markers NDSU_IND_11_47.0739 (50.68-50.75 Mb), NDSU_IND_11_47.7708 (51.50-51.53 Mb), and NDSU_IND_11_49.5223 (52.96-53.17 Mb). Based on the physical positions of the flanking BARCBean6k_3 SNPs, these three InDel markers lie outside the most-significant COL QTL interval from 52.16-52.84 Mb.

DISCUSSION

Post-processing color retention is an important quality trait in black beans. To identify genomic regions controlling this trait, black bean RIL populations were developed. Two half-sibling populations were selected for genetic mapping, Population 76 and Population 86. These populations shared a common female parent, B14311, that had poor post-processing color retention. Populations derived from this MSU breeding line were purposefully selected over the other similarly poor-canning breeding lines because B14311 had greater seed coat integrity when canned, reflected in higher appearance ratings [Table 1]. Having acceptable canned appearance (e.g. no splits) was important to the study design in order to minimize the effect of pigment leaching due to mechanical breakdown or splitting of the seed coat. This also mitigates potential bias amongst reviewers who may unintentionally confound appearance and color instead of treating them as distinct characteristics. Both B12724 and Zenith exhibit a similar level of superior post-processing color retention, yet possess different genetic backgrounds that may uniquely contribute to color retention [Supplemental Figures 4 and 5]. Results from this study reveal both population-specific QTL and those shared across populations, meaning that the superior-canning parents contain both unique and shared QTL for post-processing color retention.

Comparing Methods of Quantitative Color Measurement

The MSU dry bean breeding program has traditionally measured canned bean color objectively with a Hunter Labscan XE spectrophotometer to obtain *L**, *a**, and *b** values. Of these measurements, *L** was thought to be the closest representation of black bean darkness, but has been shown in this study to be less accurate at describing perceived darkness than previously thought. The Hunter Labscan XE is easy-to-use, quick, and has been used for many years, but comes with some disadvantages. For one, this instrument can only measure a small portion of a canned sample at a time (4.4 cm diameter), which may not be representative of the entire sample. Furthermore, this instrument was designed to measure color according to human perception, so glare and glossiness are included in measurements. While rinsing the canned samples before imaging is important to remove brine, excess water on the seed coat surface creates glare that introduces varying amounts of reflection on each sample. To address these drawbacks associated with the current methodology, a new protocol was developed to measure CIE *L**, *a**, and *b** values from digital images of canned beans using ImageJ software (Schneider et al., 2012). CIE *L**, *a**, and *b** values were different between measurement methods, which was to be expected due to the difference in sample size and confounding effect of glare. Using the same CIELAB color space for color components derived from both Hunter Labscan and ImageJ analysis enabled comparison between the two methods to determine which was more effective at measuring canned black bean color.

The Hunter Labscan XE spectrophotometer and ImageJ software measured color components with varying degrees of labor input and accuracy. When canned bean samples underwent machine phenotyping after reviewer evaluation, capturing digital images took longer than measuring CIELAB values from the Hunter Labscan spectrophotometer. This was mostly due

to the preparation time involved in "plating" the sample for photographing. After rinsing, each canned bean sample was placed on a tray where it was manually distributed to a uniform depth that completely covered the bottom of the tray. The plated sample then had to be precisely positioned beneath the digital camera to fill the viewing area. Before taking the photograph, the can code for each sample had to be manually entered so that each image file was accurately recorded. In practice, the digital imaging process took about 30-40 seconds per sample, compared to approximately 20 seconds per sample from the Hunter Labscan. Once images were collected in a folder, the ImageJ macro took 5-10 seconds to process a single image before automatically moving on to the next one. A major advantage of digital images is that they hold a large amount of spatial information that can be used in a myriad of downstream analyses (e.g. creation of custom color spaces, segmentation of beans, and measurement of distances and angles).

Quantitative color components of L^*, a^*, and b^* were similarly correlated to visual color ratings in both populations [Table 4]. Color values derived from the ImageJ macro were more accurate and precise compared to those from the Hunter Labscan across years and populations [Table 4; Figure 11]. Regardless of measurement method, the b^* component was most strongly correlated with visual color ratings, though b^*I values from the ImageJ macro were more strongly correlated with visual color ratings than the b^*H values from the Hunter Labscan. Considering only measurements from 2017, the L^*H values from the Hunter Labscan were strongly correlated with visual color ratings (r = -0.73 to -0.83), but were less descriptive than the L^*I values from the ImageJ analysis (r = -0.87 to -0.91). Using two years of ImageJ-derived L^*I values further improves the correlation with visual color ratings (r = -0.87 to -0.91), though the two-year averages of L^*I did not reach the strength of the two-year averages of b^*I (r = -0.93 to -0.96). The Hunter

Labscan-derived *L**H value has typically been treated as the standard for quantitative color measurement of black beans, a practice that needs to be re-visited in light of these findings.

Instead of relying on *L** values, *b** values should be used to measure perceived seed coat darkness of canned black beans. Considering only measurements from 2017, the Hunter Labscan *b**H values had a very strong correlation (r = -0.82 to -0.93) with visual color ratings, but did not exceed the ImageJ *b**I correlation coefficients of -0.91 to -0.93. When two years of ImageJ *b**I values were used, there was a nearly perfect negative correlation with visual color ratings (r = -0.93 to -0.96). In reality, the *b**I value may be a more accurate measurement of canned bean color than the consensus reviewer rating. Although reviewers were trained and provided physical copies of the 1-5 visual color scale, their ratings of canned beans may be influenced by the rating experience of the reviewers, brine on the surface of the seed coats, or fatigue and loss of focus from the large number of samples. All of these aforementioned issues can be mitigated through machine-derived measurements of color.

Interestingly, *L**, *a**, and *b** were moderately correlated with reviewers' visual appearance ratings across populations and measurement methods [Table 4]. This could be caused by reviewers confounding color ratings with appearance ratings or by the machines measuring the exposed cotyledon tissue of split beans, thereby increasing the mean brightness of the digital image. Regardless of the potential cause, *L** values were more strongly correlated to visual appearance ratings than *a** and *b** values. The ImageJ *L**I values were similarly correlated to visual appearance ratings (r = -0.46 to -0.52) than the Hunter Labscan *L**H values (r = -0.42 to -0.49). While simple measurements from machine vision can provide unbiased and repeatable measurements of canned color, further improvements are required to more accurately describe canned appearance. Research by Mendoza et al. (2017) utilized digital images of canned black

beans and brine to develop partial least square regression (PLSR) models for prediction of reviewers' color and appearance ratings. In the study, digital images of canned beans underwent an additional segmentation process that separated the canned beans from the background. Information from the segmented beans was combined with several other image features into PLSR models for color and appearance. The models returned correlation coefficients of 0.873 to 0.937 for color ratings and 0.806 to 0.871 for appearance ratings. However, implementation of the methodology used by Mendoza et al. (2017) in breeding programs may be hindered by the lack of a comprehensive, easy-to-use phenotyping pipeline. Overall, research from the present study has shown that color retention of canned black beans can be accurately measured by CIE *L**, *a**, and *b** values generated after minimal post-processing of digital images. Using ImageJ to measure color components from digital images is a more reliable method than the traditional Hunter Labscan, and *b** values are more strongly correlated with reviewers' visual color ratings than *L** values.

Heritability Estimates of Canning Quality Traits

Heritability estimates of canned bean color retention have not been previously reported. Broad-sense heritabilities of reviewer color ratings were high in both Population 76 (0.87) and Population 86 (0.91) [Figure 11]. This suggests that a consensus approach can be effective at phenotyping this trait. However, CIELAB color components as measured by ImageJ analysis were also highly heritable in these populations, with *b**I and *L**I having heritabilities near 0.90 in both populations. These results validate anecdotal evidence suggesting that color retention is moderately to highly heritable in the MSU dry bean breeding program (J. Kelly, pers. comm.).

Furthermore, color retention heritabilities estimated by objective measurements can meet or exceed those provided by subjective reviewer ratings.

Populations 76 and 86 both had appearance heritabilities near 0.58 [Figure 11], which is nearly identical to the 0.58 estimated by Walters et al. (1997) for visual appearance ('VIS') in navy beans. However, Posa-Macalincag et al. (2002) estimated the narrow-sense heritability of canned kidney bean appearance as approximately 0.84.

Estimates of broad-sense heritabilities for canned bean texture ranged from 0.46 to 0.67 in Populations 86 and 76, respectively. These were comparable to the estimate of 0.64 determined by Walters et al. (1997).

Broad-sense heritabilities of washed and drained weight were very low [Figure 11]. In Population 76, the heritability was just 0.06 and in Population 86, the heritability was 0.30. Contrastingly, Walters et al. (1997) determined a moderate heritability of 0.67 for washed and drained mass, an equivalent measurement of washed and drained weight.

QTL Nomenclature

QTL are named according to the guidelines proposed by Miklas and Porch (2010). Briefly, each trait is assigned a two- to three-letter abbreviation. Common abbreviations are listed in a separate document (unpublished), but canning quality QTL are uncommon traits so new trait abbreviations were created for this study. After the abbreviation, the linkage group or chromosome number is listed. This study mapped QTL on each of the 11 *Phaseolus vulgaris* chromosomes so all numbers 1 through 11 are used. Specific QTL within a linkage group are noted successively by adding a '.' followed by a number. Precedence is given toward previously discovered QTL. Lastly, QTL are tagged according to the population in which they were discovered. This study uses "76"

for QTL found in Population 76 (B14311/Zenith) and "86" for QTL found in Population 86 (B14311/B12724). These population descriptors are useful for consistency within the context of this study, but may need to be changed to "BZ" (B14311/Zenith) and "BB" (B14311/B12724) in future publications to maintain compliance with nomenclature guidelines.

QTL Mapping of Post-Processing Color Retention

A complete list of QTL for post-processing color retention is located in Table 6. QTL graphs from Population 76 are located in Figure 12, and QTL graphs from Population 86 are located in Figure 13.

Color Ratings (COL)

QTL for visual color ratings were detected on five chromosomes: Pv02, Pv03, Pv05, Pv08, Pv10, and Pv11. As expected, QTL contributed by the B14311 parent decreased color ratings, except in a single instance. Many significant, yet small-effect QTL were detected across and within the two RIL populations. Previous studies by Wright and Kelly (2011) and Cichy et al. (2014) also measured canned black bean color, but used methods that differed from this study. Wright and Kelly (2011) used HunterLAB color space *L* value as a proxy for color, while Cichy et al. (2014) used a 1-7 hedonic ("liking") scale where reviewers rated bean color retention according to preference.

The COL2.1^{76} QTL on Pv02 was detected by color ratings from 2017 and the two-year average (COL_2017 and COL_2YA, respectively) and was specific to Population 76. This QTL influenced color ratings only slightly, but co-localized with QTL for quantitative color measurements like *L**2.1^{76} and *b**2.1^{76} which were both detected by ImageJ software in 2017.

LOD peaks for the Hunter Labscan *L**H and *b**H values also co-localized to this region, but were below the significance threshold. The 2017 ratings mapped to a smaller interval than the two-year average ratings, but both shared a terminal flanking marker, ss715651061 located at 17.24 Mb. Neither Wright and Kelly (2011), nor Cichy et al. (2014) detected COL QTL on Pv02, but co-localization with quantitative color measurements supports the detection of a population-specific COL QTL in this region.

COL QTL on Pv03 were detected in both populations, but in different years for each. In Population 76, the COL3.1^{76} QTL was detected from 2016 and the two-year average color ratings (COL_2016 and COL_2YA, respectively). Both measurements were found within the same, small physical interval of 2.02-2.43 Mb and had small effects on color retention, explaining just 6% of the phenotypic variation and affecting color ratings by approximately 0.15. This COL3.1^{76} QTL co-localized with QTL for ImageJ color measurements. A QTL for *L**I from 2017 RILs (*L**3.1^{76}) mapped to the same region, while a QTL for *b**I from 2016 (*b**31.^{76}) mapped slightly upstream.

In Population 86, a 2017 COL QTL was detected near the top of Pv03 from 1.19-1.30 Mb, named COL3.1^{86}. This QTL had an extremely small effect on color retention, but co-localized with the APP3.1^{86} QTL detected from 2016 and two-year average and the *b**3.1^{86} QTL from ImageJ software in RILs grown in 2017. Another small effect COL QTL (COL3.2^{86}), this one from 2016, was detected near the distal end of the chromosome from 47.28-50.39 Mb. Both of these COL QTL in Population 86 mapped to regions of sparse marker coverage, and overall Population 86 had fewer markers mapping to unique positions on Pv03 (n=22) than Population 76 (n=50). For example, COL3.2^{86} at the distal end of Pv03 had a left-flanking marker that mapped to 102.4 cM (47.28 Mb) and the next closest upstream marker was located at 75.4 cM (37.2 Mb).

The COL5.1[86] QTL on Pv05 mapped to a small physical interval from 38.84-38.92 Mb and contributed very little to color retention. The QTL mapped within the interval for the two-year average color rating, though the two-year average color ratings fell just short of the permutation LOD threshold. Interestingly, COL5.1[86] was the only COL QTL that mapped independently of quantitative color measurements, which somewhat weakens its validity.

A highly-significant COL QTL was detected across populations on Pv08. In Population 76, the COL8.1[76] QTL was detected by color ratings from 2016, 2017, and the two-year average and mapped to a tight region near 53 cM, although the 2016 ratings extended further upstream than the others. Each of these individual measurements contributed a moderate amount toward color retention by explaining 12-16% of phenotypic variation and influencing color ratings by approximately 0.25 on the 1-5 rating scale. Although this region spanned a large map distance of nearly 50 cM, the physical interval was 1.53-7.25 Mb. Only four markers were located within that interval, and there was a large 4 Mb gap from 1.53-5.86 Mb without any markers. This means that this region may actually contain several QTL if mapping resolution was increased. Nevertheless, this region was a "hotspot" for post-processing color retention because QTL for all quantitative color measurements like *L**, *a**, and *b** co-localized in or near this interval.

Likewise, the COL8.1[86] QTL from Population 86 was detected by ratings from 2016, 2017, and the two-year average (COL_2016, COL_2017, and COL8_2YA, respectively) and mapped to the interval 15.32-60.37 cM, which corresponded to a physical region of 1.57-53.68 Mb. This COL QTL explained a similar amount of phenotypic variation as those identified in Population 76, with nearly identical effect sizes. However, COL8.1[86] spanned a much larger interval overall. The region encompassed by COL_2017 in Population 86 had the smallest physical interval from 1.57-6.27 Mb, which fits within the interval of the Population 76 COL8.1[76] QTL (1.53-7.25 Mb). As

mentioned before, this region of Pv08 contained major gaps in marker coverage. In Population 86, there were no markers from 1.58-6.27 Mb or from 6.27-53.59 Mb, which contributed to the large QTL interval. Like Population 76, quantitative color measurements co-localized with COL QTL in this population, as well.

Overall, the region from 1.5-7.25 Mb on Pv08 was found to be a key determinant of post-processing color retention in both populations. The Co-4 locus conditioning resistance to anthracnose (*Colletotrichum lindemuthianum*) resides within this interval at approximately 2.8 Mb (Oblessuc et al., 2015), and the complex C locus [C R Prp] also maps in this region (McClean et al., 2002). Interestingly, all loci within the complex C locus are involved in pigmentation: C determines seed coat patterning (Prakken, 1974); R determines red seed coat coloration (Prakken, 1974); and Prp determines pod pigmentation (Bassett, 1994). While the complex C locus is an important determinant of pigmentation of dry beans, it is unknown if it also plays a role in seed coat color retention of canned beans. In any case, this region of Pv08 is crucial to dry bean pigmentation and canned color retention, but additional markers are needed to determine the actual physical location of the COL QTL identified in this study.

Genes within the 1.5-7.3 Mb QTL interval were examined using PhytoMine (DOE-JGI and USDA-NIFA, http://phytozome.jgi.doe.gov/phytomine/begin.do) to generate a list of 599 genes (data not shown). Genes encoded for unknown proteins, leucine-rich repeat proteins, and transferases involved in flavonoid biosynthesis, among many others. Gene ontology (GO) terms were generated [Supplemental Figure 7]. However, deducing the biological mechanism(s) behind post-processing color retention was beyond the scope of this study.

A single QTL on Pv10 (COL10.1^{86}) was found in Population 86 that had a very minor effect on color retention. It was noteworthy because it was the only COL QTL found in this study

where the B14311 parent contributed a beneficial allele for color retention. COL10.1^{86} co-localized with QTL for *a**, APP, and TXT over a 12 cM map interval corresponding to a smaller physical interval of 42.22-43.29. A QTL for *L** (*L**10.1^{86}) mapped just upstream.

COL QTL on Pv11 were major determinants of post-processing color retention and were identified across populations and instruments. In Population 76, the COL11.1^{76} QTL detected by ratings from 2016, 2017, and the two-year average mapped to a region near the distal end of the chromosome from 52.16-52.84 Mb. These individual regions explained a range of phenotypic variation from 8.4-14.3% and influenced color ratings by 0.19-0.25. QTL for quantitative color measurements of *L** (*L**11.1^{76}) and *b** (*b**11.1^{76}) co-localized to this region as well, showing that the COL QTL at this location can be detected consistently by machine phenotyping.

In Population 86, the COL11.1^{86} QTL mapped to the end of Pv11 just like the COL11.1^{76} QTL from Population 76. This COL11.1^{86} QTL was detected across all years (2016, 2017, and the two-year average), and had associated LOD scores greater than any other color ratings in the study, at 10.55, 12.74, and 12.96, respectively. Individually, they explained 19-22% of the phenotypic variation and influenced color ratings by nearly a third of a score. These regions associated with yearly color ratings all mapped to the exact same physical interval from 52.47-52.84 Mb, which lies within the interval of the COL11.1^{76} QTL detected in Population 76. In Population 86, COL11.1^{86} co-localized with all measurements of *L** (*L**11.1^{86}) and *b** (*b**11.1^{86}), with the exception of *L**H measured by the HunterLab spectrophotometer on 2017 RILs. Taken together, the Pv11 COL QTL represent the most influential source of color retention detected in this study.

Previous work by Cichy et al. (2014) also revealed QTL associated with color on Pv11. In that study, significant QTL for hedonic color ratings in 2010 and 2011 mapped near the top of the chromosome and co-localized with QTL for putative *L**H, *a**H, and *b**H values measured by a

Hunter Labscan spectrophotometer. Their QTL cluster was reported as a 0-13 cM interval at the top of chromosome 11. However, the mapping positions must have been mistakenly inverted, since physical positions of the flanking SNPs are actually located around 52-53 Mb in the v2.1 dry bean genome. The SNP marker M27933 was closest to QTL for color retention in both years, *L**H in 2011, and *b**H in both years. No sequence data was provided for M27933, but a BLAST query of adjacent markers D05338 and D30369 placed them at 52.61 and 53.47 Mb, respectively. Disregarding the published genetic positions in favor of the latest physical positions, the QTL identified by Cichy et al. (2014) are in the same physical region as the co-localizing QTL for color retention identified in the present study.

This region of COL QTL co-localization on the distal end of Pv11 is nearby several loci conferring disease resistance in dry beans. Slightly upstream of the QTL, the 51-52.2 Mb interval contains many genes encode leucine-rich repeat proteins, sulfotransferases, and albumins (data not shown). Furthermore, the anthracnose resistance locus Co-2 (Geffroy et al., 1998) maps to the distal end of chromosome Pv11, along with loci involved in rust resistance, Ur-3, Ur-6, Ur-11, and Ur-Dorado (Miklas et al., 2006). Of these loci, physical positions have been determined for Ur-11 near 51.93 Mb (McClean, unpublished) and Ur-3 from 46.97-47.01 Mb (Hurtado-Gonzales et al., 2017).

The region from 52.41-52.85 Mb was screened for candidate genes using PhytoMine (DOE-JGI and USDA-NIFA, http://phytozome.jgi.doe.gov/phytomine/begin.do). This region contained genes encoding unknown proteins, aspartyl proteases, and annexins [Supplemental Table 2]. The biological role of aspartyl proteases is not completely understood, but their ability to hydrolyze proteins may contribute to protein storage or disease resistance (Simões and Faro, 2004). An *Arabidopsis thaliana* homolog, CDR1, was found to confer resistance to *Pseudomonas*

syringae (Xia et al., 2004). According to PhytoMine results, putative aspartyl protease genes Phvul.011G208100 and Phvul.011G208900 had perfectly correlated expression levels with paralogs related to pectin breakdown: Phvul.007G202000, Phvul.007G271650, and Phvul.007G271600. Annexins are thought to have several cellular functions, ranging from Ca^{2+}-dependent membrane binding (Gerke et al., 2005) to polar growth and stress response (Konopka-Postupolska et al., 2011). However, the focus of the present study was toward genetic mapping of post-processing color retention; the biological mechanism behind the phenotype was not explored. Additional experiments like microscopy, NIL development, metabolomic analyses, RNA-Seq, and comparative mapping may be useful in deducing a biological mechanism behind post-processing color retention.

*L**

*L** values describe the luminosity of a sample on a 0-100 scale where 0 is black and 100 is white. *L** values from a Hunter Labscan XE spectrophotometer (Hunter Associates Laboratory Inc., Reston, VA) have traditionally been used by the MSU breeding program as a quantitative method of black bean post-processing color and are referred to in this study as *L**H. While these *L**H values are able to detect phenotypic variation in canned black beans, the measurement process can create artifacts (F. Mendoza, pers. comm.). In an attempt to improve color measurements, an experimental macro was developed for ImageJ that measured *L**, *a**, and *b** values from processed digital images of canned beans. QTL for *L** values from the digital imaging software (*L**I) were more detectable and co-localized more frequently with QTL for color retention than QTL for *L**H values from the Hunter LabScan XE spectrophotometer. Hunter Labscan-derived *L**H QTL from this study can be compared to previous studies by and Wright and Kelly (2011) and Cichy et al.

(2014) where both authors used a Hunter Labscan XE to measure QTL for 'Color' and '*L**' respectively.

The *L**2.1[76] QTL was detected by ImageJ analysis and located on Pv02 in Population 76. This QTL had a small, yet detectable effect on *L**I and co-localized with QTL detected by visual color rating (COL2.1[76]) and *b**I (*b**2.1[76]). Overlapping this QTL, LOD scores were elevated for *L**H and *b**H values measured by the Hunter Labscan, but were below the significance threshold.

Another lone *L** QTL (*L**3.1[76]) mapped to a 2.02-2.43 Mb physical interval on Pv03. This QTL co-localized with COL3.1[76] and *b**3.1[76]. The *L**3.1[76] QTL was significant, but did not have a major effect on *L** value due to a low R^2 of 6.2% and low additive effect of 0.40. Wright and Kelly (2011) detected a putative *L**H QTL on Pv03 in 2005 that accounted for 21% of the phenotypic variation, but the nearest marker (F9R1.150) was not given a physical position.

QTL *L**5.1[86] mapped to a physical region of 34.33-35.96 Mb on Pv05. The peak LOD was located toward the right side of interval above the significance threshold. While this QTL appeared to be near the region associated with the two-year average color ratings (COL_2YA), they are actually separated by 40 cM (4 Mb). Wright and Kelly (2011) identified a putative *L**H QTL on Pv05 that was found in years 2005 and 2006. The 2005 QTL was nearest marker IAC96 and explained 10% of the phenotypic variation, while the 2006 QTL was nearest marker F22R1.400 and explained 13% of the phenotypic variation. A BLAST query of the SSR marker IAC96 against the v2.1 dry bean genome gave a top hit at the physical position near 3.2 Mb, which is very distant from the physical interval of the *L**5.1[86] QTL detected in the present study. In the Cichy et al. (2014) study, putative *L**H QTL ('L*10' and 'L*11') also mapped to Pv05 where they explained approximately 10% of the phenotypic variation and co-localized with QTL for *b** and color ratings. The DArT marker sequences from the Cichy et al. (2014) study were provided by K. Cichy and

used in BLAST queries against the v2.1 dry bean genome. Based on the nearest marker, D33359, the 'L*10' QTL on Pv05 maps to 8.42 Mb, and the closest flanking markers are located several Mb away at 5.4 and 18.0 Mb. The nearest marker to the 'L*11' QTL on Pv05 was D23441 at 106.28 cM (18 Mb); however, this same genetic position was shared with markers that have physical positions as far away as 16.76 and 27.6 Mb. The physical intervals from the Cichy et al. (2014) study did not match the physical interval of the *L**5.1[86] QTL detected in the present study. Both studies have large gaps on Pv05 that require additional markers to more accurately determine QTL locations.

*L** QTL were found on Pv08 in both populations. As mentioned in the COL QTL section, *L** QTL co-segregated with COL QTL around a 1.53-7.25 Mb region in both populations. Surprisingly, in Population 76, the region associated with the Hunter Labscan-derived values (*L**H_2017) was more tightly co-localized with COL_2017 and COL_2YA, while the region associated with ImageJ-derived values (*L**I_2016 and *L**I_2017) co-localized with color ratings from 2016 (COL_2016). In Population 86, ImageJ-derived measurements from both years (*L**I_2016 and *L**I_2017) tightly co-localized with the COL8.1[86] QTL, while the Hunter Labscan-derived values were unable to detect the QTL.

Three separate *L** QTL were detected by ImageJ software that mapped to Pv09. In Population 76, *L**9.1[76] and *L**9.2[76] were detected in the absence of QTL for COL or other color measurements. While both QTL occupied tight intervals, *L**9.1[76] had a tight LOD peak from 10.30-10.32 Mb, and *L**9.2[76] had a more gradual peak from 13.55-13.71 Mb. The *L**9.1[76] QTL had a higher LOD score, more explained phenotypic variation, and larger additive effect. In Population 86, *L**9.1[86] had a very small effect on the *L** value and was noteworthy as the only *L** QTL where the B14311 allele had an additive effect that darkened *L** values.

Pv10 contained the *L**10.1[86] QTL that mapped to a very small physical interval from 41.96-42.01 Mb. However, its LOD scores had an extremely gradual ascent over a 50 cM region where no markers were present, which cast a level of uncertainty on its actual position. It was located slightly upstream of QTL for color rating (COL10.1[86]) and *a** value (*a**10.1[86]).

*L** QTL were found on Pv11 in both populations. In Population 76, the *L**11.1[76] QTL was comprised of regions from individual years (*L**I_2016, *L**I_2017, and *L**H_2017) that all explained less than 10% of the phenotypic variation, but neatly co-localized with the COL11.1[76] QTL near 52.47-52.87 Mb. In Population 86, *L**11.1[86] was comprised of ImageJ-derived *L**I_2016 and *L**I_2017 regions that mapped to a 400 kb interval containing COL11.1[86] and *b**11.1[86] QTL within its 52.47-52.87 Mb region. Wright and Kelly (2011) detected a putative *L**H QTL ('Color') on Pv11 in 2007 near marker F5R10.475 that explained 9% of the phenotypic variation. Cichy et al. (2014) detected putative *L**H QTL ('L*10' and 'L*11') near the proximal end of Pv11 that both explained approximately 25% of the phenotypic variation. However, re-locating the Cichy et al. (2014) *L** QTL to their correct physical positions at the distal end of Pv11 places them near 52.6-53.4 Mb in the v2.1 genome, which is similar to the physical region of the COL, *L**, and *b** QTL detected in the present study.

*a**

QTL for *a** were almost exclusively located on Pv08 where they co-localized with QTL for color ratings, *L** values, and *b** values across populations. Other instances on Pv03 and Pv05 show regions of elevated, but insignificant LOD scores that co-localized with *L** QTL.

In Population 76, the *a**8.1[76] QTL was detected by all measurements of *a** that mapped within a region from 0.48-7.25 Mb. Strangely, the *a** measurements from 2016 ImageJ (*a**I_2016)

mapped to two peaks on either end of the major color-determining region, but the first peak was more in-line with other color measurements and was subsequently the one selected for visualization in MapChart. Aside from the 2016 measurements, *a**I_2017 and *a**H_2017 explained a surprisingly large amount of phenotypic variation for the trait; values of R^2 for *a**I_2017 and *a**H_2017 were 27.0% and 21.4%, respectively. In Population 86, the *a**8.1^{86} QTL was also detected across all *a** measurements, but mapped more closely with other color values than *a**8.1^{76} from Population 76 [Figure 13H]. Again, the range of explained phenotypic variation for the underlying regions associated with *a**8.1^{86} was moderately large, from 17-21.4%. Interestingly, *a**H measurements from the Hunter Labscan explained this trait as well as *a**I measurements from the ImageJ software, which was not the case for QTL derived from the other color component measurements *L** and *b**. However, the *a** value does not seem to be as strongly correlated with visual color ratings as *L** and *b**. [Table 4].

A small-effect *a** QTL (*a**10.1^{86}) was detected by ImageJ in 2017 RILs on Pv10. The QTL mapped to a small physical interval of 42.22-42.29 Mb that was in between an *L** QTL from 2016 (*L**10.1^{86}) and a COL QTL from 2017 (COL10.1^{86}). Despite having minor effects, both the *a** QTL and the COL QTL were the only instances of the B14311 parent contributing a beneficial additive effect on color retention. The B14311 *a**10.1^{86} allele decreased the *a**I value by 0.31, while the COL10.1^{86} allele improved color ratings by 0.15.

Cichy et al. (2014) mapped putative *a**H QTL ('a10' and 'a11') on Pv07 and Pv11 to regions containing clusters of QTL involved in color ratings. Interestingly, their *a**H QTL consistently mapped adjacent to, not inside, these clusters, a pattern that was also observed for the *a**H QTL detected in this study on Pv08.

*b**

QTL for *b** were detected on Pv02 in Population 76 and Pv03, Pv08, and Pv11 in both populations [Table 6]. The *b** value measures color on a scale of blue to yellow, where smaller values are more blue and larger values are more yellow.

On Pv02, a single small-effect *b** QTL from 2017 (*b**2.1^{76}) co-localized with QTL for color ratings (COL2.1^{76}) and *L** (*L**2.1^{76}). The Hunter Labscan measurement of *b**H was unable to detect a significant QTL, though elevated LOD scores were found over the same interval, similar to what happened with *L**H from the Hunter Labscan [Figure 12B]. This is evidence that ImageJ software is generally more accurate at detecting color retention QTL than the spectrophotometer.

A *b** QTL mapped near the top of chromosome Pv03 in both populations. Across the two populations, both *b** QTL shared the flanking marker ss715646396 at 1.19 Mb. In Population 76, *b**3.1^{76} mapped to an interval of 1.00-1.19 Mb slightly upstream of QTL for COL and *L**. In Population 86, *b**3.1^{86} tightly co-localized with QTL for COL and APP over the interval 1.19-1.30 Mb. The *b**3.1^{76} QTL from Population 76 explained nearly double the phenotypic variation compared to the *b**3.1^{86} QTL from Population 86, but both had very small effects on this trait.

Although Cichy et al. (2014) detected a putative *b**H QTL ('b*11') on Pv05 that co-localized with QTL for color, *L**, and anthocyanin content of canned beans, no *b** QTL were found on Pv05 in the present study.

Significant LOD scores for all measurements of *b** were detected on Pv08, resulting in *b** QTL for both populations. Both the *b**8.1^{76} QTL from Population 76 and the *b**8.1^{86} QTL from Population 86 co-localized with QTL for color ratings, *a** values, and *L** values. In Population 76, the *b** QTL mapped more closely to the COL QTL than the *L** QTL, while in Population 86, both *b** and *L** QTL mapped to the exact same intervals. Due to the absence of markers in the regions

1.58-6.27 Mb and 6.27-53.59 Mb, it remains unclear if the *b** QTL on Pv08 are identical or if there are multiple QTL contributing to *b** in this interval.

Pv11 contained *b** QTL that were detected by all methods and years, similar to Pv08. These QTL, *b**11.1^{76} in Population 76 and *b**11.1^{86} in Population 86, had component regions explaining a range of phenotypic variation from 11.4% to over 27%. The individual measurements associated with *b** in this region mapped to a similar or smaller interval than COL or *L** QTL. Even *b**H values from the HunterLab spectrophotometer were strongly significant, though they explained a lesser amount of phenotypic variation compared to the *b**I QTL from the ImageJ analysis. QTL for *b** were mapped in both populations and co-localized with color ratings to a small physical interval on the distal end of Pv11.

Cichy et al. (2014) also identified putative *b**H QTL on Pv11 ('b*10' and 'b*11') that co-localized with QTL for color ratings ('color10' and 'color11') and putative *L**H values ('L*10' and 'L*11'). In that study, the putative *b**H QTL explained a larger amount of phenotypic variation (33-44%) than determined in the present study. As mentioned previously, these QTL were all placed near the top of Pv11, but should be re-positioned to the distal end of the chromosome.

QTL Mapping of Other Canning Quality Traits

A complete list of QTL for appearance, washed and drained weight, and texture is located in Table 7. QTL graphs from Population 76 are located in Figure 12, and QTL graphs from Population 86 are located in Figure 13.

Appearance Ratings (APP)

Recently, new methods of canning evaluation have been implemented by the MSU breeding program that differ from previous canning quality studies. Walters et al. (1997) and Posa-Macalincag et al. (2002) used a 1-7 hedonic "liking" scale to evaluate canned navy beans and kidney beans, respectively. In Wright and Kelly (2011), canned bean appearance ('visual appearance') was rated by reviewers on a 1-7 hedonic "liking" scale that also factored in the perceived darkness of the seed coat color. Similarly, reviewers from Cichy et al. (2014) rated canned bean appearance ('overall appearance') on a 1-7 hedonic "liking" scale that also included seed coat color. In the present study, appearance and color were rated as distinct characteristics on 1-5 scales based on seed coat integrity and perceived darkness of seed coat color, respectively [Figure 4].

In most instances, APP QTL typically mapped independently of COL QTL and were detected on many chromosomes. Furthermore, the percentage of phenotypic variation explained by any one APP QTL was always less than 10%. Interestingly, the poor-canning parent B14311 was responsible for improved appearance ratings in four out of nine detected APP QTL.

APP QTL on Pv02 differed across years, populations, and physical positions, which weakens their reliability. For example, APP2.1^{76} was detected in 2017 and mapped in isolation near 40 Mb, while APP2.1^{86} was detected in 2016 and co-localized with QTL for 2016 texture (TXT2.1^{86}) and 2016 washed and drained weight (WDW2.1^{86}) near 4 Mb. The co-localization of these QTL in Population 86 lends validity to this region because the QTL involved could realistically be explaining a shared physiological mechanism. When the allele was contributed by B14311, APP2.1^{86} decreased appearance scores (more split beans), TXT2.1^{86} decreased texture

scores (mushier beans), and WDW2.1[86] increased washed and drained weights (more hydrated beans).

Appearance ratings for 2016 and the two-year average were combined into the APP3.1[86] QTL that co-localized with QTL for COL and *b** on Pv03. These APP QTL mapped to a relatively tight physical interval of 1.2-1.3 Mb, but explained very little phenotypic variation.

An APP QTL on Pv04 (APP4.1[86]) mapped to a small physical interval from 2.75-2.89 Mb. Unexpectedly, it co-localized with QTL for several agronomic traits: height, desirability score and seed weight. A QTL for 2016 washed and drained weights did not meet the permutation threshold, but showed a region of elevated LOD scores mapping slightly upstream of the APP4.1[86] QTL.

Pv05 contained an APP QTL (APP5.1[76]) over a 300 kb interval from 4.47-4.75 Mb. This APP QTL mapped in complete isolation of other QTL. Wright and Kelly (2011) also detected an appearance QTL on Pv05 that shared its nearest marker IAC96 with a putative *L**H QTL (reported as 'Color' by the authors). Querying the primer sequence of IAC96 against the v2.1 dry bean genome placed it near 3.2 Mb, which is moderately close to the physical position of the APP5.1[76] QTL detected in this study.

The APP6.1[86] QTL on Pv06 mapped to the small physical interval of 28.97-29.04 Mb. The LOD scores for this QTL fluctuated around 2.4 LOD over the entire chromosome outside of the peak. Only 8 markers mapped to unique genetic positions on Pv08, so this QTL is somewhat questionable. In the Cichy et al. (2014) study, the authors found an isolated, yet highly significant APP QTL on Pv06 that explained nearly 20% of the phenotypic variation. A BLAST query of the closest DArT marker D17956 against the v2.1 dry bean genome returned a top hit near 18.74 Mb, which is approximately 10 Mb upstream of the APP QTL identified in the present study.

Two independent APP QTL (APP8.1[76] and APP8.2[76]) mapped to Pv08 in Population 76. APP8.1[76] co-localized with the washed and drained weight QTL WDW8.1[76] and also with QTL for agronomic traits BRZ, DF, SY, and SW. The co-localization of APP QTL and agronomic QTL was also observed on Pv04. These QTL may be located in gene-rich areas or exhibit pleiotropic effects. APP8.2[76] co-localized to the top of Pv08 along with many QTL related to color retention: color ratings, *L** values, *a** values, and *b** values. Color ratings and appearance ratings were weakly positively correlated (r = 0.24) [Table 4] and reviewers may inadvertently rate severely split beans with poor color ratings. Conversely, if the canned color is dark black, cotyledon staining may conceal splits and reviewers may be more "forgiving" with appearance ratings.

Wright and Kelly (2011) detected a 'visual appearance' QTL on Pv08 that was nearest marker TE1/6.340. This marker was also the closest marker for a putative *L**H QTL ('Color') and a seed weight QTL ('seed size'). While both studies were somewhat limited by low marker number, it is very interesting to observe that canned appearance has co-segregated with seed weight in three different instances.

The APP10.1[86] QTL mapped to Pv10 and co-localized with QTL for texture (TXT10.1[86]) and color (COL10.1[86]) near the distal end of the chromosome. Although the map intervals between markers in this region were large, APP10.1[86] mapped to a relatively small region from 42.22-44.22 Mb. This was just the second instance of APP QTL co-localizing with COL QTL, which supports the practice of rating both traits separately.

Cichy et al. (2014) identified an APP QTL on Pv11 ('app11') that mapped near putative QTL for COL, *L**H, *a**H, and *b**H at the proximal end of the linkage group. In this case, co-localization of visual appearance and color ratings may have been confounded by rating color according to "liking" and not strictly darkness of the seed coat.

Texture (TXT)

Six TXT QTL were identified across four chromosomes. Two minor-effect TXT QTL on Pv02 mapped to opposite ends of the chromosome. When donated by B14311, TXT2.1[76] increased texture measurements by 2.64 kg, while the TXT2.1[86] decreased texture measurements by 2.25 kg. Both were detected in just one population-year and explained very little phenotypic variation, casting doubt on their validity.

The TXT5.1[76] QTL on Pv05 was comprised of texture measurements from 2016 and 2017 that mapped to the exact same physical positions from 27.70-36.79 Mb. Both TXT_2016 and TXT_2017 had strong LOD scores, and the reproducibility across years lends credence to the QTL. Unfortunately, there was a large gap in marker coverage from 27.72-35.96 Mb, which would need to be addressed in future mapping projects.

Wright and Kelly (2011) detected a TXT QTL on Pv06 near marker F8R2.350, which was not given a physical position. Cichy et al. (2014) detected a consistent TXT QTL over two years that co-localized with other canning quality measurements at the Asp locus on Pv07.

TXT9.1[76] mapped to a large region on Pv09 from 16.26-39.61 cM (7.87-13.55 Mb). This interval overlapped with QTL for agronomic desirability scores and *L**I values measured by ImageJ software. It was not surprising for this TXT QTL to overlap with unrelated QTL because of its large interval.

The TXT10.1[86] QTL on Pv10 was detected in 2016 and mapped to a small interval at the distal end of the chromosome from 43.29-44.22 Mb. TXT10.1[86] co-localized with QTL for APP (APP10.1[86]), COL (COL10.1[86]), and also 2017 texture measurements that showed an elevated LOD score, but did not reach the significance threshold. Taking into account the high LOD score

(11.3), large R^2, small physical interval, and potential for replication across years, the region near TXT10.1[86] may be useful in future research on the trait.

Washed and Drained Weight (WDW)

Only two WDW QTL were detected in this study, which was partly expected due to minimal variation for this trait in the parental lines. WDW2.1[86] mapped to the top arm of Pv02 and spanned a very large physical interval from 3.90-30.15 Mb. As mentioned in the discussion section for APP QTL, WDW2.1[86] co-localized with QTL for APP and TXT. On Pv08, a WDW QTL (WDW8.1[76]) also mapped near an APP QTL (APP8.1[76]). Again, this co-localization is discussed in the previous section pertaining to APP QTL. Finer mapping and more contrasting phenotypes would be needed to refine the WDW QTL identified in this study.

Wright and Kelly (2011) detected WDW QTL on Pv03 and Pv10, but did not provide physical positions. Cichy et al. (2014) detected QTL for a trait called washed drained coefficient ('WDC'). This trait was calculated by dividing a canned sample's WDW by the dry weight of the sample before canning. Two WDC QTL ('wdc10' and 'wdc11') mapped to the Asp locus on Pv07 along with many other QTL involved in water uptake. Parental lines in the present study both contained the recessive *asp* allele (matte seed coat) and the Asp locus was not a factor in this study.

QTL Mapping of Agronomic Traits

This study was mostly concerned with canning quality traits so agronomic traits were only measured to identify RILs that might be useful for breeding goals. Parents were not greatly different for agronomic traits, and many of these traits are under complex genetic control, which limited detection of significant QTL. Furthermore, agronomic traits were only measured in one

environment (SVREC) and year (2017) with significant, but mostly negligible effects. Considering these major limitations, small-effect QTL detected for agronomic traits may not be compelling enough for further validation. A complete list of QTL for agronomic traits is located in Table 8. QTL graphs from Population 76 are located in Figure 12, and QTL graphs from Population 86 are located in Figure 13.

Seed Yield (SY)

Although the parents differed slightly in seed yield, it was not a mapping priority in this study. Two SY QTL were detected on Pv08, each with high LOD scores, but a small effect on the trait. $SY8.1^{76}$ mapped to the distal end of the chromosome in Population 76, while $SY8.1^{86}$ mapped to the proximal end of the chromosome in Population 86. Interestingly, $SY8.1^{86}$ co-localized to the exact same interval as QTL for DS ($DS8.1^{86}$) and HT ($HT8.1^{86}$). In Population 86, $SY8.1^{76}$ mapped to a tight window from 60.07-60.56 Mb that may be of interest if genomic selection methods gain popularity in dry bean breeding. While both QTL are currently impractical as breeding targets, they may be useful to document for future agronomic studies.

Seed Weight (SW)

Measurements of seed weight can vary drastically for a genotype, even within years or replications. The parents in this study varied only slightly for seed weight in 2016, but were consistent with previous years' seed weights. Zenith generally had the largest seed size, followed by B12724, and then B14311 [Table 2; Table 3].

A major SW QTL on Pv03 was found in both populations. $SW3.1^{76}$ and $SW3.1^{86}$ explained a large amount of phenotypic variation (R^2 = 22.7 and 12.2, respectively) and mapped to a similar

physical interval. SW3.1[76] had a physical region of 11.47-11.82 Mb, and SW3.1[86] had a physical region of 3.82-12.30 Mb that included the region of the SW QTL in Population 76. These may be the same QTL detected across populations, although there were large gaps in marker coverage over the SW3.1[86] interval, which limited resolution.

SW QTL on Pv04 were also detected in both populations. SW4.1[76], SW4.1[86], and SW4.2[86] had smaller effects than the SW QTL on Pv03, but still mapped closely together. Although the two SW QTL from Population 86 appear separate based on a LOD graph, these may actually be the same QTL. They were separated by a single marker ss715646243, that upon further inspection was separated from neighboring markers by a 20 cM gap despite differing in physical positions of less than 100 kb. This is evidence that the marker did not fit well at its mapped location. When the marker was temporarily excluded, the two peaks were joined, but the right-most peak from SW4.1[86] was still the most prominent.

A SW QTL on Pv05 (SW5.1[86]) mapped to a relatively tight peak from 35.96-36.79 Mb. It had a minor effect on the trait and mapped to a similar location as *L**5.1[86].

The QTL SW7.1[76] was detected in the interval from 4.25-4.39 Mb on Pv07. It spanned a large map distance that was slightly downstream of a QTL for canopy height, HT7.1[76].

A SW QTL on Pv08 (SW8.1[76]) was found over a 200 kb region near 62 Mb. This QTL was part of a cluster that contained agronomic QTL (SY, DF, BRZ) and canning quality QTL (APP, WDW), all detected from RILs grown in 2017. Wright and Kelly (2011) found putative SW ('seed size') QTL on Pv05, Pv06, Pv08, and Pv11 that were mostly year-dependent. Cichy et al. (2014) found three putative SW ('seedwt') QTL on Pv08 over two years that mapped in isolation from each other. DArT markers near the Cichy et al. (2014) SW QTL on Pv08 were BLASTed against the v2.1 dry bean genome and returned top hits from 61-62 Mb, which is in the same physical

region as SW8.1[76] detected in the present study. As exemplified in other studies, SW QTL are strongly year-dependent. SW QTL from this study were detected in just one year and require further validation.

Days to Flowering (DF)

QTL were detected for DF on three chromosomes, only in Population 76. These QTL should be regarded as somewhat questionable, given that in 2017 the parents differed in flowering date by just one day. Both DF7.1[76] and DF11.1[76] were barely significant, with LOD scores of 3.04 and 2.99, respectively. DF7.1[76] mapped in isolation, while DF11.1[76] mapped just upstream of a large cluster that contained QTL for HT and many color retention-related measurements. Wright and Kelly (2011) were able to detect a DF QTL on Pv11 in all three years that consistently mapped with marker F17R8.420, but comparison of between the studies is impossible due to lack of physical positions.

The DF QTL DF8.1[76] was the most interesting (and unexpected), given its high percentage of explained phenotypic variation (R^2=20%). As mentioned previously, this QTL mapped from 60.97-61.30 Mb along with QTL for SY, SW, BRZ, APP, and WDW. This QTL was not detected in the black bean RIL population of Wright and Kelly (2011), nor in the Middle American GWAS performed by Moghaddam et al. (2016). However, Kamfwa et al. (2015) detected a significant SNP for DF, ss715646088, reported at a physical position of 57.73 Mb. This physical position is in the vicinity of the 60.97-61.30 Mb region for DF8.1[76], but the v2.1 dry bean genome places it even closer at 61.16 Mb. Although SNP ss715646088 was not included in linkage mapping, its updated physical position is directly between the flanking markers for DF8.1[76], strongly validating the QTL.

Days to Maturity (DM)

There was very little phenotypic variation for days to maturity among the parents (and RILs) in this study. [Table 2; Table 3]. Nevertheless, a few QTL were detected that should be treated with an appropriate amount of skepticism.

QTL DM2.1[76] co-localized with the height QTL HT2.1[76]. Both of these traits are involved in agronomic adaptation and may suggest a pleiotropic effect between them. This QTL was not found in other studies.

A DM QTL on Pv04 (DM4.1[86]) mapped in isolation to a small physical region from 2.2-2.4 Mb and had the largest effect for a DM QTL by explaining 11.6% of the phenotypic variation. Moghaddam et al. (2016) found significant SNPs for DM near the top of Pv04. In their supplementary material, a DM SNP on Pv04 mapped to 1 Mb, but other significant SNPs near the proximal end of Pv04 were apparent in Supplementary Figure S1f showing Manhattan plots of days to maturity among beans from the Mesoamerican subpopulation.

A DM QTL on Pv11 (DM11.1[86]) was significant over a broad mapping interval, but small physical interval from 49.59-51.12. It is important to note that the Population 86 Pv11 linkage group was not representative of the entire chromosome; the first marker was located at 49.59 Mb and the last marker was located at 52.88 Mb. Moghaddam et al. (2016) detected GWAS peaks and candidate genes associated with DM on Pv11 at 4.3 Mb and 41 Mb. According to the authors, the peak at 4 Mb was detected in Nebraska and Michigan, while the peak at 41 Mb was detected in North Dakota. Additional mapping with a more complete linkage map is required to validate DM11.1[86].

Canopy Height (HT)

Many small-effect QTL for canopy height were detected for the 2017 field season. Normally, this would be expected since height is widely considered to be under polygenic control. However, in 2017 the parental lines only differed in height by 0.5 cm, as estimated on a per-plot basis. Lack of phenotypic variability calls into question the validity of these QTL. Most HT QTL in this study had an R^2 below 10%; QTL explaining more than 10% phenotypic variation will be otherwise noted.

The QTL, HT1.1[86] mapped in isolation to an interval of 1.30-2.85 Mb on Pv01. A few somewhat-significant peaks were observed in this region according to the first Manhattan plot in the Supplementary Figure S1r of Moghaddam et al. (2016). Other studies did not detect significant markers on Pv01.

On Pv02, HT2.1[76] mapped to a broad 6 Mb interval from 25-31 Mb that co-localized within a QTL for days to maturity, DM2.1[76]. This QTL has not been supported by other studies.

Pv03 contained a HT QTL (HT3.1[76]) from 10.69-11.25 Mb that mapped upstream of the SW3.1[76] QTL at 11.47-11.82 Mb. A significant peak was also detected near the top of the Manhattan plot for the Michigan location in the third plot of the Moghaddam et al. (2016) Supplementary Figure S1r.

On Pv04, HT4.1[86] explained over 17% of the phenotypic variation for height in Population 86. Interestingly, this QTL co-localized with other 2017 QTL for seed weight, agronomic desirability score, and canned appearance ratings. It mapped to the physical interval 2.55-2.89 Mb, which is extremely close to 2.9 Mb where Moghaddam et al. (2016) found a GWAS peak by excluding shorter statured beans with type 1 (determinate) architecture. This height QTL is the most likely to be validated in other studies.

A HT QTL on Pv07 (HT7.1[76]) was barely significant in this study and mapped to the proximal end of Pv07. This location does not match the position of the strong peak detected at 46 Mb by Moghaddam et al. (2016).

The HT8.1[86] QTL was detected within the physical interval 0.37-1.5 Mb on Pv08 that explained over 21% of the phenotypic variation. According to the third Manhattan plot of Supplementary Figure S1r in Moghaddam et al. (2016), a significant peak for height was detected near the top of Pv08. Interestingly, this peak was only observed with Mesoamerican genotypes grown in Michigan, suggesting a QTL x environment interaction.

On Pv11, HT11.1[76] mapped to a 52.16-52.65 Mb region at the end of the chromosome along with QTL for DF and nearly every measurement of canned bean color. Moghaddam et al. (2016) described a height QTL at 43 Mb that contained several SNPs within a gene having pleiotropic effect on architectural traits. Wright and Kelly (2011) also detected a height QTL on Pv11 in 2004 linked that was linked to marker F17R8.420. Neither of these previously documented QTL give strong support to HT11.1[76] given its position.

Desirability Score (DS)

The agronomic desirability score is an in-house measurement used to guide breeding decisions. The score is visually assigned on a per-plot basis and factors in a variety of agronomic characteristics from a 'breeder's eye' perspective. In 2017, the parents earned very similar desirability scores and few QTL were detected for this trait in the mapping populations. The B14311 contributed a negative additive effect in all cases. Most DS QTL mapped to relatively tight physical positions.

On Pv02, DS2.1[76] mapped near 51 cM (5.86-7.10 Mb), which was upstream of QTL for color measurements that had left-most flanking markers near 54 cM (11.03 Mb). B14311 was responsible for negative effects toward both DS and COL, and the proximity of the QTL suggests a degree of genetic linkage.

DS4.1[86] on Pv04 co-localized with QTL for height, seed weight, and canned appearance ratings to a 2.75-2.89 Mb interval. The B14311 allele lowered values for all co-localizing traits except canned appearance ratings. This region appears to be important for both agronomic and quality traits, but values of R^2 were generally low, which may prohibit effective molecular markers.

DS8.1[86] mapped to a physical interval from 0.37-1.50 Mb and neatly co-localized with QTL for yield (SY8.1[76]) and height (HT8.1[86]). This was the strongest DS QTL detected according to its LOD score of 6.7 with an R^2 value of nearly 20%. This region is clearly important for key agronomic traits and suggests the desirability score can be a useful tool when rated with a skilled 'breeder's eye.'

A DS QTL on Pv09 (DS9.1[76]) had a tight LOD peak at 7.70-7.79 Mb. This QTL overlapped with TXT9.1[76] and was also near QTL for *L** values, although these traits would seem to be unrelated.

Ozone Bronzing (BRZ)

Foliar bronzing attributed to ozone damage was observed in the 2017 field trials, however bronzing did not appear to be evenly distributed across the field. Since bronzing ratings were taken on each plot, they were included in QTL analysis in the spirit of curiosity. Several population-specific bronzing QTL from the 2017 growing season were detected. To the best of the author's

knowledge, this is the first time this trait has been mapped in dry beans, though validation in different years and populations is required. Ratings for foliar bronzing may have been confounded by CBB lesions, which may explain the proximity of bronzing QTL with known CBB QTL.

QTL BRZ5.1[86] mapped to a very tight physical interval on Pv05 from 39.24-39.34 Mb. This QTL co-localized within a QTL for canned bean color (COL5.1[86]) and explained very little phenotypic variation.

In Population 76, BRZ6.1[76] was distributed across 0.5-22.9 cM. This genetic distance covered over half of the poorly-covered linkage group representing Pv06 (40.4 cM in length). This QTL explained minimal phenotypic variation (R^2 = 6.3%).

The most-significant BRZ QTL (BRZ7.1[86]) resided on Pv07. With a peak LOD of 6.6 and a high R^2 of 30%, this QTL mapped to the tight physical interval from 3.99-4.17 Mb. This location is relatively close to the *Phs* locus that encodes for phaseolin, the main seed storage protein in dry beans (Ma and Bliss, 1978). The Phs CDS from black beans 'Jamapa' and 'Puebla 152' identified by Diniz et al. (2014) were BLASTed against the v2.1 dry bean genome. Both queries returned top hits at approximately 5.026 Mb near an annotated *P. vulgaris* gene, Phvul.007G059700.1. This gene encodes a Cupin family seed storage protein that also has an *Arabidopsis thaliana* homolog, At3g22640. Several CBB QTL have been mapped near the *Phs* locus in three independent studies: (Nodari et al., 1993b; Miklas et al., 1996; Jung et al., 1996). Interestingly, this bronzing QTL on Pv07 is extremely close to a CBB resistance locus near 4 Mb that is currently being fine-mapped (P. Miklas, pers. comm.). This may suggest that bronzing ratings in the present study were confounded by presence of CBB or that there is a similar physiological response to these stresses.

In Population 76, BRZ8.1[76] co-localized with QTL for APP, SY, SW, and DF at the proximal end of Pv08 near 61 Mb, however it did not explain much phenotypic variation. A major

CBB resistance QTL, SU91 is also located on Pv08. Shi et al. (2012) found a soybean predicted protein homolog (UDP-glycosyltransferase) associated with a tepary bean EST near the SU91 locus. A BLASTp query of the predicted protein sequence against the v2.1 dry bean genome returned top hits for genes Phvul.008G290200.1 and Phvul.008G290300.1 located at 62.81 Mb and Phvul.008G26200.1 and Phvul.008G262100.1 located at 60.89 Mb. Recently, Lobaton et al. (2018) have developed a KASP marker for the SU91 locus that has a physical position near 62.95 Mb in the v2.1 genome (B. Raatz, pers. comm.). Although the BRZ8.1[76] QTL is in the same general region as the SU91 QTL, they are most likely different QTL since the B14311 allele for BRZ8.1[76] was associated with increased foliar bronzing, whereas the B14311 allele for SU91-CG11 was associated with a reduction in foliar symptoms of CBB.

A BRZ QTL on Pv09 was also detected (BRZ9.1[86]) that mapped between 31.40-33.38 Mb. Although no published bronzing QTL were found in this region, two CBB QTL have been mapped to this chromosome from mapping populations BAT93/Jalo EEP558 (Freyre et al., 1998; Gepts, 1999; Geffroy et al., 2000) and Belnab-RR-1/A55 population (Ariyarathne et al., 1999; Jung et al., 2003; Fourie et al., 2004). These CBB QTL were not given physical positions to compare with BRZ9.1[86].

Common Bacterial Blight Resistance (CBB)

Parental lines used in this study exhibited slight, but significant phenotypic variation in CBB resistance in 2017 [Table 2]. No CBB QTL were detected, though several BRZ QTL were detected near previously-identified CBB QTL. Parents were genotyped with the codominant SCAR marker SU91-CG11 developed by Shi et al. (2012) from the SCAR marker SU91 first published by Pedraza García et al. (1997). This marker is tightly linked to a major locus governing

CBB resistance that was derived from tepary bean (*Phaseolus acutifolius*) PI 319433 via common bean XAN 159 (Miklas et al., 2003). Parental lines B12724 and B14311 were shown to have the product size corresponding to CBB resistance, while Zenith did not [Supplemental Figure 8]. Although SU91 has been mapped to Pv08, no CBB QTL were detected by SNP markers on Pv08 in Population 76 (B14311/Zenith) that should have segregated at the SU91 locus. Absence of CBB QTL might be explained by mild or uneven disease pressure in the field, confounding effects of ozone-induced foliar bronzing, and the paucity of markers on the Pv08 linkage map (n=20).

Molecular Marker Analysis

Parental lines were genotyped with InDel markers developed by Moghaddam et al. (2014) that were located near COL QTL on Pv08 [Figure 14A]. This region contained QTL for post-processing color retention, *L**, *a**, and *b**, but all spanned a large physical interval from approximately 1.5-7 Mb. The region from 5.43-7.13 Mb was selected for exploratory genotyping because several highly-significant SNPs mapped to the region. Seven markers polymorphic across navy, black, and light red kidney market classes were selected based on their proximity to the physical positions of SNPs included on the BARCBean6k_3 BeadChip. InDel markers from non-black market classes were included because there were not many in the region, with only five InDel markers spanning the 6.00 to 7.00 Mb interval. The B14311 parent was not polymorphic to both parents for any marker; however, B12724 and Zenith were polymorphic to the other genotypes for markers NDSU_IND_8_6.2923. and NDSU_IND_8_7.0078. Although none of the tested markers were able to discriminate B14311 against the other parents, fine-mapping the 1.5-7 Mb interval could refine detected QTL or uncover multiple QTL.

Parental lines were also genotyped with InDel markers developed by Moghaddam et al. (2014) that were located near COL QTL at the distal end of Pv11 [Figure 14B]. Six markers polymorphic in the black bean market class were selected based on their proximity to the physical positions of SNPs included on the BARCBean6k_3 BeadChip. The B14311 parent was polymorphic to the other parents for three of these markers, though these three markers were located outside of the physical region from 52.16-52.84 Mb. Within the region of interest, B14311 had the same product size as Zenith and B12724, except for marker NDSU_IND_11.487818 where B14311 and Zenith had a larger product size than B12724. Additional InDel markers developed by Moghaddam et al. (2014) are polymorphic in other market classes and are located near this region, but their usefulness in genotyping black beans for color retention is untested.

CONCLUSIONS

Black beans are an increasingly popular dietary option for US consumers. In order to meet consumer demand for a bean that remains dark black after processing, it is necessary to explore improvements on both phenotypic and genetic aspects of this trait. In this study, a novel and comprehensive method of phenotyping canned bean color via digital image analysis was developed. Extracting CIELAB color values from canned bean photographs eliminated many confounding factors associated with traditional phenotyping such as high reflectance, small sample size, and time-consuming (and often highly-variable) reviewer ratings. On the genetic side, the RIL mapping populations that were developed through this research were used to identify regions in the dry bean genome associated with color retention. Many small-effect QTL were detected for black bean post-processing color retention, supporting previous research that this trait is under polygenic control. Several of these QTL co-localized to the same genomic regions on Pv03, Pv08,

and Pv11 across years, phenotyping methods and populations, while other QTL were population- or year-dependent and require additional validation. QTL for other canning quality traits and agronomic traits were also detected.

In most cases, marker development for these QTL is impractical for two reasons: most QTL explained only a small amount of the total phenotypic variation and lack of markers limited the resolution of mapping intervals. That said, if markers were to be developed for color retention QTL, they may be useful to screen early generation material for canning quality potential. Those regions on Pv03, Pv08, and Pv11 where visual color ratings co-localize with quantitative color values would be the best areas to target for molecular marker development. The region from 52.5-52.9 Mb on Pv11 shows potential for molecular marker development due to a high R^2 and small physical interval. Alternatively, genomic selection for canning quality traits would be an interesting continuation of this research, as many small-effect loci are involved that may not always be detectable from year to year. This study gives dry bean breeders and scientists a better understanding of the genetics controlling color retention so that they can generate darker-colored processed black beans to meet the growing consumer demand.

APPENDIX

Table 1. Agronomic and canning quality traits guiding parental selection for black bean RIL populations.

		Agronomic Traits								Canning Traits			
Parent	**Pedigree**	**SY**	**SW**	**DF**	**DM**	**HT**	**DS**	**CBB**	**ANT$_{73}$**	**COL**	**APP**	**WDW**	**TXT**
		(kg/ha)	(g)	(days)	(days)	(cm)	(1-7)	(1-5)	(R/S)	(1-5)	(1-5)	(g)	(kg)
B14303	B09197/B11334	3571	18.9	45	96	51	5.8	1	R	1.7	2.8	256.8	40
B14302	B09197/B11334	3386	18.2	45	97	51.3	5.8	1	R	2.2	2.5	256.3	36
B14311	B11338/B10241	2907	18.7	45	96	48.3	5	1	S	1.7	3.7†	255.4	34
Zenith	B04644/ZORRO	2803	22.4	44	96	50.5	4.8	4.3	R	5*	4.2	255.8	29
B12724	B09184/B09135	2638	21.2	45	101	49.3	3.5	1.8	R	4.8*	3.5	257.4	35
(ZORRO)	B00103*/X00822	2211	19.4	45	97	50.3	4.3	4.3	S	3.5	3.3	262.2	36
	Mean (n=30)	2856	20.3	44.9	95.8	48.5	4.1	3					
	LSD (.05)	424	1.1	0.7	1.7	1.5	0.6	0.7					
	CV (%)	12.6	4.5	0.9	1.5	2.7	13.4	18.8					

Parental lines are bolded and shaded according to color of their canned seed. *Zenith and B12724 have excellent color retention, while breeding lines B14302, B14303, and B14311 have poor color retention. †B14311 has reasonably high appearance ratings. Zorro is a black bean variety widely-grown in Michigan. Data: MSU 2015 Standard Black Bean Yield Trial.
Abbreviations: SY: seed yield, SW: 100-seed weight, DF: days to flowering, DM: days to maturity, HT: canopy height, DS: desirability score, CBB: common bacterial blight resistance, ANT$_{73}$: resistance to anthracnose race 73, COL: canned color rating, APP: canned appearance rating, WDW: washed and drained weight; TXT: texture; BRZ: ozone bronzing (not measured in 2015)

Table 2. Phenotypic variation in canning quality and agronomic traits for Population 76 (B14311/Zenith).

Population 76	B14311	Zenith		RILs		
Trait	Mean	Mean	*p* value	Mean ± SD	Range	*p* value
Color (1-5)[1]	1.37	4.91	<.0001	3.13 ± 0.56	1.54-4.55	<.0001
*L**I[2]	17.07	10.49	<.0001	12.72 ± 1.27	9.6-16.41	<.0001
*a**I	7.93	3.49	<.0001	5.34 ± 0.91	3.16-7.72	<.0001
*b**I	9.18	1.90	<.0001	5.85 ± 1.22	2.39-8.71	<.0001
*L**H	19.08	12.64	N/A	16.32 ± 1.34	11.89-20.11	N/A
*a**H	8.50	3.29	N/A	5.73 ± 0.81	4.13-8.46	N/A
*b**H	6.62	1.42	N/A	3.65 ± 0.93	1.54-6.24	N/A
Appearance (1-5)[3]	2.81	3.91	0.0012	3.12 ± 0.33	2.28-3.88	<.0001
Washed and drained weight (g)[4]	255.2	261.3	0.2783	258.6 ± 4.2	247.9-274.8	0.3268
Texture (kg)[5]	54.9	43.8	0.0078	53.2 ± 4.4	41.5-62.1	<.0001
Seed yield (kg/ha)	3328	2977	0.761	3073 ± 351	1326-3776	0.0013
Seed weight (g/100 seeds)	20.7	25.1	<.0001	21.9 ± 1.5	18.2-25.6	<.0001
Days to flowering	46	47	0.0769	46.8 ± 1	45-50	<.0001
Days to maturity	93	95	0.0491	93.2 ± 1.2	91-98	<.0001
Lodging (1-5)	1	1	1	1 ± 0	1-1	1
Height (cm)	46.5	46.5	1	46.1 ± 1.3	43-49	<.0001
Desirability score (1-5)	4.5	4.5	1	4.4 ± 0.5	3-6	0.0141
Bronzing (1-5)	2	2	0.392	2.3 ± 0.9	1-5	<.0001
CBB (1-5)	1	3	0.0026	2.2 ± 0.7	1-4.5	<.0001

Means of canning traits are listed as two-year averages, except for Hunter Labscan-derived *L**H, *a**H, and *b**H values which were only measured on 2017 samples. Means of agronomic traits are listed as plot averages from 2017.

[1] Color ratings of canned beans were averaged across reviewers on 2016 and 2017 samples.

[2] *L**, *a**, *b**: CIELAB color values, where *L** measures lightness, *a** measures greenness/redness, *b** measures blueness/yellowness. 'I' indicates values measured by ImageJ analysis and 'H' indicates values measured by a Hunter Labscan.

[3] Appearance ratings of canned beans were averaged across reviewers on 2016 and 2017 samples.

[4] Washed and drained weights were measured after briefly rinsing canned beans under cool water.

[5] Texture was measured as the peak force (kg) required to compress a 100 g sample of canned beans.

Table 3. Phenotypic variation in canning quality and agronomic traits for Population 86 (B14311/B12724).

Population 86	B14311	B12724		RILs		
Trait	Mean	Mean	*p* value	Mean ± SD	Range	*p* value
Color (1-5)[1]	1.58	4.93	<.0001	3.25 ± 0.64	1.72-4.96	<.0001
*L**I[2]	15.97	10.23	<.0001	12.11 ± 1.4	8.4-15.95	<.0001
*a**I	6.60	2.90	<.0001	4.63 ± 0.86	2.2-6.68	<.0001
*b**I	8.42	1.53	<.0001	5.3 ± 1.42	1.73-8.54	<.0001
*L**H	16.44	9.95	N/A	11.92 ± 1.5	8.56-16.45	N/A
*a**H	6.87	3.51	N/A	4.69 ± 0.97	1.88-7.05	N/A
*b**H	8.52	1.92	N/A	5.26 ± 1.46	1.51-8.77	N/A
Appearance (1-5)[3]	3.15	3.72	0.06	3.22 ± 0.4	2.19-4.01	<.0001
Washed and drained weight (g)[4]	250.2	255.6	0.7409	255.7 ± 4.5	244.6-266.8	0.7922
Texture (kg)[5]	61.8	63.0	0.8382	59.5 ± 5.7	44.8-72.3	0.0001
Seed yield (kg/ha)	3346	3690	0.5704	3315 ± 314	2285-3959	0.0442
Seed weight (g/100 seeds)	21.8	23.1	0.1257	22.3 ± 1.1	19.7-26.2	<.0001
Days to flowering	45	47	0.1098	46 ± 0.9	44-49	0.001
Days to maturity	93	93	1	93.3 ± 1.1	91-96	<.0001
Lodging (1-5)	1	1	1	1 ± 0	1-1.5	0.5
Height (cm)	47	47	1	46.7 ± 1.2	44-49.5	<.0001
Desirability score (1-5)	5.5	5	0.3744	4.6 ± 0.5	3.5-6	0.0233
Bronzing (1-5)	3	1	0.0039	1.6 ± 0.6	1-3	0.0001
CBB (1-5)	N/A	N/A	N/A	N/A	N/A	N/A

Means of canning traits are listed as two-year averages, except for Hunter Labscan-derived *L**H, *a**H, and *b**H values which were only measured on 2017 samples. Means of agronomic traits are listed as plot averages from 2017.

[1] Color ratings of canned beans were averaged across reviewers on 2016 and 2017 samples.

[2] *L**, *a**, *b**: CIELAB color values, where *L** measures lightness, *a** measures greenness/redness, *b** measures blueness/yellowness. 'I' indicates values were measured by ImageJ analysis and 'H' indicates values were measured by a Hunter Labscan.

[3] Appearance ratings of canned beans were averaged across reviewers on 2016 and 2017 samples.

[4] Washed and drained weights were measured after briefly rinsing canned beans under cool water.

[5] Texture was measured as the peak force (kg) required to compress a 100 g sample of canned beans.

Table 4. Correlation matrix for canning quality traits in two black bean RIL populations.

Pop. 86 Canning Traits Pearson Correlation Coefficients (n=145 RILs)														
Pop. 76 Canning Traits Pearson Correlation Coefficients (n=145 RILs)	Pop. 86 → / Pop. 76 ↓		Hunter Labscan '17			ImageJ '17			ImageJ 2YA					
		COL	***L***H*	***a***H*	***b***H*	***L***I*	**a*I**	***b***I*	***L***I*	***a***I*	***b***I*	**APP**	**WDW**	**TXT**
	COL	COL	-0.83	-0.74	-0.93	-0.87	-0.74	-0.92	-0.91	-0.83	-0.96	0.31	0.07	-0.10
			<.0001	<.0001	<.0001	<.0001	<.0001	<.0001	<.0001	<.0001	<.0001	<.0001	0.41	0.22
Hunter Labscan '17	***L***H*	-0.73	*L**H '17	0.69	0.85	0.76	0.60	0.75	0.94	0.73	0.82	-0.49	0.10	0.03
		<.0001		<.0001	<.0001	<.0001	<.0001	<.0001	<.0001	<.0001	<.0001	<.0001	0.25	0.68
	aH*	-0.72	0.39	*a**H '17	0.78	0.63	0.58	0.61	0.70	0.89	0.72	-0.21	-0.10	0.13
		<.0001	<.0001		<.0001	<.0001	<.0001	<.0001	<.0001	<.0001	<.0001	0.01	0.24	0.11
	bH*	-0.82	0.53	0.84	*b**H '17	0.80	0.65	0.89	0.88	0.80	0.97	-0.26	-0.05	0.09
		<.0001	<.0001	<.0001		<.0001	<.0001	<.0001	<.0001	<.0001	<.0001	0.00	0.51	0.28
ImageJ '17	***L***I*	-0.91	0.75	0.69	0.84	*L**I '17	0.59	0.78	0.94	0.68	0.81	-0.36	-0.12	0.04
		<.0001	<.0001	<.0001	<.0001		<.0001	<.0001	<.0001	<.0001	<.0001	<.0001	0.14	0.61
	aI*	-0.74	0.57	0.69	0.59	0.74	*a**I '17	0.80	0.63	0.89	0.75	-0.24	0.08	0.20
		<.0001	<.0001	<.0001	<.0001	<.0001		<.0001	<.0001	<.0001	<.0001	0.00	0.32	0.02
	bI*	-0.91	0.73	0.66	0.86	0.91	0.71	*b**I '17	0.82	0.80	0.97	-0.29	0.03	0.09
		<.0001	<.0001	<.0001	<.0001	<.0001	<.0001		<.0001	<.0001	<.0001	0.00	0.73	0.27
ImageJ 2YA	***L***I*	-0.87	0.71	0.62	0.77	0.94	0.68	0.83	*L**I	0.75	0.87	-0.46	-0.01	0.03
		<.0001	<.0001	<.0001	<.0001	<.0001	<.0001	<.0001		<.0001	<.0001	<.0001	0.91	0.68
	aI*	-0.80	0.55	0.72	0.58	0.74	0.91	0.69	0.71	*a**I	0.82	-0.26	-0.01	0.18
		<.0001	<.0001	<.0001	<.0001	<.0001	<.0001	<.0001	<.0001		<.0001	0.00	0.94	0.03
	bI*	-0.93	0.71	0.61	0.81	0.85	0.64	0.95	0.80	0.71	*b**I	-0.29	-0.01	0.09
		<.0001	<.0001	<.0001	<.0001	<.0001	<.0001	<.0001	<.0001	<.0001		0.00	0.91	0.30
	APP	0.33	-0.42	-0.12	-0.29	-0.43	-0.12	-0.34	-0.52	-0.15	-0.34	APP	-0.46	0.08
		<.0001	<.0001	0.13	0.00	<.0001	0.13	<.0001	<.0001	0.08	<.0001		<.0001	0.32
	WDW	0.02	0.04	-0.11	-0.03	-0.02	-0.06	-0.02	-0.03	-0.04	-0.01	0.03	WDW	-0.21
		0.80	0.65	0.20	0.76	0.83	0.48	0.84	0.76	0.62	0.86	0.74		0.01
	TXT	-0.28	0.11	0.23	0.19	0.13	0.23	0.27	0.04	0.29	0.33	-0.04	-0.36	TXT
		0.00	0.17	0.01	0.02	0.11	0.01	0.00	0.62	0.00	<.0001	0.65	<.0001	

Correlations for Population 76 (B14311/Zenith) are on the left axis, while correlations for Population 86 (B14311/B12724) are on the top axis. Abbreviations for traits are given in Table 1. 'I' indicates values measured by ImageJ analysis and 'H' indicates values measured by a Hunter Labscan. Pearson correlation coefficients and p-values are given for each comparison.

Table 5. Correlation matrix for agronomic and selected canning quality traits in two black bean RIL populations.

Pop. 76 Agronomic Traits Pearson Correlation Coefficients (n=145 RILs)	Pop. 86 Agronomic Traits Pearson Correlation Coefficients (n=145 RILs)													
Pop. 86 → Pop. 76 ↓	**SY**	**SW**	**DF**	**DM**	**LDG**	**HT**	**DS**	**BRZ**	**CBB**	**COL**	***L***I*	***a***I*	***b***I*	**APP**
SY	SY	0.22 0.01	0.13 0.11	0.26 0.00	-0.03 0.72	0.59 <.0001	0.53 <.0001	0.03 0.72	-	0.07 0.40	-0.01 0.90	-0.03 0.73	-0.02 0.80	-0.32 <.0001
SW	0.16 0.05	SW	-0.10 0.22	0.23 0.01	0.13 0.12	0.28 0.00	0.16 0.05	0.03 0.69	-	0.22 0.01	-0.17 0.04	-0.27 0.00	-0.22 0.01	0.00 0.98
DF	-0.05 0.51	0.25 0.00	DF	-0.02 0.82	0.00 0.96	0.02 0.78	-0.02 0.77	0.00 0.95	-	0.11 0.20	-0.07 0.43	-0.04 0.59	-0.09 0.27	-0.10 0.22
DM	-0.09 0.29	0.48 <.0001	0.42 <.0001	DM	0.05 0.52	0.55 <.0001	0.40 <.0001	-0.07 0.37	-	0.01 0.92	0.04 0.67	-0.14 0.10	0.04 0.61	-0.29 0.00
LDG	-	-	-	-	LDG	0.06 0.47	0.08 0.36	0.19 0.02	-	0.04 0.62	0.04 0.66	-0.05 0.51	-0.01 0.95	-0.16 0.06
HT	0.26 0.00	0.42 <.0001	0.25 0.00	0.56 <.0001	-	HT	0.78 <.0001	-0.06 0.48	-	0.03 0.76	0.03 0.70	-0.10 0.23	0.03 0.74	-0.35 <.0001
DS	0.46 <.0001	0.25 0.00	0.05 0.54	0.32 <.0001	-	0.73 <.0001	DS	0.01 0.88	-	-0.01 0.92	0.06 0.45	-0.03 0.68	0.04 0.59	-0.33 <.0001
BRZ	0.08 0.35	-0.11 0.17	-0.31 0.00	-0.23 0.01	-	-0.07 0.38	0.04 0.67	BRZ	-	0.19 0.02	-0.15 0.07	-0.11 0.18	-0.16 0.05	0.02 0.80
CBB	-0.12 0.17	-0.10 0.23	0.06 0.47	-0.05 0.55	-	-0.06 0.48	-0.14 0.09	0.10 0.21	CBB	-	-	-	-	-
COL	0.03 0.74	0.14 0.09	-0.04 0.65	0.09 0.30	-	-0.01 0.92	0.01 0.91	-0.01 0.91	0.12 0.14	COL	-0.91 <.0001	-0.83 <.0001	-0.96 <.0001	0.31 <.0001
LI*	-0.02 0.80	-0.07 0.40	0.15 0.07	-0.01 0.88	-	-0.05 0.53	-0.09 0.27	-0.11 0.19	-0.11 0.21	-0.87 <.0001	*L**I	0.75 <.0001	0.87 <.0001	-0.46 <.0001
aI*	-0.09 0.29	-0.11 0.18	-0.02 0.84	-0.04 0.63	-	-0.06 0.47	-0.10 0.23	0.04 0.59	-0.06 0.46	-0.80 <.0001	0.71 <.0001	*a**I*	0.82 <.0001	-0.26 0.00
bI*	0.01 0.93	-0.17 0.04	0.05 0.57	-0.10 0.24	-	0.01 0.91	-0.01 0.91	-0.04 0.63	-0.10 0.21	-0.93 <.0001	0.80 <.0001	0.71 <.0001	*b**I*	-0.29 0.00
APP	-0.07 0.41	-0.14 0.09	-0.22 0.01	-0.06 0.50	-	-0.01 0.94	-0.03 0.68	0.13 0.12	0.04 0.59	0.33 <.0001	-0.52 <.0001	-0.15 0.08	-0.34 <.0001	APP

Correlations for Population 76 (B14311/Zenith) are on the left axis, while correlations for Population 86 (B14311/B12724) are on the top axis. Abbreviations for traits are given in Table 1. 'I' indicates values measured by ImageJ analysis and 'H' indicates values measured by a Hunter Labscan. Pearson correlation coefficients and p-values are given for each comparison.

Table 6. QTL for measurements of post-processing color retention in two black bean RIL populations.

QTL	Chr[1]	Year	Peak Pos (cM)[2]	Peak LOD[3]	R^2 (%)[4]	a[5]	Map interval (cM)	Physical interval (Mb)	Left-flanking SNP	Right-flanking SNP
Color rating										
COL2.1[76]	***Flanking region***			**3.2-3.7**	**4.9-6.2**	**-(0.14-0.16)**	**54.0-74.1**	**11.03-17.24**	**ss715649088**	**ss715651061**
	Shared region						**61.1-74.1**	**12.78-17.24**	**ss715649961**	**ss715651061**
COL_2017	2	2017	63.1	3.7	6.2	-0.16	54.0-74.1	11.03-17.24	ss715649088	ss715651061
COL_2YA	2	2YA	64.1	3.2	4.9	-0.14	61.1-74.1	12.78-17.24	ss715649961	ss715651061
COL3.1[76]	***Shared region***			**3.5-4.0**	**6.3**	**-(0.15-0.16)**	**26.4-32.8**	**2.02-2.43**	**ss715646879**	**ss715647570**
COL_2016	3	2016	26.4	3.5	6.3	-0.16	26.4-32.8	2.02-2.43	ss715646879	ss715647570
COL_2YA	3	2YA	26.4	4.0	6.3	-0.15	26.4-32.8	2.02-2.43	ss715646879	ss715647570
COL3.1[86]	3	2017	0.0	2.8	3.6	-0.13	0-1.51	1.19-1.30	ss715646396	ss715646392
COL3.2[86]	3	2016	102.4	2.9	4.4	-0.17	102.4-121.7	47.28-50.39	ss715650580	ss715647338
COL5.1[86]	5	2017	170.5	3.1	4.3	-0.14	167.5-170.7	38.84-38.92	ss715645449	ss715645459
COL8.1[76]	***Flanking region***			**5.8-7.4**	**11.8-16.2**	**-(0.23-0.26)**	**16.8-62.3**	**1.53-7.25**	**ss715647112**	**ss715648559**
	Shared region						**17.5-62.3**	**1.54-7.25**	**ss715647113**	**ss715648559**
COL_2016	8	2016	41.6	5.8	16.2	-0.26	16.8-62.3	1.53-7.254	ss715647112	ss715648559
COL_2017	8	2017	53.4	7.4	13.0	-0.25	17.5-62.3	1.54-7.254	ss715647113	ss715648559
COL_2YA	8	2YA	53.4	7.0	11.8	-0.23	17.5-62.3	1.54-7.254	ss715647113	ss715648559

Table 6. (cont'd)

QTL	Chr[1]	Year	Peak Pos (cM)[2]	Peak LOD[3]	R^2 (%)[4]	a[5]	Map interval (cM)	Physical interval (Mb)	Left-flanking SNP	Right-flanking SNP
COL8.1[86]	***Flanking region***			**6.7-8.0**	**12.3-13.7**	**-(0.26-0.27)**	**15.3-60.4**	**1.57-53.68**	**ss715647115**	**ss715648232**
	Shared region						**15.3-40.1**	**1.57-6.27**	**ss715647115**	**ss715647905**
COL_2016	8	2016	39.8	6.7	12.3	-0.27	15.3-60.4	1.57-53.68	ss715647115	ss715648232
COL_2017	8	2017	35.8	7.0	13.7	-0.27	15.3-40.1	1.57-6.27	ss715647115	ss715647905
COL_2YA	8	2YA	39.8	8.0	13.4	-0.26	15.3-60.4	1.57-53.68	ss715647115	ss715648232
COL10.1[86]	10	2017	75.7	2.9	4.5	0.15	69.7-82.1	42.22-43.29	ss715645524	ss715645501
COL11.1[76]	***Shared region***			**4.8-7.4**	**8.4-14.3**	**-(0.19-0.25)**	**144.3-150.9**	**52.16-52.84**	**ss715649459**	**ss715640405**
COL_2016	11	2016	149.3	7.4	14.3	-0.25	144.3-149.6	52.16-52.65	ss715649459	ss715650816
COL_2017	11	2017	149.6	4.8	8.4	-0.19	149.6-150.6	52.65-52.84	ss715650816	ss715649382
COL_2YA	11	2YA	149.6	7.0	11.9	-0.21	149.6-150.9	52.65-52.84	ss715650816	ss715640405
COL11.1[86]	***Shared region***			**10.6-13.0**	**18.7-22.0**	**-(0.31-0.32)**	**22.9-30.5**	**52.47-52.84**	**ss715648350**	**ss715640405**
COL_2016	11	2016	28.4	10.6	18.7	-0.31	22.9-30.5	52.47-52.84	ss715648350	ss715640405
COL_2017	11	2017	28.4	12.7	22.0	-0.32	22.9-30.5	52.47-52.84	ss715648350	ss715640405
COL_2YA	11	2YA	28.4	13.0	21.2	-0.31	22.9-30.5	52.47-52.84	ss715648350	ss715640405
L value*										
***L**2.1[76]**	2	2017	61.6	4.7	8.8	0.43	61.1-74.1	12.78-17.24	ss715649961	ss715651061
***L**3.1[76]**	3	2017	26.4	3.1	5.2	0.33	26.4-32.8	2.02-2.43	ss715646879	ss715647570
***L**5.1[86]**	5	2017	125.9	3.8	6.2	0.40	121.9-126.9	34.33-35.96	ss715647683	ss715639578

Table 6. (cont'd)

QTL	Chr[1]	Year	Peak Pos (cM)[2]	Peak LOD[3]	R^2 (%)[4]	a[5]	Map interval (cM)	Physical interval (Mb)	Left-flanking SNP	Right-flanking SNP
***L**8.1[76]**	***Shared region***			**4.1-7.7**	**8.4-14.4**	**0.43-0.60**	**0-62.3**	**0.48-7.25**	**ss715646686**	**ss715648559**
*L**I_2016	8	2016	15.0	4.1	8.4	0.43	0-15.2	0.484-1.41	ss715646686	ss715647114
*L**I_2017	8	2017	52.4	7.7	14.4	0.60	16.8-62.3	1.53-7.25	ss715647112	ss715648559
*L**H_2017	8	2017	51.4	4.2	10.5	0.47	17.54-62.3	1.54-7.25	ss715647113	ss715648559
***L**8.1[86]**	***Flanking region***			**4.4-7.8**	**8.4-16.7**	**0.49-0.67**	**15.3-40.1**	**1.57-6.27**	**ss715647115**	**ss715647905**
	Shared region						**15.8-40.1**	**1.58-6.27**	**ss715647116**	**ss715647905**
*L**I_2016	8	2016	39.83	4.4	8.4	0.49	15.8-40.1	1.58-6.27	ss715647116	ss715647905
*L**I_2017	8	2017	38.83	7.8	16.7	0.67	15.3-40.1	1.57-6.27	ss715647115	ss715647905
***L**9.1[76]**	9	2016	27.0	6.8	13.9	0.53	27.0-27.1	10.30-10.32	ss715646178	ss715646179
***L**9.2[76]**	9	2017	39.6	3.1	4.8	0.31	39.6-40.1	13.55-13.71	ss715647980	ss715647985
***L**9.1[86]**	9	2016	2.7	3.5	5.5	-0.38	2.6-5.8	27.58-29.10	ss715647620	ss715649156
***L**10.1[86]**	10	2016	66.6	3.8	6.8	0.48	65.6-67.3	41.96-42.01	ss715645508	ss715645510
***L**11.1[76]**	***Shared region***			**3.0-4.5**	**7.3-8.8**	**0.41-0.43**	**149.6-154.0**	**52.65-52.87**	**ss715650816**	**ss715650160**
*L**I_2016	11	2016	149.6	4.5	8.8	0.43	149.6-150.6	52.65-52.84	ss715650816	ss715649382
*L**I_2017	11	2017	149.6	4.4	8.1	0.41	149.6-150.6	52.65-52.84	ss715650816	ss715649382
*L**H_2017	11	2017	150.9	3.0	7.3	0.41	150.9-154.0	52.84-52.87	ss715640405	ss715650160

Table 6. (cont'd)

QTL	Chr[1]	Year	Peak Pos (cM)[2]	Peak LOD[3]	R^2 (%)[4]	a[5]	Map interval (cM)	Physical interval (Mb)	Left-flanking SNP	Right-flanking SNP
***L**11.1[86]**	***Flanking region***			**8.1-8.9**	**15.0-18.0**	**0.62-0.68**	**22.9-30.8**	**52.47-52.87**	**ss715648350**	**ss715650160**
	Shared region						**22.9-30.5**	**52.47-52.84**	**ss715648350**	**ss715640405**
*L**I_2016	11	2016	30.5	8.9	18.0	0.68	22.9-30.8	52.47-52.87	ss715648350	ss715650160
*L**I_2017	11	2017	28.4	8.1	15.0	0.62	22.9-30.5	52.47-52.84	ss715648350	ss715640405
a value*										
***a**8.1[76]**	***Flanking region***			**3.9-9.8**	**8.6-27.0**	**0.34-0.57**	**0-62.3**	**0.48-7.25**	**ss715646686**	**ss715648559**
	Shared region						**15.2-17.5**	**1.41-1.54**	**ss715647114**	**ss715647113**
*a**I_2016	8	2016	15.0	3.9	8.6	0.34	0-17.5	0.48-1.54	ss715646686	ss715647113
*a**I_2017	8	2017	23.6	9.8	27.0	0.57	15.2-62.3	1.41-7.25	ss715647114	ss715648559
*a**H_2017	8	2017	36.6	7.2	21.4	0.40	16.8-62.3	1.53-7.25	ss715647112	ss715648559
***a**8.1[86]**	***Flanking region***			**6.6-8.7**	**17.3-20.7**	**0.46-0.55**	**15.3-60.4**	**1.53-53.68**	**ss715647115**	**ss715648232**
	Shared region						**15.3-40.1**	**1.57-6.27**	**ss715647115**	**ss715647905**
*a**I_2016	8	2016	39.8	8.7	20.7	0.49	15.3-60.4	1.57-53.68	ss715647115	ss715648232
*a**I_2017	8	2017	35.8	6.6	17.3	0.46	15.3-40.1	1.57-6.27	ss715647115	ss715647905
*a**H_2017	8	2017	37.8	7.7	20.6	0.55	15.3-40.1	1.57-6.27	ss715647115	ss715647905
***a**10.1[86]**	10	2017	69.7	3.8	8.3	-0.31	69.7-82.1	42.22-43.29	ss715645524	ss715645501
b value*										
***b**2.1[76]**	2	2017	64.1	4.4	8.6	0.41	54.0-74.1	11.03-17.24	ss715649088	ss715651061
***b**3.1[76]**	3	2016	14.2	3.5	7.2	0.41	3.4-14.7	1.01-1.19	ss715650435	ss715646396
***b**3.1[86]**	3	2017	0.0	2.7	3.9	0.31	0-1.5	1.19-1.30	ss715646396	ss715646392

Table 6. (cont'd)

QTL	Chr[1]	Year	Peak Pos (cM)[2]	Peak LOD[3]	R^2 (%)[4]	a[5]	Map interval (cM)	Physical interval (Mb)	Left-flanking SNP	Right-flanking SNP
***b**8.1[76]**	***Flanking region***			**3.5-7.8**	**6.7-16.4**	**0.39-0.47**	**16.8-62.3**	**1.53-7.25**	**ss715647112**	**ss715648559**
	Shared region						**17.5-54.1**	**1.54-7.04**	**ss715647113**	**ss715640331**
*b**I_2016	8	2016	51.4	4.9	10.8	0.47	17.5-50.4	1.54-6.00	ss715647113	ss715648337
*b**I_2017	8	2017	53.4	3.5	6.7	0.39	50.4-54.1	6.00-7.04	ss715648337	ss715640331
*b**H_2017	8	2017	52.4	7.8	16.4	0.41	16.8-62.3	1.53-7.25	ss715647112	ss715648559
***b**8.1[86]**	***Flanking region***			**4.3-7.0**	**9.1-12.6**	**0.45-0.55**	**15.3-60.4**	**1.57-53.68**	**ss715647115**	**ss715648232**
	Shared region						**15.8-40.1**	**1.58-6.27**	**ss715647116**	**ss715647905**
*b**I_2016	8	2016	38.8	7.0	11.7	0.55	15.3-60.37	1.57-53.68	ss715647115	ss715648232
*b**I_2017	8	2017	36.8	4.3	9.1	0.49	15.8-40.1	1.58-6.27	ss715647116	ss715647905
*b**H_2017	8	2017	39.8	6.8	12.6	0.45	15.3-40.1	1.57-6.27	ss715647115	ss715647905
***b**11.1[76]**	***Flanking region***			**5.3-8.8**	**11.4-20.7**	**0.31-0.66**	**123.3-150.9**	**51.12-52.84**	**ss715649251**	**ss715640405**
	Shared region						**144.3-149.6**	**52.16-52.65**	**ss715649459**	**ss715650816**
*b**I_2016	11	2016	149.3	8.8	20.7	0.66	144.3-149.6	52.16-52.65	ss715649459	ss715650816
*b**I_2017	11	2017	149.3	6.9	13.9	0.51	123.3-149.6	51.12-52.65	ss715649251	ss715650816
*b**H_2017	11	2017	149.3	5.3	11.4	0.34	144.3-150.9	52.16-52.84	ss715649459	ss715640405
***b**11.1[86]**	***Shared region***			**13.3-14.6**	**25.9-27.3**	**0.62-0.81**	**22.9-30.5**	**52.47-52.84**	**ss715648350**	**ss715640405**
*b**I_2016	11	2016	28.4	14.6	26.3	0.79	22.9-30.5	52.47-52.84	ss715648350	ss715640405
*b**I_2017	11	2017	28.4	13.3	27.3	0.81	22.9-30.5	52.47-52.84	ss715648350	ss715640405
*b**H_2017	11	2017	28.4	13.5	25.9	0.62	22.9-30.5	52.47-52.84	ss715648350	ss715640405

Table 6. (cont'd)

QTL	Chr[1]	Year	Peak Pos (cM)[2]	Peak LOD[3]	R^2 (%)[4]	a[5]	Map interval (cM)	Physical interval (Mb)	Left-flanking SNP	Right-flanking SNP
***L**11.1[86]**	***Flanking region***			**8.1-8.9**	**15.0-18.0**	**0.62-0.68**	**22.9-30.8**	**52.47-52.87**	**ss715648350**	**ss715650160**
	Shared region						**22.9-30.5**	**52.47-52.84**	**ss715648350**	**ss715640405**
*L**I_2016	11	2016	30.5	8.9	18.0	0.68	22.9-30.8	52.47-52.87	ss715648350	ss715650160
*L**I_2017	11	2017	28.4	8.1	15.0	0.62	22.9-30.5	52.47-52.84	ss715648350	ss715640405
a value*										
***a**8.1[76]**	***Flanking region***			**3.9-9.8**	**8.6-27.0**	**0.34-0.57**	**0-62.3**	**0.48-7.25**	**ss715646686**	**ss715648559**
	Shared region						**15.2-17.5**	**1.41-1.54**	**ss715647114**	**ss715647113**
*a**I_2016	8	2016	15.0	3.9	8.6	0.34	0-17.5	0.48-1.54	ss715646686	ss715647113
*a**I_2017	8	2017	23.6	9.8	27.0	0.57	15.2-62.3	1.41-7.25	ss715647114	ss715648559
*a**H_2017	8	2017	36.6	7.2	21.4	0.40	16.8-62.3	1.53-7.25	ss715647112	ss715648559
***a**8.1[86]**	***Flanking region***			**6.6-8.7**	**17.3-20.7**	**0.46-0.55**	**15.3-60.4**	**1.53-53.68**	**ss715647115**	**ss715648232**
	Shared region						**15.3-40.1**	**1.57-6.27**	**ss715647115**	**ss715647905**
*a**I_2016	8	2016	39.8	8.7	20.7	0.49	15.3-60.4	1.57-53.68	ss715647115	ss715648232
*a**I_2017	8	2017	35.8	6.6	17.3	0.46	15.3-40.1	1.57-6.27	ss715647115	ss715647905
*a**H_2017	8	2017	37.8	7.7	20.6	0.55	15.3-40.1	1.57-6.27	ss715647115	ss715647905
***a**10.1[86]**	10	2017	69.7	3.8	8.3	-0.31	69.7-82.1	42.22-43.29	ss715645524	ss715645501
b value*										
***b**2.1[76]**	2	2017	64.1	4.4	8.6	0.41	54.0-74.1	11.03-17.24	ss715649088	ss715651061
***b**3.1[76]**	3	2016	14.2	3.5	7.2	0.41	3.4-14.7	1.01-1.19	ss715650435	ss715646396
***b**3.1[86]**	3	2017	0.0	2.7	3.9	0.31	0-1.5	1.19-1.30	ss715646396	ss715646392

Table 6. (cont'd)

QTL	Chr[1]	Year	Peak Pos (cM)[2]	Peak LOD[3]	R^2 (%)[4]	a[5]	Map interval (cM)	Physical interval (Mb)	Left-flanking SNP	Right-flanking SNP
***b**8.1[76]**	***Flanking region***			**3.5-7.8**	**6.7-16.4**	**0.39-0.47**	**16.8-62.3**	**1.53-7.25**	**ss715647112**	**ss715648559**
	Shared region						**17.5-54.1**	**1.54-7.04**	**ss715647113**	**ss715640331**
*b**I_2016	8	2016	51.4	4.9	10.8	0.47	17.5-50.4	1.54-6.00	ss715647113	ss715648337
*b**I_2017	8	2017	53.4	3.5	6.7	0.39	50.4-54.1	6.00-7.04	ss715648337	ss715640331
*b**H_2017	8	2017	52.4	7.8	16.4	0.41	16.8-62.3	1.53-7.25	ss715647112	ss715648559
***b**8.1[86]**	***Flanking region***			**4.3-7.0**	**9.1-12.6**	**0.45-0.55**	**15.3-60.4**	**1.57-53.68**	**ss715647115**	**ss715648232**
	Shared region						**15.8-40.1**	**1.58-6.27**	**ss715647116**	**ss715647905**
*b**I_2016	8	2016	38.8	7.0	11.7	0.55	15.3-60.37	1.57-53.68	ss715647115	ss715648232
*b**I_2017	8	2017	36.8	4.3	9.1	0.49	15.8-40.1	1.58-6.27	ss715647116	ss715647905
*b**H_2017	8	2017	39.8	6.8	12.6	0.45	15.3-40.1	1.57-6.27	ss715647115	ss715647905
***b**11.1[76]**	***Flanking region***			**5.3-8.8**	**11.4-20.7**	**0.31-0.66**	**123.3-150.9**	**51.12-52.84**	**ss715649251**	**ss715640405**
	Shared region						**144.3-149.6**	**52.16-52.65**	**ss715649459**	**ss715650816**
*b**I_2016	11	2016	149.3	8.8	20.7	0.66	144.3-149.6	52.16-52.65	ss715649459	ss715650816
*b**I_2017	11	2017	149.3	6.9	13.9	0.51	123.3-149.6	51.12-52.65	ss715649251	ss715650816
*b**H_2017	11	2017	149.3	5.3	11.4	0.34	144.3-150.9	52.16-52.84	ss715649459	ss715640405
***b**11.1[86]**	***Shared region***			**13.3-14.6**	**25.9-27.3**	**0.62-0.81**	**22.9-30.5**	**52.47-52.84**	**ss715648350**	**ss715640405**
*b**I_2016	11	2016	28.4	14.6	26.3	0.79	22.9-30.5	52.47-52.84	ss715648350	ss715640405
*b**I_2017	11	2017	28.4	13.3	27.3	0.81	22.9-30.5	52.47-52.84	ss715648350	ss715640405
*b**H_2017	11	2017	28.4	13.5	25.9	0.62	22.9-30.5	52.47-52.84	ss715648350	ss715640405

QTL names (bolded) are assigned according to the dry bean QTL nomenclature established by Miklas and Porch (2010). QTL names consist of an abbreviated trait name, the chromosome of detection, unique number identifier on the chromosome, and the population of detection in superscript. QTL detected by multiple years or methods are listed below the putative QTL. Population 76 was derived from B14311/Zenith, and Population 86 was derived from B14311/B12724. 'I' indicates values measured by ImageJ analysis and 'H' indicates values measured by a Hunter Labscan.[1]Chr: chromosome number; [2]Peak Pos: genetic position of the peak LOD; [3]LOD: logarithm of odds; [4]R^2: percentage of phenotypic variation explained; [5]a: additive effect of the allele donated by breeding line B14311

Table 7. QTL for canning quality traits in two black bean RIL populations.

QTL	Chr[1]	Year	Peak Pos (cM)[2]	Peak LOD[3]	R^2 (%)[4]	a[5]	Map interval (cM)	Physical interval (Mb)	Left-flanking SNP	Right-flanking SNP
Appearance rating										
APP2.1[76]	2	2017	164.0	4.2	8.9	-0.12	142.8-164.4	37.81-44.97	ss715648834	ss715647236
APP2.1[86]	2	2016	1.0	3.8	8.8	-0.16	0-1.8	3.90-4.48	ss715647803	ss715639861
APP3.1[86]	***Shared region***			**3.3-4.5**	**6.7-9.7**	**-(0.11-0.16)**	**0-1.5**	**1.19-1.30**	**ss715646396**	**ss715646392**
APP_2016	3	2016	0.0	4.5	9.7	-0.16	0-1.5	1.19-1.30	ss715646396	ss715646392
APP_2YA	3	2YA	0.0	3.3	6.7	-0.11	0-1.5	1.19-1.30	ss715646396	ss715646392
APP4.1[86]	4	2016	52.1	3.3	7.1	0.13	51.1-52.1	2.75-2.89	ss715646227	ss715646218
APP5.1[76]	5	2016	49.2	3.1	7.5	-0.12	40.6-57.1	4.47-4.75	ss715648066	ss715649111
APP6.1[86]	6	2016	21.0	3.2	6.0	0.13	20.9-21.7	28.97-29.04	ss715645203	ss715645202
APP8.1[76]	8	2017	49.7	3.2	6.6	-0.10	49.7-50.4	5.86-6.00	ss715650193	ss715648337
APP8.2[76]	8	2016	146.5	3.0	7.0	0.12	145.5-147.0	60.97-61.30	ss715646515	ss715646092
APP10.1[86]	10	2017	89.2	3.6	9.5	0.14	69.7-90.2	42.22-44.22	ss715645524	ss715649823

Table 7. (cont'd)

QTL	Chr[1]	Year	Peak Pos (cM)[2]	Peak LOD[3]	R^2 (%)[4]	a[5]	Map interval (cM)	Physical interval (Mb)	Left-flanking SNP	Right-flanking SNP
Texture										
TXT2.1[76]	2	2016	85.7	4.1	7.7	2.64	81.8-88.9	17.31-20.44	ss715650059	ss715651192
TXT2.1[86]	2	2016	0.0	3.1	5.9	-2.25	0-1.8	3.90-4.48	ss715647803	ss715639861
TXT5.1[76]	***Shared region***			**7.0-11.6**	**13.7-25.2**	**2.4-2.5**	**128.2-141.5**	**27.70-36.79**	**ss715649539**	**ss715646996**
TXT_2016	5	2016	138.8	7.0	13.7	2.38	128.2-141.5	27.70-36.79	ss715649539	ss715646996
TXT_2017	5	2017	137.1	11.6	25.2	2.49	128.2-141.5	27.70-36.79	ss715649539	ss715646996
TXT9.1[76]	9	2017	33.5	3.9	7.6	-1.38	16.3-39.6	7.87-13.55	ss715645741	ss715647980
TXT10.1[86]	10	2016	89.2	11.3	26.4	-4.45	82.1-90.2	43.29-44.22	ss715645501	ss715649823
Washed drained weight										
WDW2.1[86]	2	2016	0.0	4.5	10.2	1.64	0-25.4	3.90-30.15	ss715647803	ss715647526
WDW8.1[76]	8	2016	158.4	4.4	11.6	-2.43	158.4-160.1	62.27-62.75	ss715646764	ss715647397

QTL names (bolded) are assigned according to the dry bean QTL nomenclature established by Miklas and Porch (2010). QTL names consist of an abbreviated trait name, the chromosome of detection, unique number identifier on the chromosome, and the population of detection in superscript. QTL detected by multiple years or methods are listed below the putative QTL. Population 76 was derived from B14311/Zenith, and Population 86 was derived from B14311/B12724. [1]Chr: chromosome number; [2]Peak Pos: genetic position of the peak LOD; [3]LOD: logarithm of odds; [4]R^2: percentage of phenotypic variation explained; [5]a: additive effect of the allele donated by breeding line B14311

Table 8. QTL for agronomic traits in two black bean RIL populations.

QTL	Chr[1]	Year	Peak Pos (cM)[2]	Peak LOD[3]	R^2 (%)[4]	a[5]	Map interval (cM)	Physical interval (Mb)	Left-flanking SNP	Right-flanking SNP
Seed yield										
SY8.1[76]	8	2017	137.7	3.5	8.9	-110	137.7-144.2	60.07-60.56	ss715646529	ss715646508
SY8.1[86]	8	2017	0.0	6.8	14.8	-130	0-12.9	0.37-1.50	ss715646680	ss715647128
Seed weight										
SW3.1[76]	3	2017	119.3	12.4	22.7	0.79	119.3-122.7	11.47-11.82	ss715646286	ss715646290
SW3.1[86]	3	2017	59.8	4.5	12.2	0.42	43.6-60.2	3.82-12.30	ss715649325	ss715649868
SW4.1[76]	4	2017	12.8	8.1	13.2	-0.60	10.3-20.6	0.16-1.90	ss715648682	ss715646916
SW4.1[86]	4	2017	0.7	3.4	7.7	-0.33	0.7-1.2	2.20-2.41	ss715647817	ss715646249
SW4.2[86]	4	2017	54.7	4.3	9.6	-0.38	51.1-63.9	2.75-3.59	ss715646227	ss715650365
SW5.1[86]	5	2017	132.9	4.1	9.3	0.36	126.9-133.3	35.96-36.79	ss715639578	ss715646996
SW7.1[76]	7	2017	90.1	3.3	6.2	0.50	83.1-109.5	4.25-4.39	ss715646463	ss715646455
SW8.1[76]	8	2017	155.7	5.6	8.2	-0.45	151.1-158.4	62.06-62.27	ss715646750	ss715646764
Days to flowering										
DF7.1[76]	7	2017	211.3	3.0	5.0	-0.25	203.9-215.0	27.48-30.85	ss715650972	ss715639231
DF8.1[76]	8	2017	145.5	10.0	20.5	-0.47	145.5-147.0	60.97-61.30	ss715646515	ss715646092
DF11.1[76]	11	2017	143.7	3.0	4.8	0.23	143.7-144.0	51.95-51.96	ss715649909	ss715640836

Table 8. (cont'd)

QTL	Chr[1]	Year	Peak Pos (cM)[2]	Peak LOD[3]	R^2 (%)[4]	a[5]	Map interval (cM)	Physical interval (Mb)	Left-flanking SNP	Right-flanking SNP
Days to maturity										
DM2.1[76]	2	2017	113.1	4.7	11.0	-0.43	110.1-113.2	31.67-33.65	ss715647744	ss715647098
DM4.1[86]	4	2017	0.7	4.3	11.6	-0.39	0.7-1.2	2.20-2.41	ss715647817	ss715646249
DM11.1[86]	11	2017	4.0	3.7	8.3	0.35	0-10.8	49.59-51.12	ss715649023	ss715649251
Canopy height										
HT1.1[86]	1	2017	43.6	4.5	6.7	-0.34	43.6-63.7	1.29-2.85	ss715646260	ss715647676
HT2.1[76]	2	2017	110.1	4.9	9.6	-0.45	95.3-110.1	25.39-31.67	ss715648526	ss715647744
HT3.1[76]	3	2017	108.3	3.1	5.8	0.35	92.4-108.8	10.69-11.25	ss715647445	ss715649740
HT4.1[86]	4	2017	50.9	10.6	17.2	-0.49	44.5-52.1	2.55-2.89	ss715646239	ss715646218
HT7.1[76]	7	2017	8.9	3.1	5.5	0.34	5.8-9.43	0.65-0.91	ss715645687	ss715645692
HT8.1[86]	8	2017	0.0	12.8	21.5	-0.59	0-12.9	0.37-1.50	ss715646680	ss715647128
HT11.1[76]	11	2017	144.3	4.6	9.0	0.42	144.3-149.6	52.16-52.65	ss715649459	ss715650816

Table 8. (cont'd)

QTL	Chr[1]	Year	Peak Pos (cM)[2]	Peak LOD[3]	R^2 (%)[4]	a[5]	Map interval (cM)	Physical interval (Mb)	Left-flanking SNP	Right-flanking SNP
Desirability score										
DS2.1[76]	2	2017	50.6	3.0	6.8	-0.14	50.6-51.0	5.86-7.10	ss715650567	ss715649765
DS4.1[86]	4	2017	52.1	3.6	7.3	-0.12	51.1-52.1	2.75-2.89	ss715646227	ss715646218
DS8.1[86]	8	2017	0.0	6.7	14.5	-0.19	0-12.9	0.37-1.50	ss715646680	ss715647128
DS9.1[76]	9	2017	14.9	4.9	11.1	-0.18	14.8-15.8	7.70-7.79	ss715645748	ss715645745
Bronzing										
BRZ5.1[86]	5	2017	178.5	3.2	7.4	-0.19	174.7-188.5	39.24-39.34	ss715645318	ss715645331
BRZ6.1[76]	6	2017	9.6	3.4	6.3	-0.25	0.5-22.9	12.21-13.75	ss715649979	ss715647424
BRZ7.1[86]	7	2017	46.1	6.6	16.9	-0.30	46.1-49.8	3.99-4.17	ss715649276	ss715646465
BRZ8.1[76]	8	2017	151.1	5.0	10.3	0.31	144.8-158.4	60.71-62.27	ss715646503	ss715646764
BRZ9.1[86]	9	2017	19.0	3.5	7.3	0.18	12.1-19.2	31.40-33.38	ss715646279	ss715645631

QTL names (bolded) are assigned according to the dry bean QTL nomenclature established by Miklas and Porch (2010). QTL names consist of an abbreviated trait name, the chromosome of detection, unique number identifier on the chromosome, and the population of detection in superscript. QTL detected by multiple years or methods are listed below the putative QTL. Population 76 was derived from B14311/Zenith, and Population 86 was derived from B14311/B12724. [1]Chr: chromosome number; [2]Peak Pos: genetic position of the peak LOD; [3]LOD: logarithm of odds; [4]R^2: percentage of phenotypic variation explained; [5]a: additive effect of the allele donated by breeding line B14311

Figure 1. US production of black beans for the year 2016.

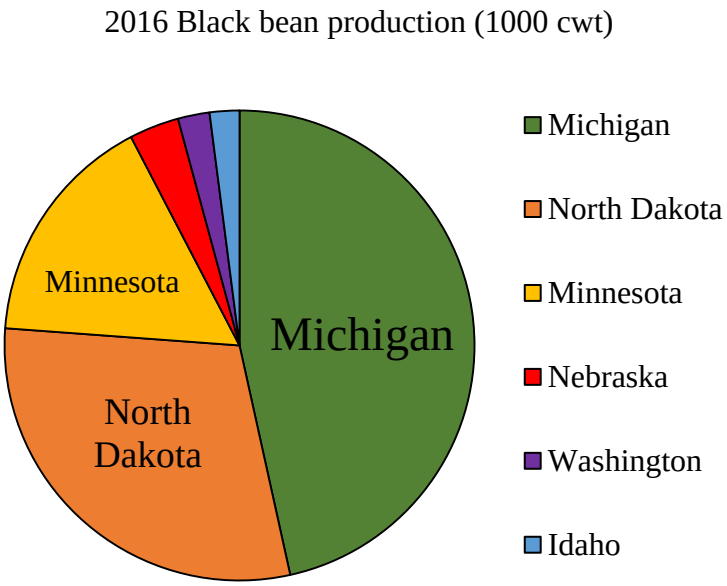

Michigan led the nation with 113,624 US tons produced (47% of total production). Data: 2017 USDA-NASS Crop Production Summary.

Figure 2. US per capita consumption of *P. vulgaris* dry beans.

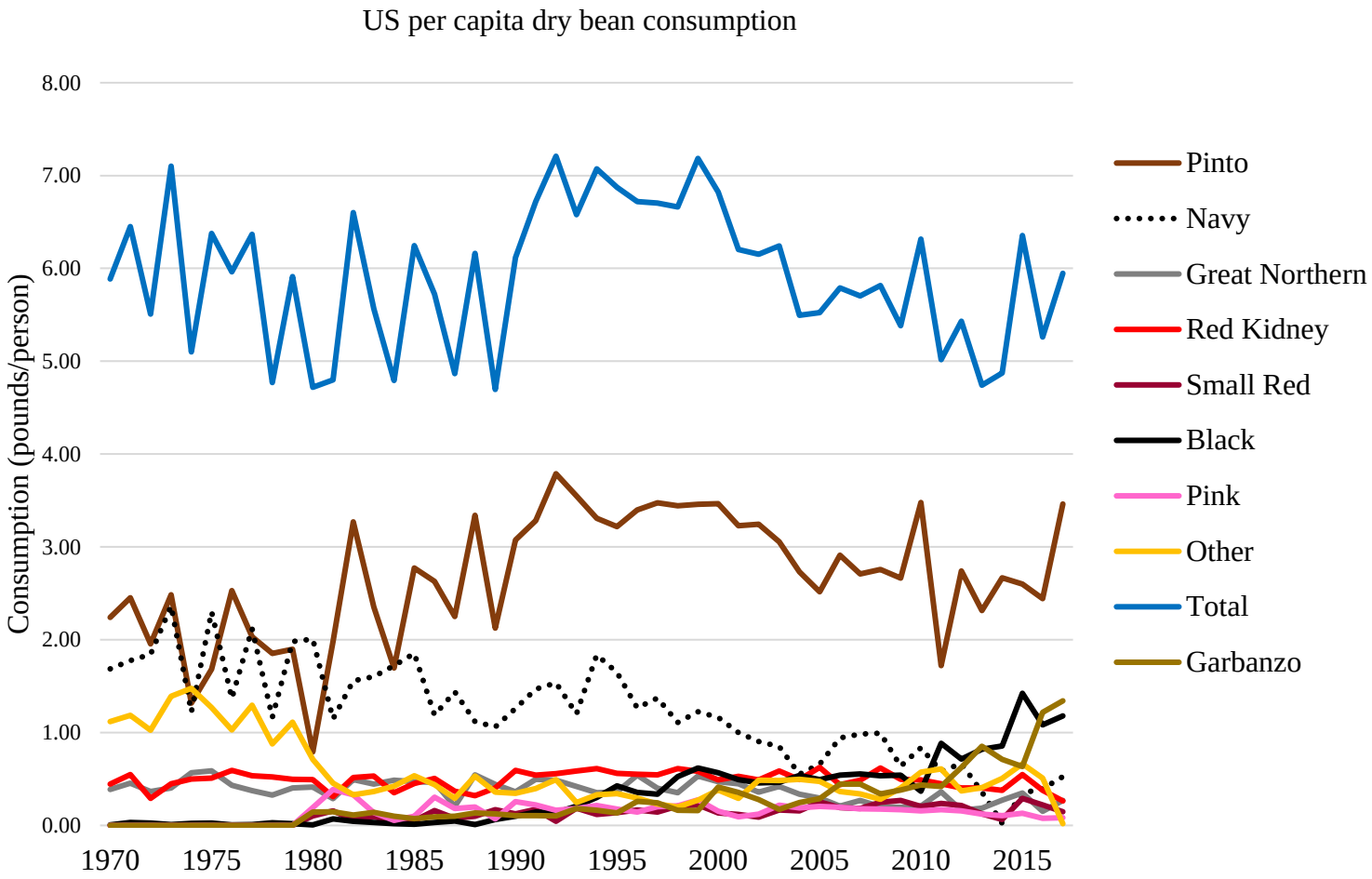

Market types classified as "other" include small white, cranberry, and all other dry edible beans after 1979. Garbanzo beans (*Cicer aritinum*) are also included for comparison. Data: Oct. 2017 Vegetable and Pulse Yearbook Table 5. USDA-ERS.

Figure 3. US per capita consumption of black beans.

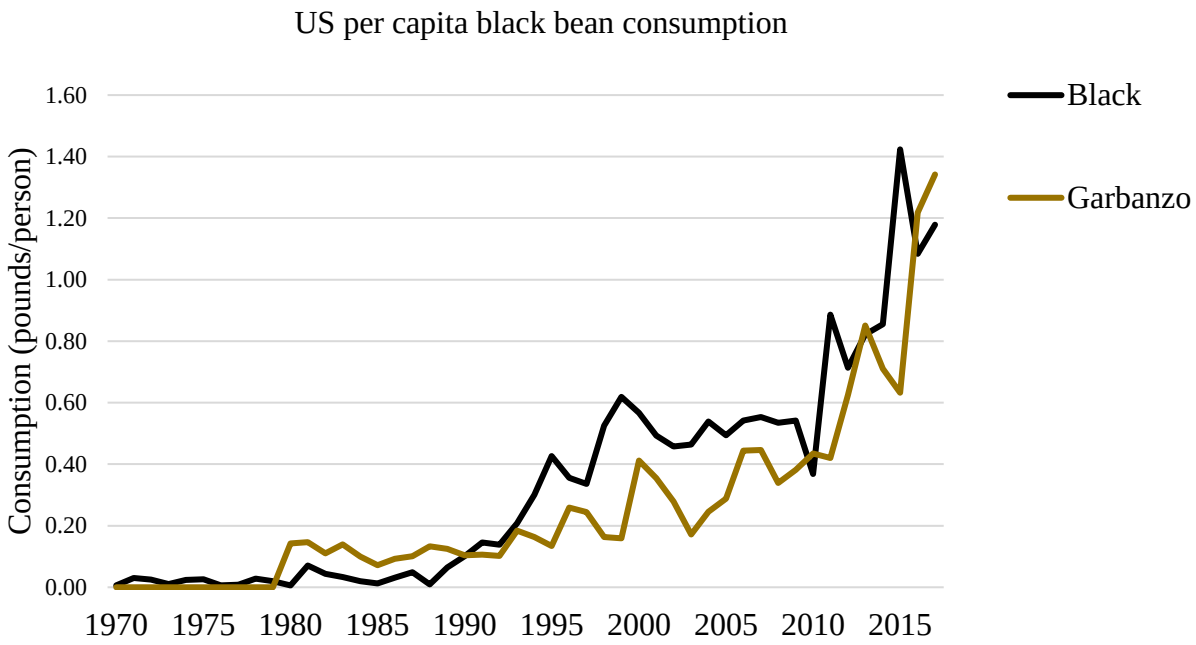

Consumption of black beans (*Phaseolus vulgaris*) is compared with consumption of garbanzo beans (*Cicer arietinum*). Data: Oct. 2017 Vegetable and Pulse Yearbook Table 5. USDA-ERS.

Figure 4. Canning quality evaluation guidelines.

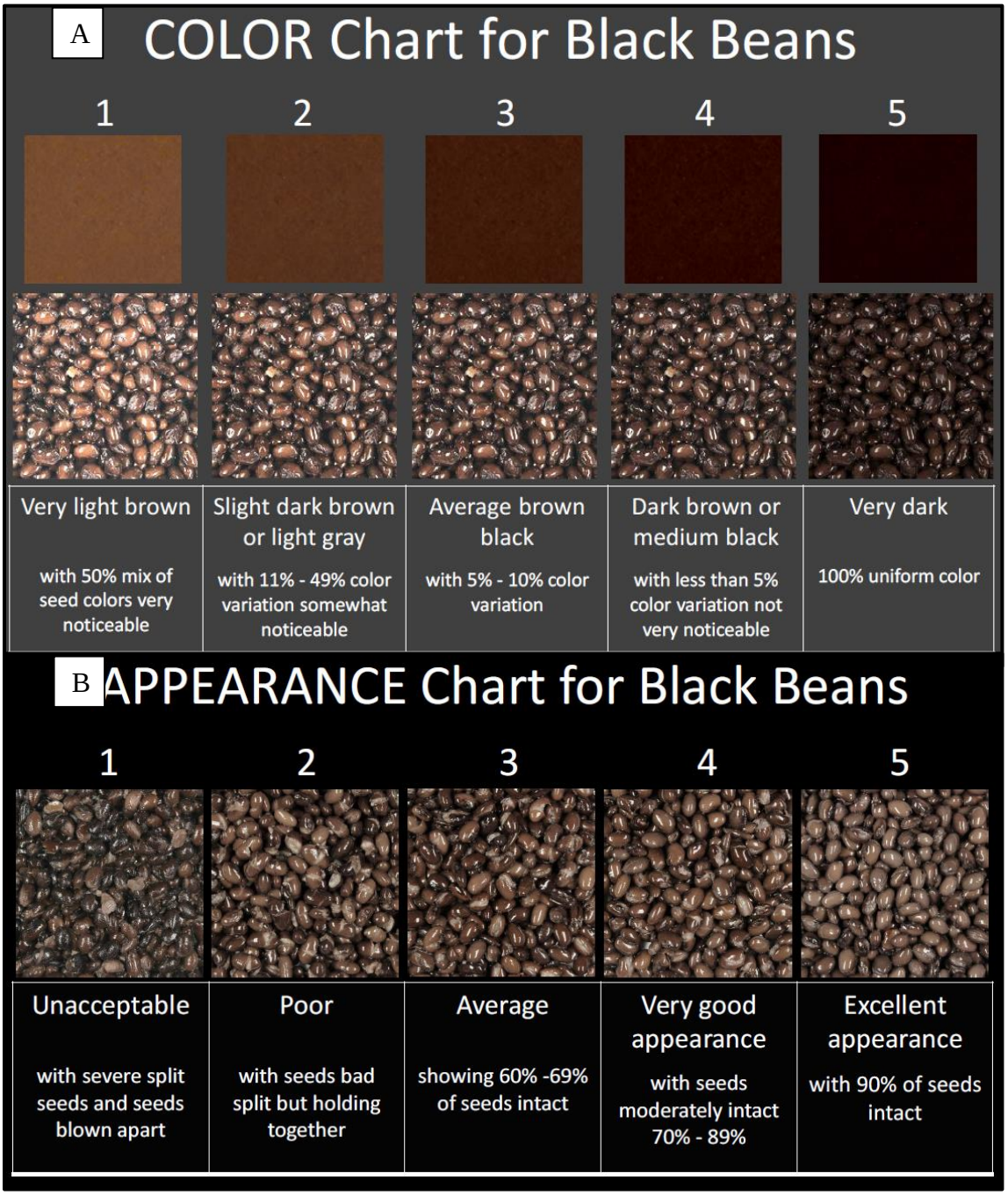

Evaluation charts were developed by Mendoza et al. (2017) and provided to reviewers during evaluations. Canned bean color and canned bean appearance are rated as independent traits.
A: Color ratings are based on the perceived color of the seed coat darkness.
B: Appearance ratings are mostly based on seed coat integrity, but may take into account brine consistency, clumping, extruded starch, and seed size.

Figure 5. Distribution of color ratings for Population 76 (B14311/Zenith) and Population 86 (B14311/B12724).

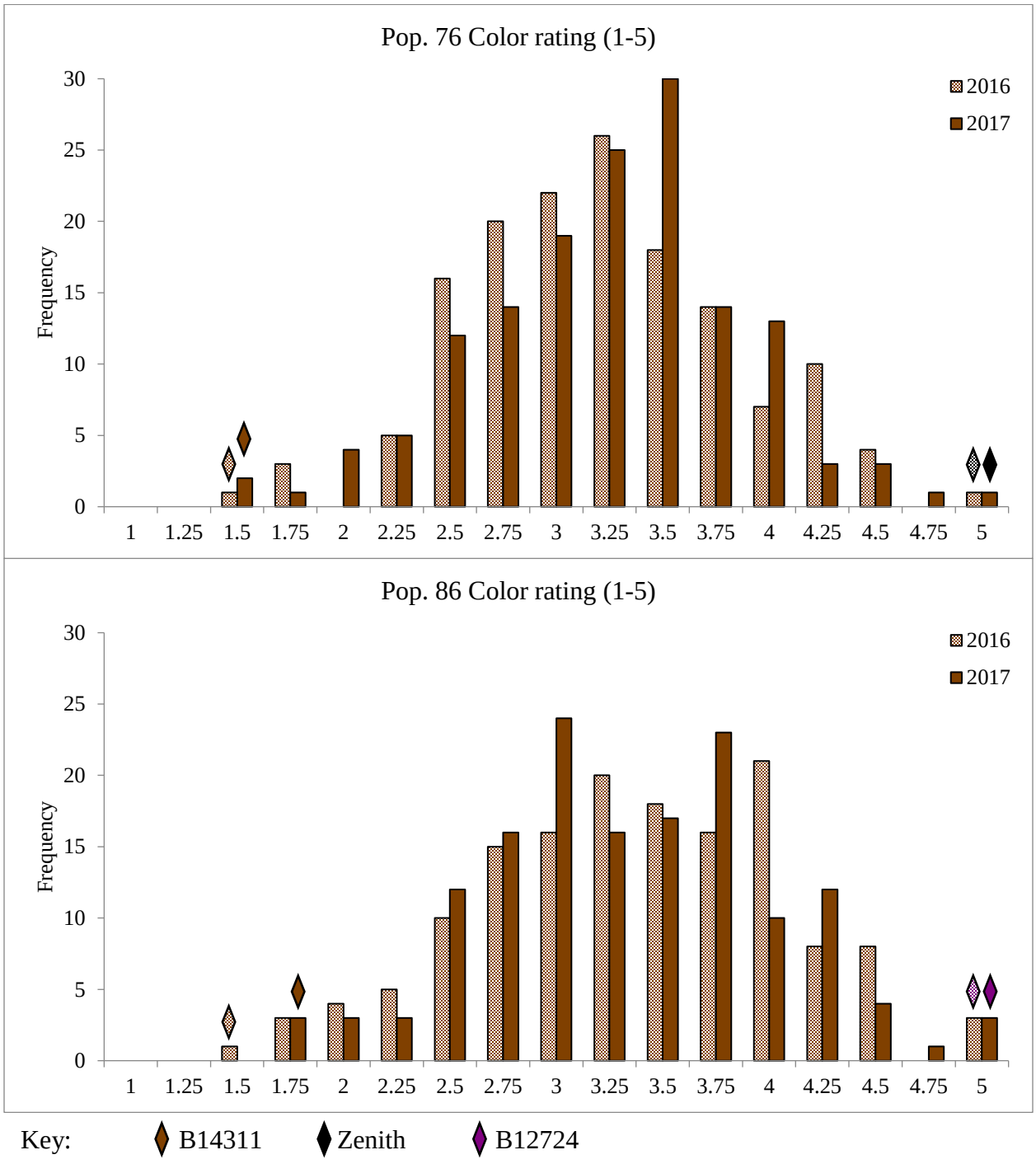

Color ratings for each genotype were averaged across reviewers within years.

Figure 6. Distribution of CIELAB color values in Population 76 (B14311/Zenith).

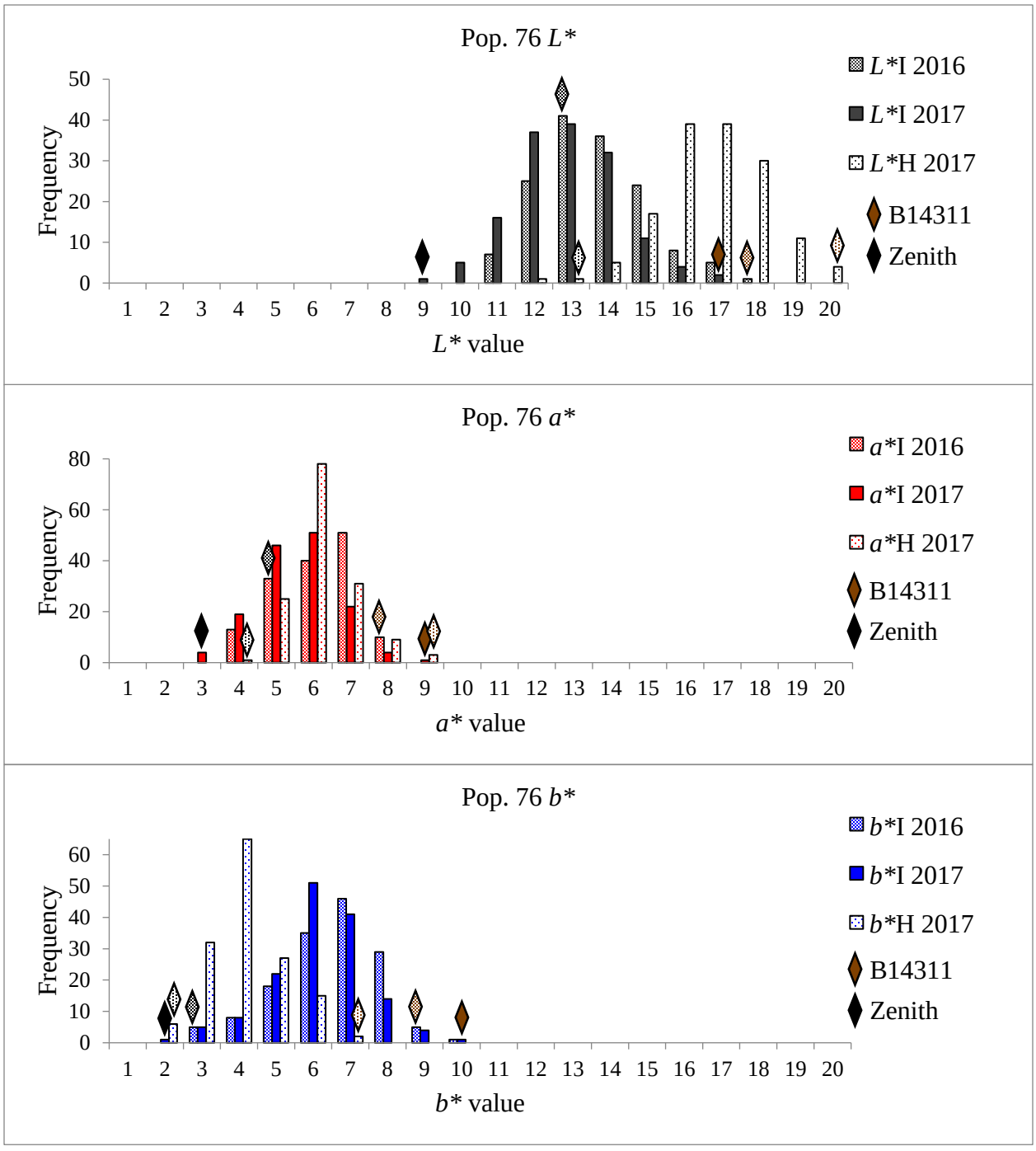

'I' indicates values measured by ImageJ analysis and 'H' indicates values measured by a Hunter Labscan.

Figure 7. Distribution of CIELAB color values in Population 86 (B14311/B12724).

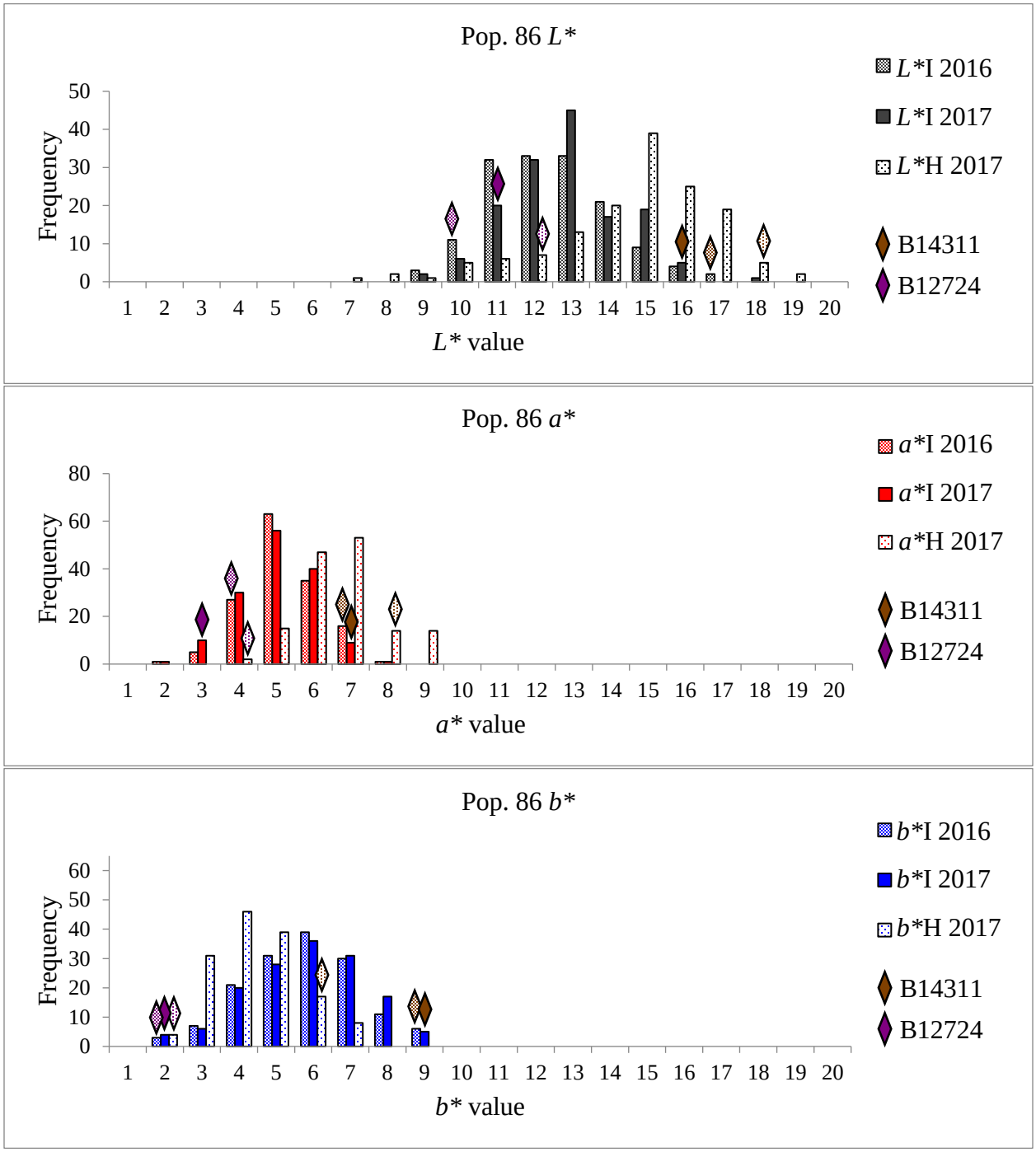

'I' indicates values measured by ImageJ analysis and 'H' indicates values measured by a Hunter Labscan.

Figure 8. Distribution of canning quality traits for Population 76 (B14311/Zenith) and Population 86 (B14311/B12724).

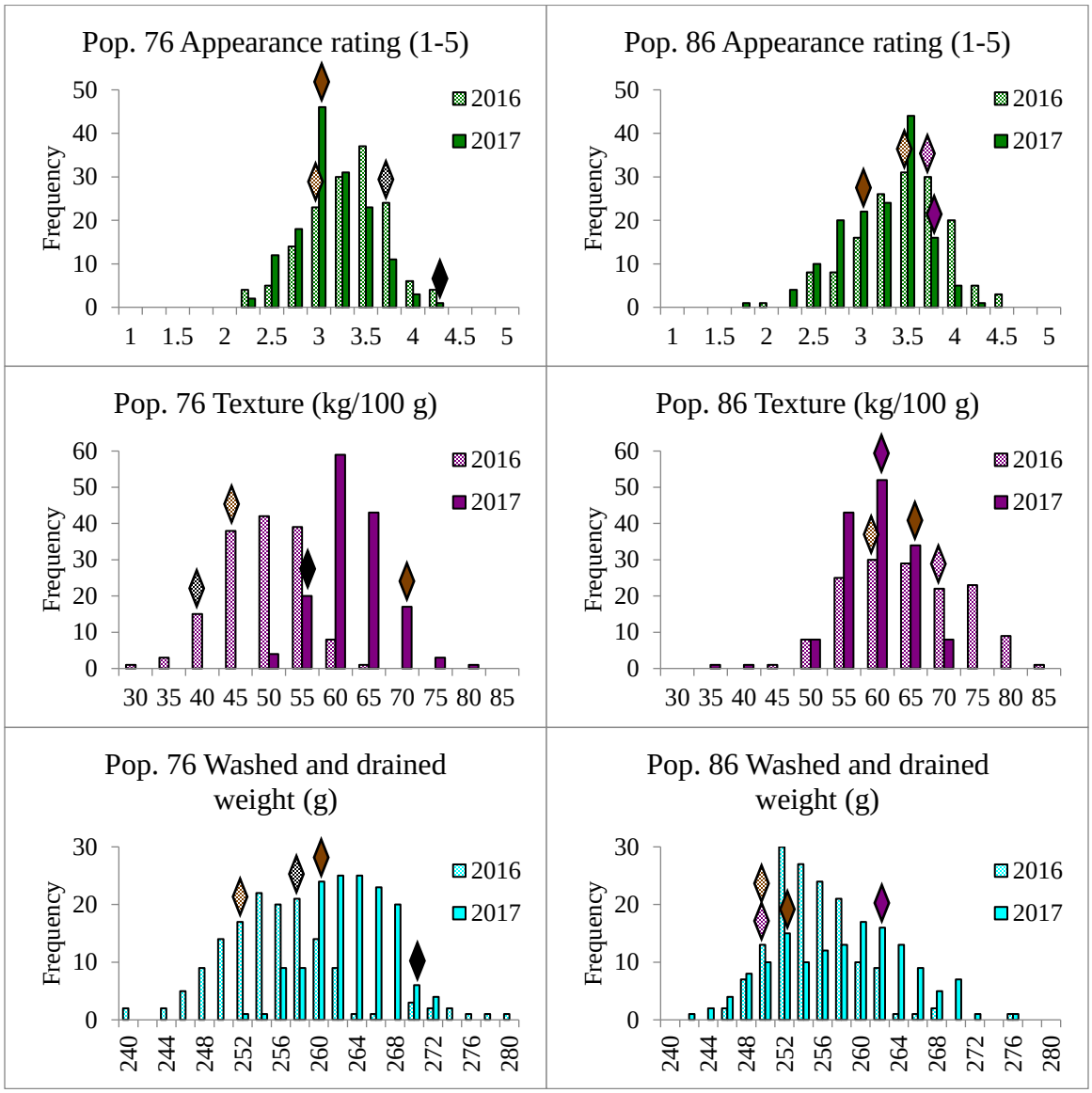

Key: B14311 Zenith B12724

Appearance ratings for each genotype were averaged across reviewers within years. Washed and drained weights and textures were not replicated within years.

Figure 9. Heritability estimates of canning quality traits in two black bean RIL populations.

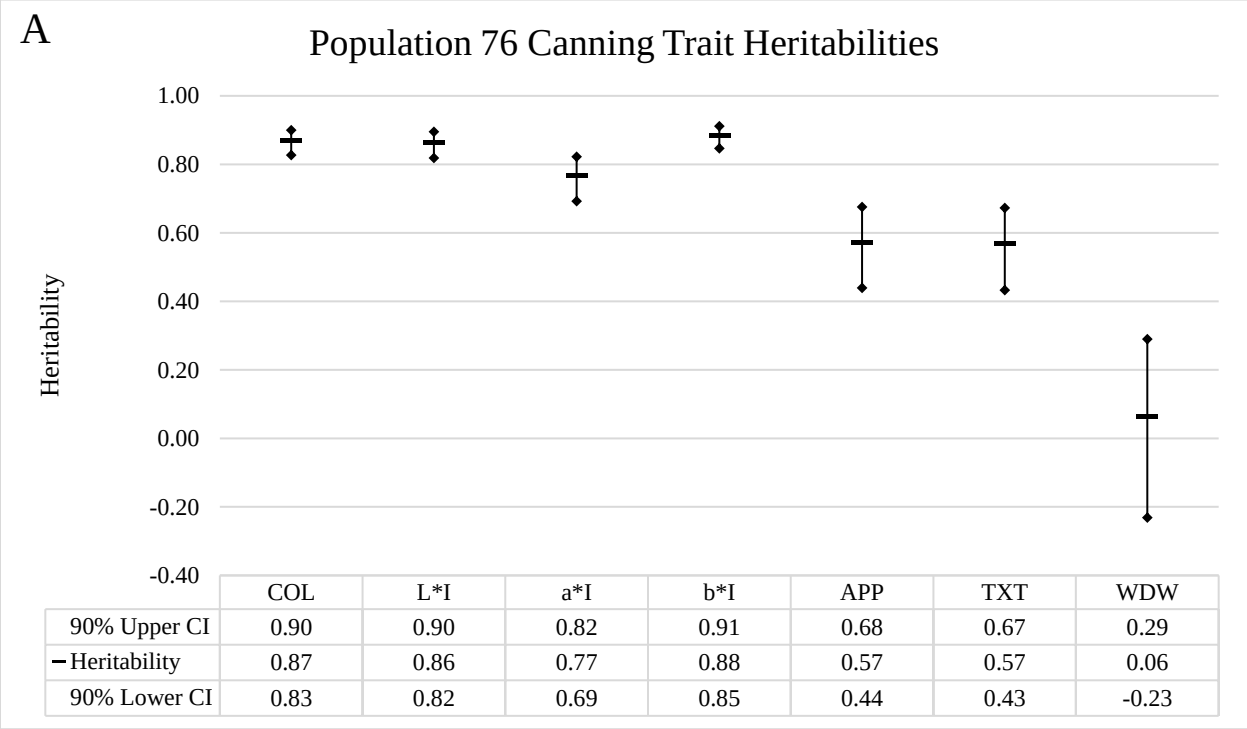

	COL	L*I	a*I	b*I	APP	TXT	WDW
90% Upper CI	0.90	0.90	0.82	0.91	0.68	0.67	0.29
Heritability	0.87	0.86	0.77	0.88	0.57	0.57	0.06
90% Lower CI	0.83	0.82	0.69	0.85	0.44	0.43	-0.23

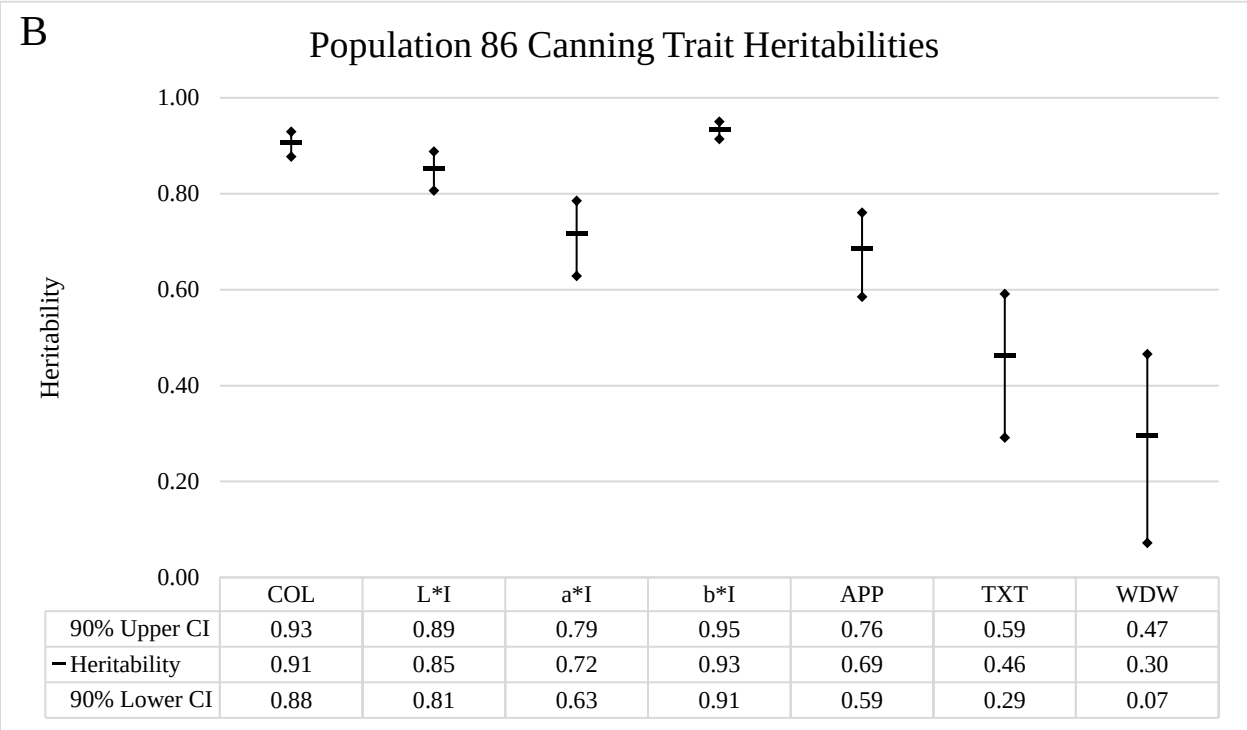

	COL	L*I	a*I	b*I	APP	TXT	WDW
90% Upper CI	0.93	0.89	0.79	0.95	0.76	0.59	0.47
Heritability	0.91	0.85	0.72	0.93	0.69	0.46	0.30
90% Lower CI	0.88	0.81	0.63	0.91	0.59	0.29	0.07

A: Population 76 is derived from B14311/Zenith.
B: Population 86 is derived from B14311/B12724.

Figure 10. Distribution of agronomic traits in two black bean RIL populations.

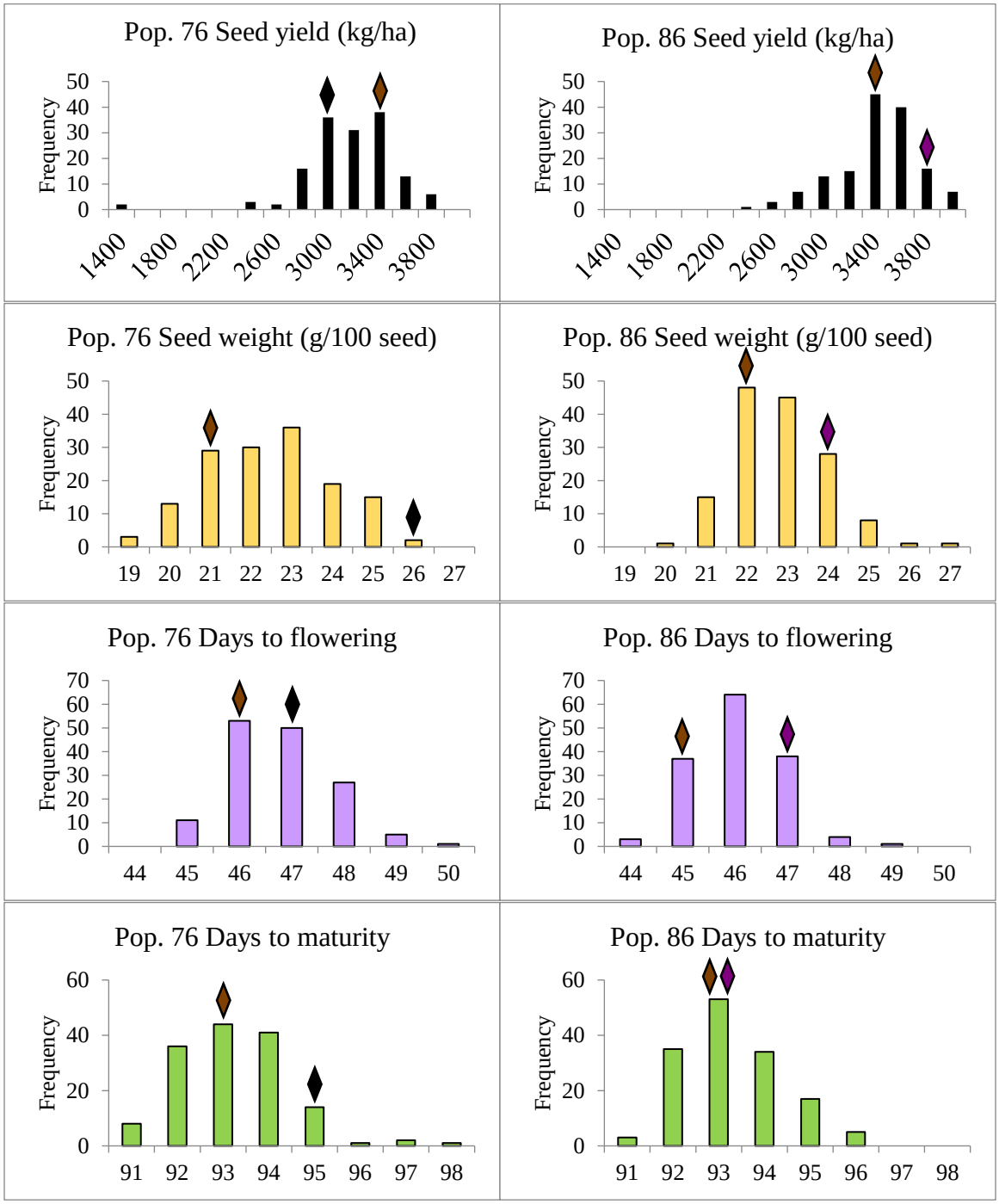

Figure 10. (cont'd)

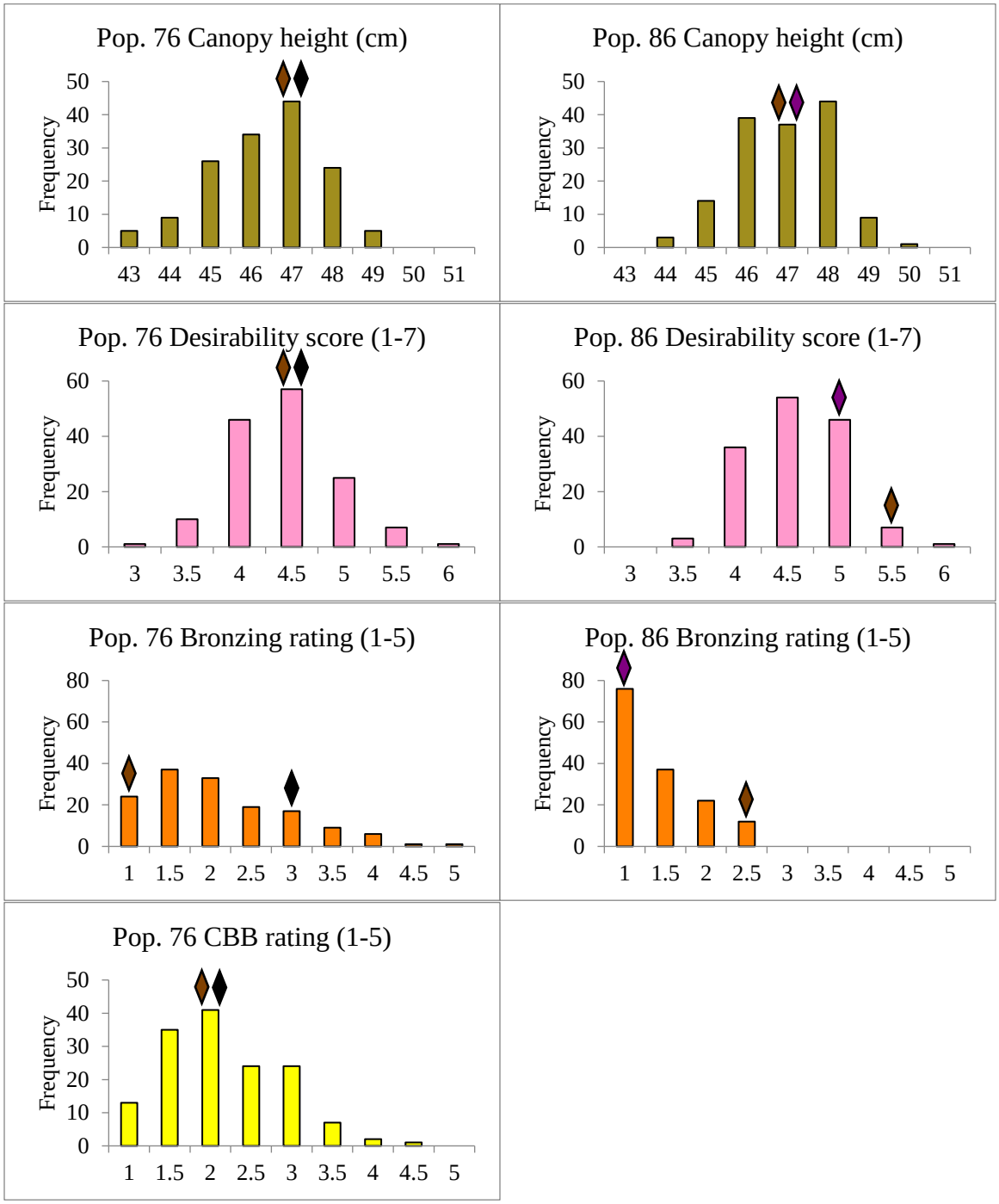

Key: B14311 Zenith B12724

Measurements for each genotype were averaged across 2017 field replications.

Figure 11. Regression of color components and mean visual rating of canned color.

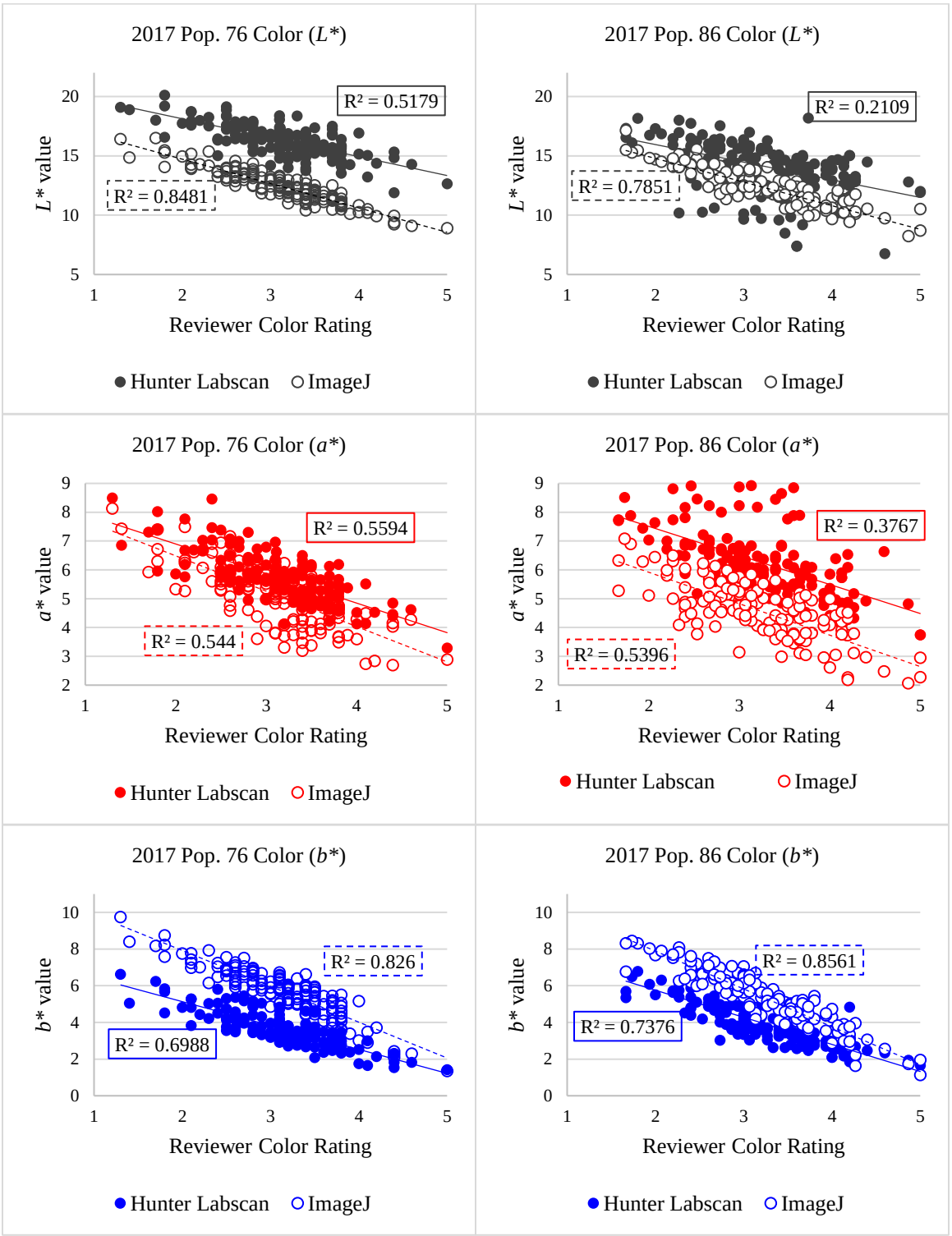

ImageJ gives more precise measurements, and *L** and *b** are good descriptors of perceived color.

Figure 12. QTL graphs for Population 76 (B14311/Zenith).

A: Pop. 76 Pv01 (no QTL detected)

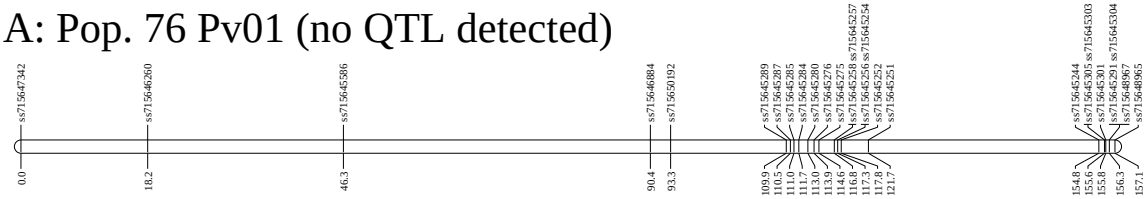

B: Pop. 76 Pv02

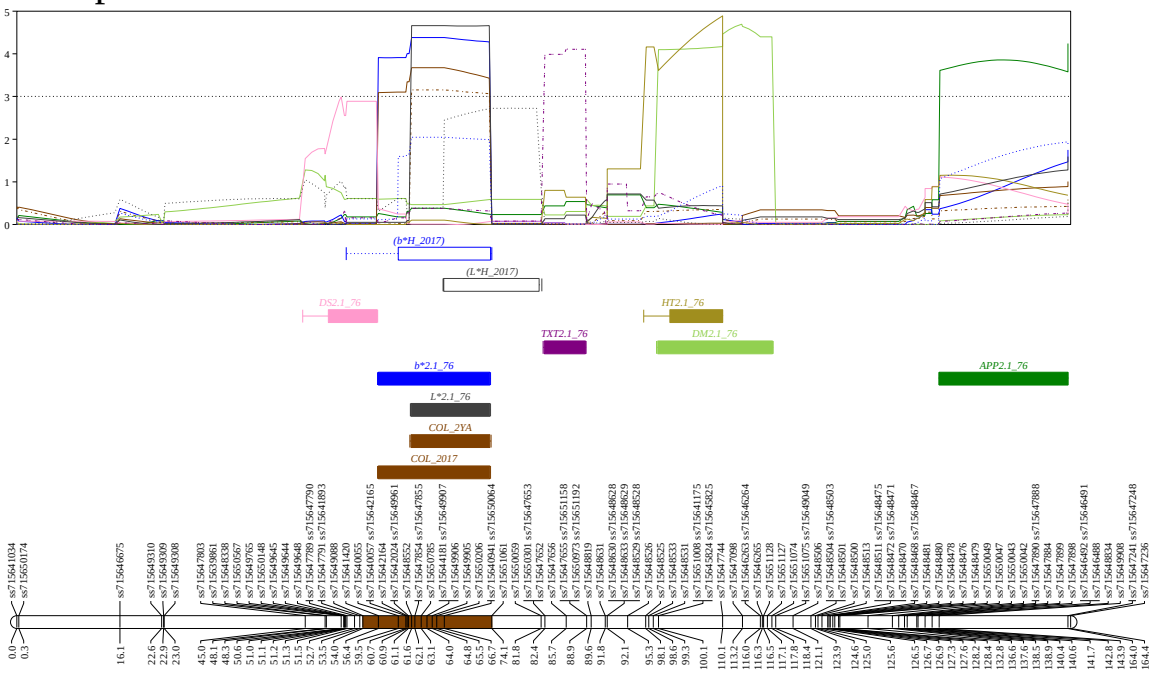

Figure 12. (cont'd)

C: Pop. 76 Pv03

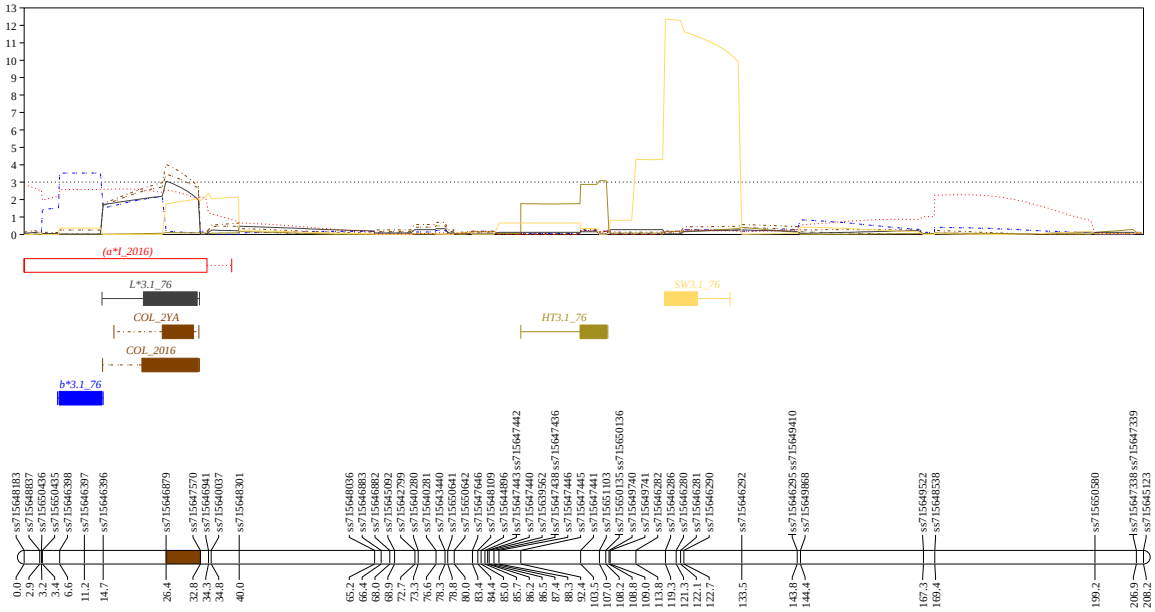

D: Pop. 76 Pv04

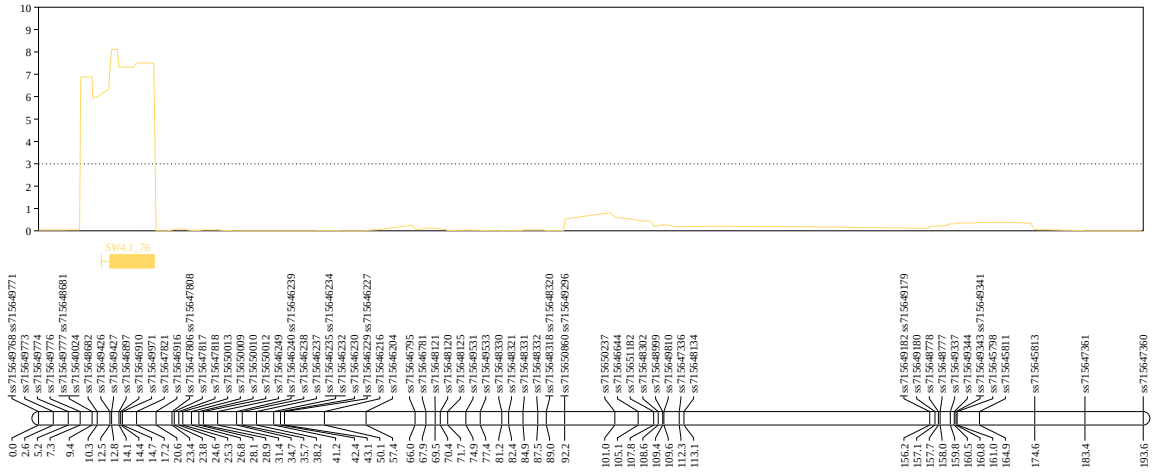

Figure 12. (cont'd)

E: Pop. 76 Pv05

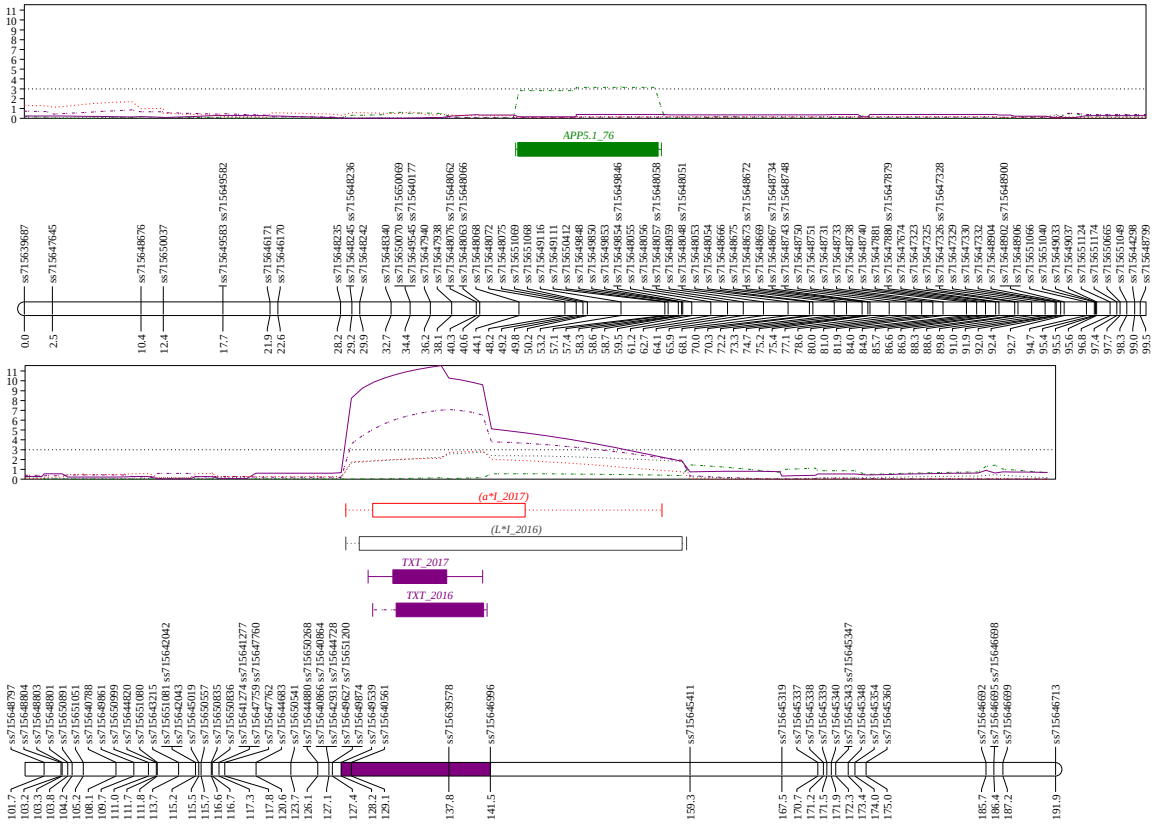

F: Pop. 76 Pv06

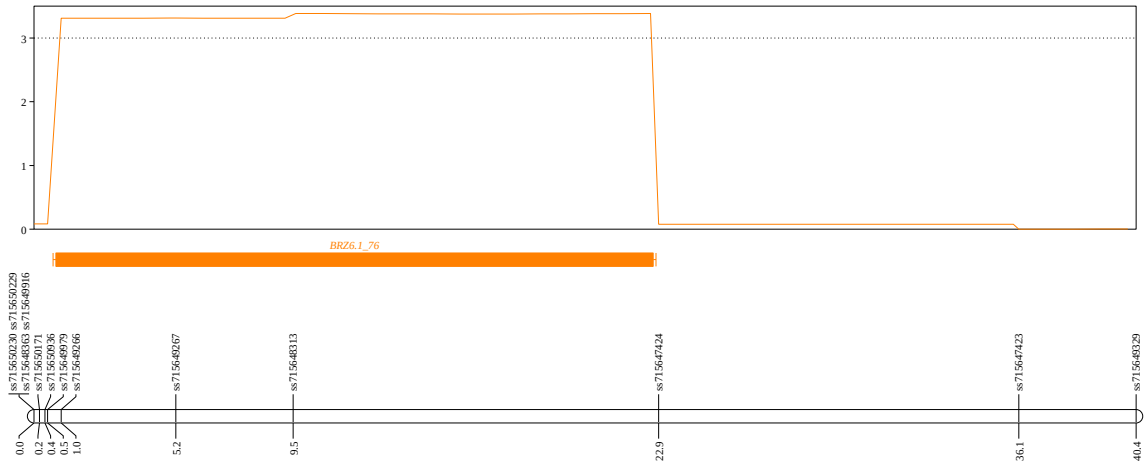

Figure 12. (cont'd)

G: Pop. 76 Pv07

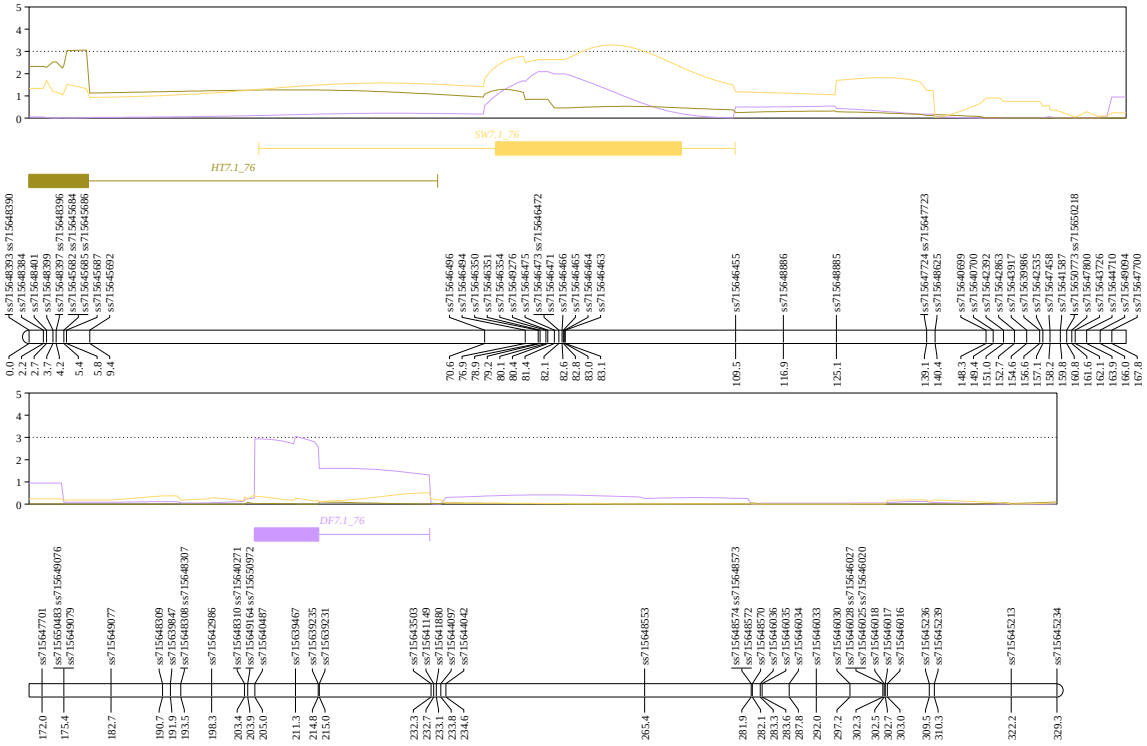

Figure 12. (cont'd)

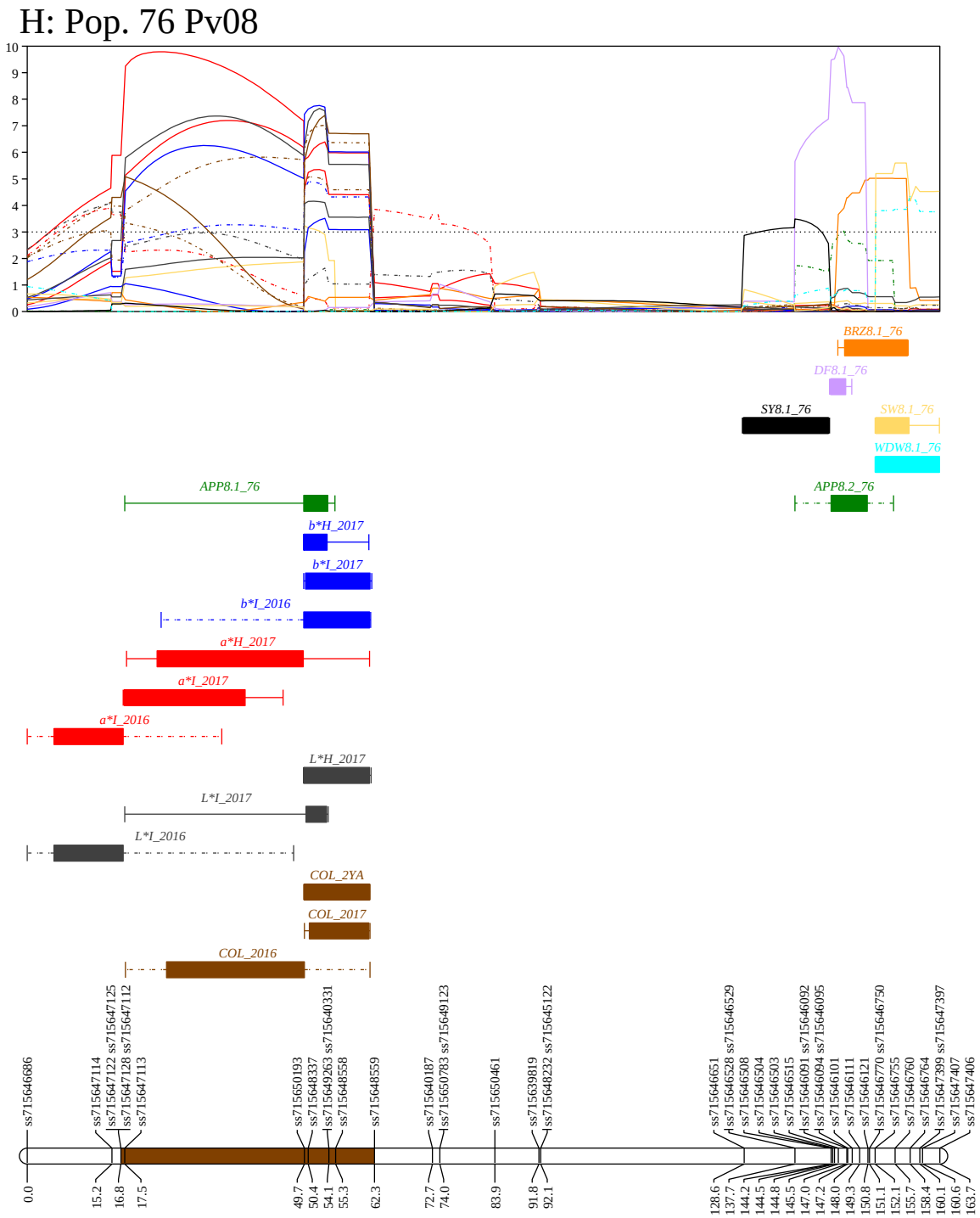

Figure 12. (cont'd)

I: Pop. 76 Pv09

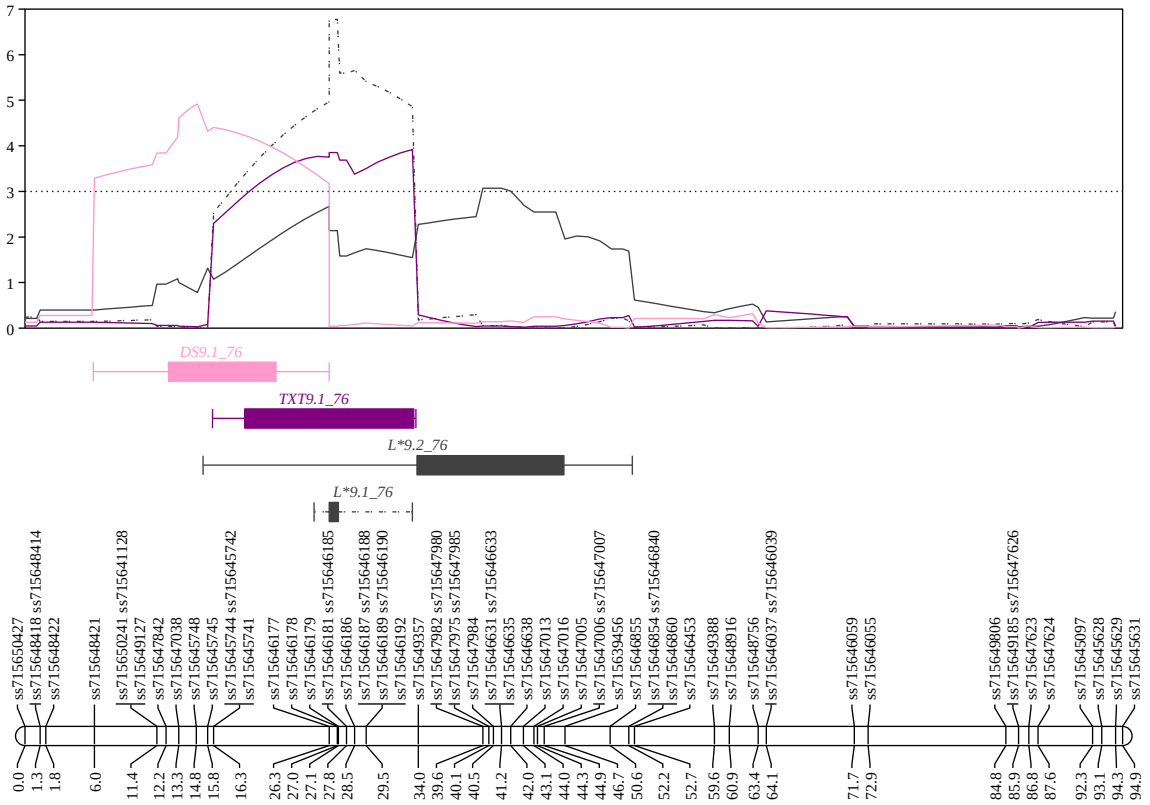

J: Pop. 76 Pv10 (no QTL detected)

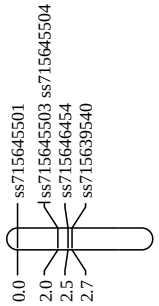

Figure 12. (cont'd)

K: Pop. 76 Pv11

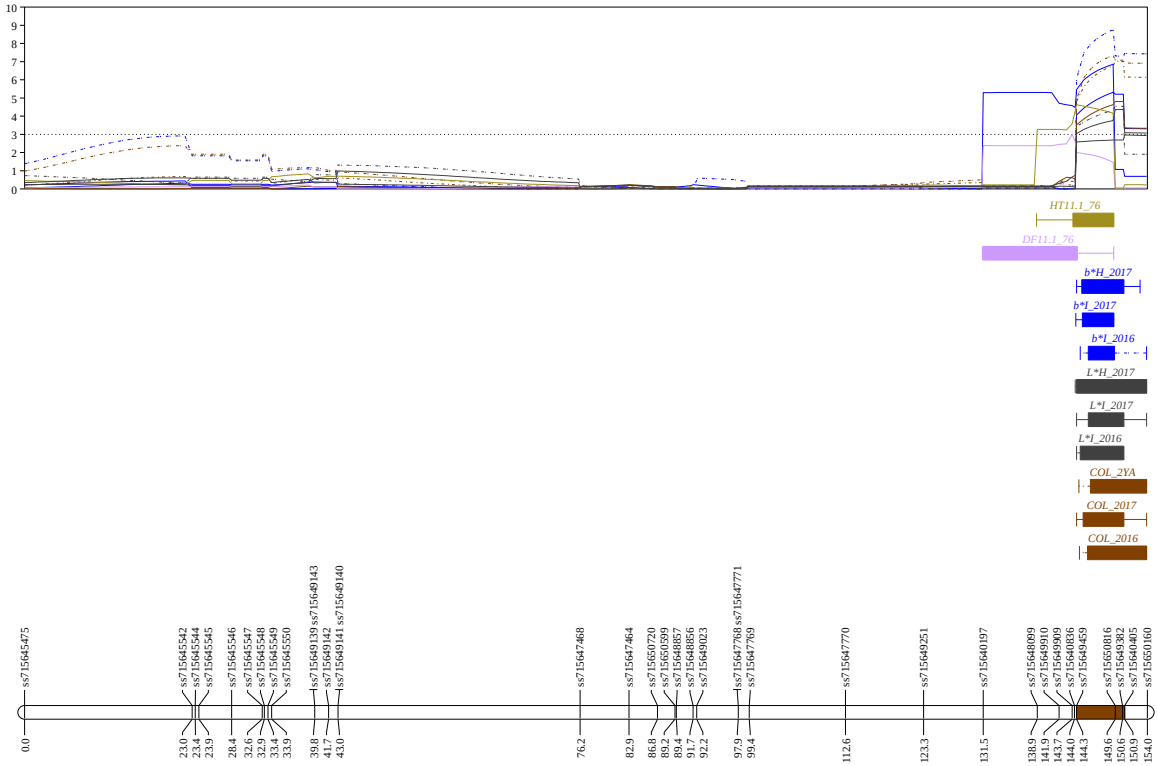

SNP markers and their genetic positions in centimorgans (cM) are shown on linkage maps. Abbreviations: COL: canned color rating, APP: canned appearance rating, TXT: texture; WDW: washed and drained weight; SY: seed yield, SW: 100-seed weight, DF: days to flowering, DM: days to maturity, HT: canopy height, DS: desirability score, BRZ: ozone bronzing, CBB: common bacterial blight resistance

Figure 13. QTL graphs for Population 86 (B14311/B12724).

A: Pop. 86 Pv01

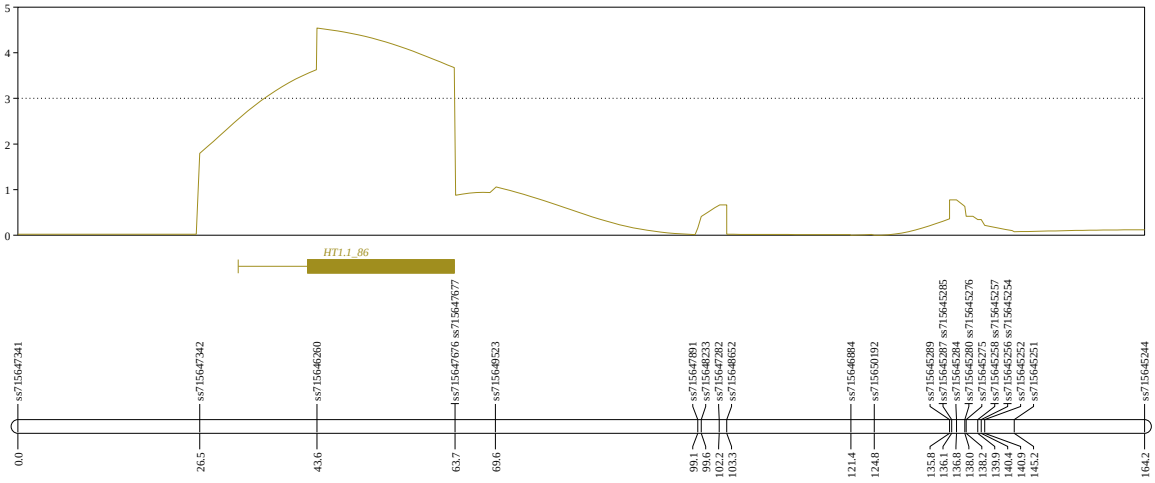

B: Pop. 86 Pv02

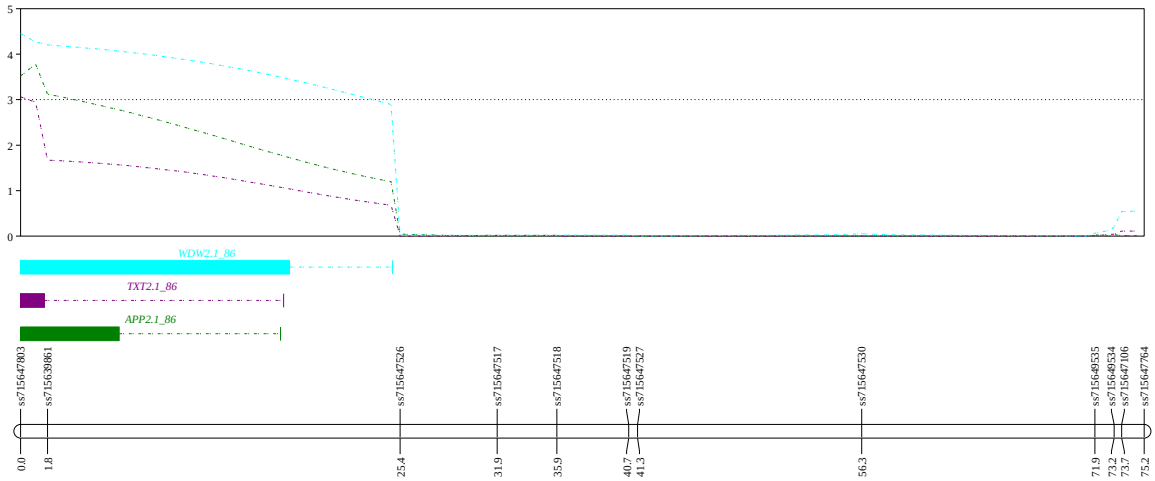

Figure 13. (cont'd).

C: Pop. 86 Pv03

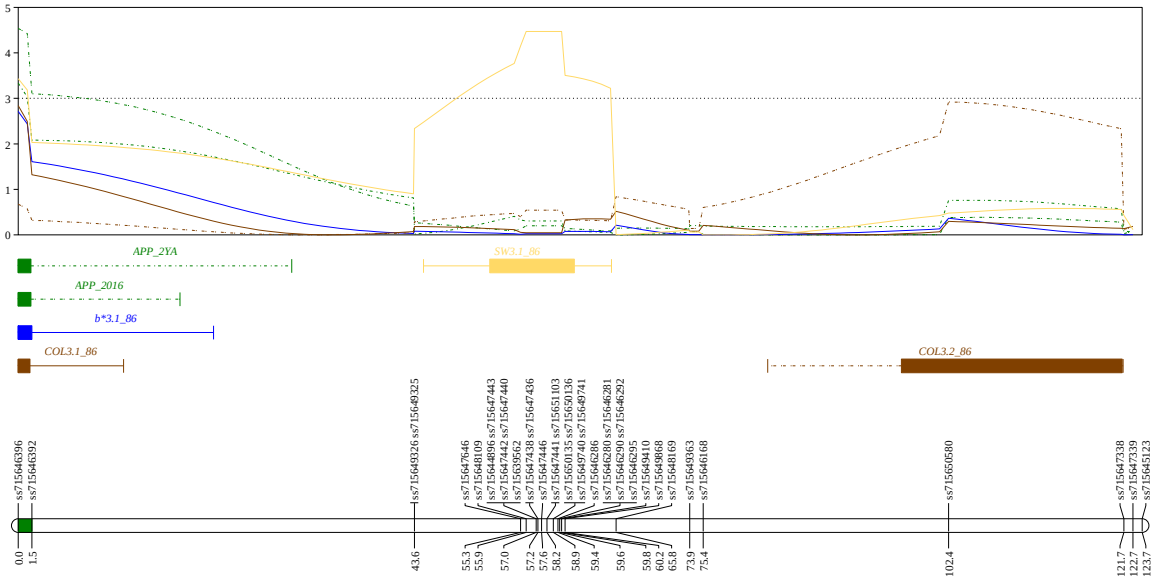

D: Pop. 86 Pv04

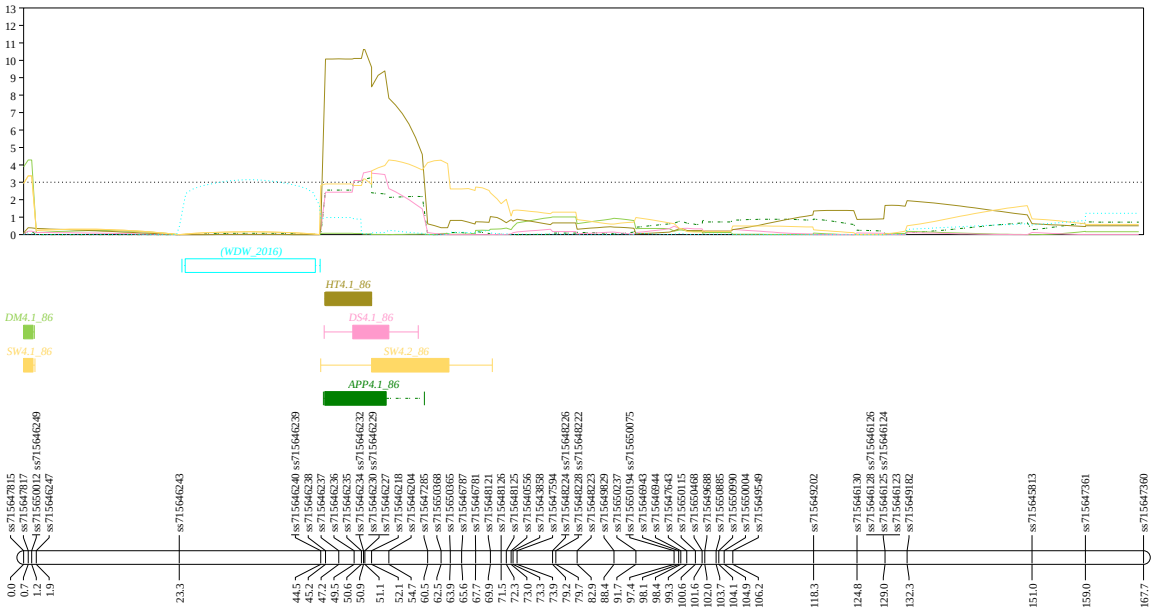

Figure 13. (cont'd).

E: Pop. 86 Pv05

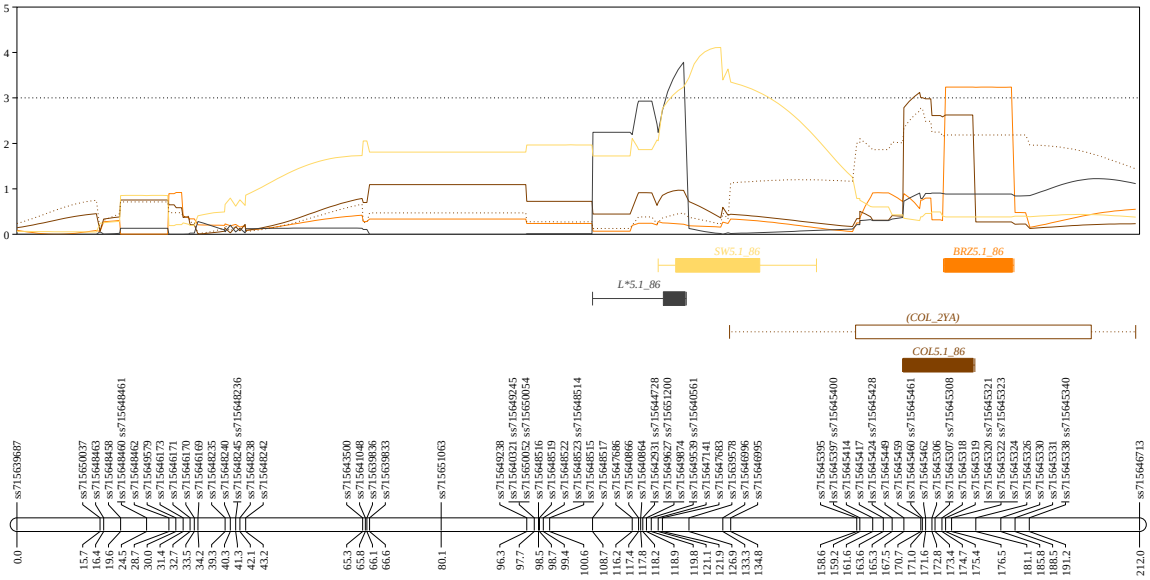

F: Pop. 86 Pv06

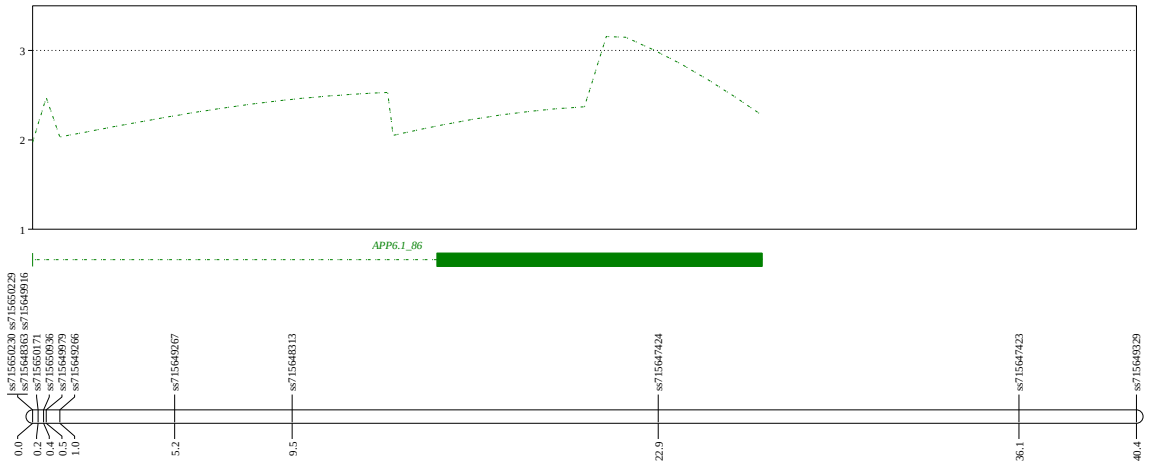

Figure 13. (cont'd).

G: Pop. 86 Pv07

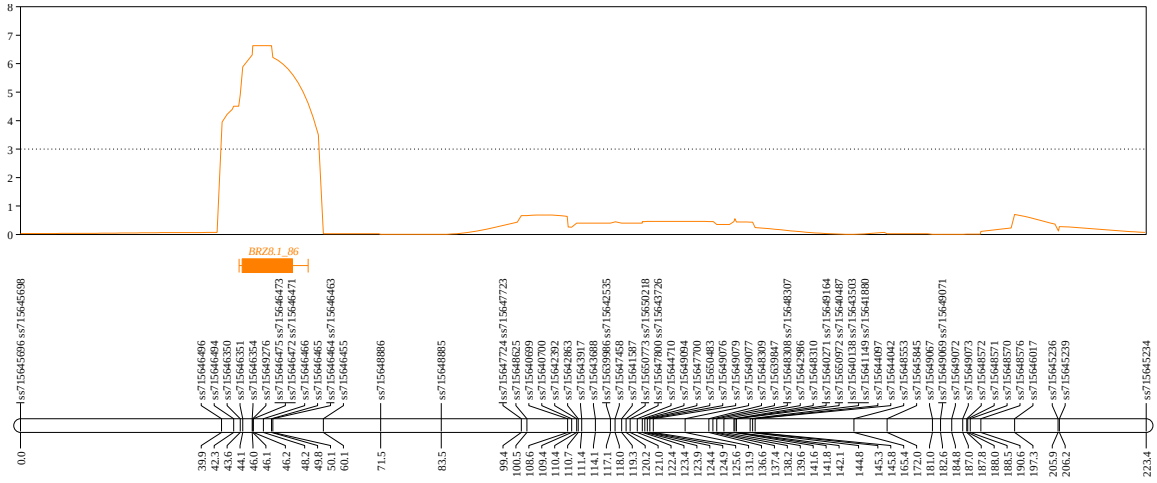

H: Pop. 86 Pv08

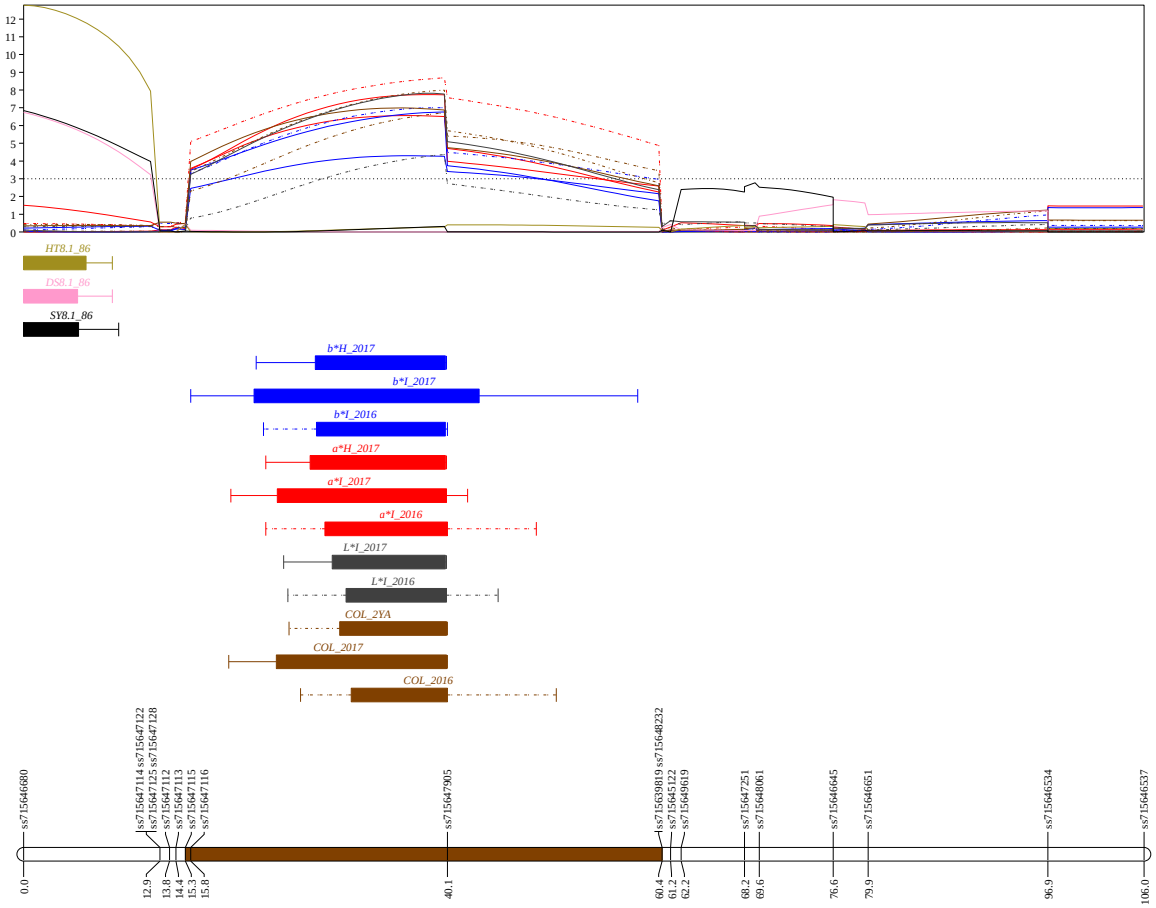

Figure 13. (cont'd).

I: Pop. 86 Pv09

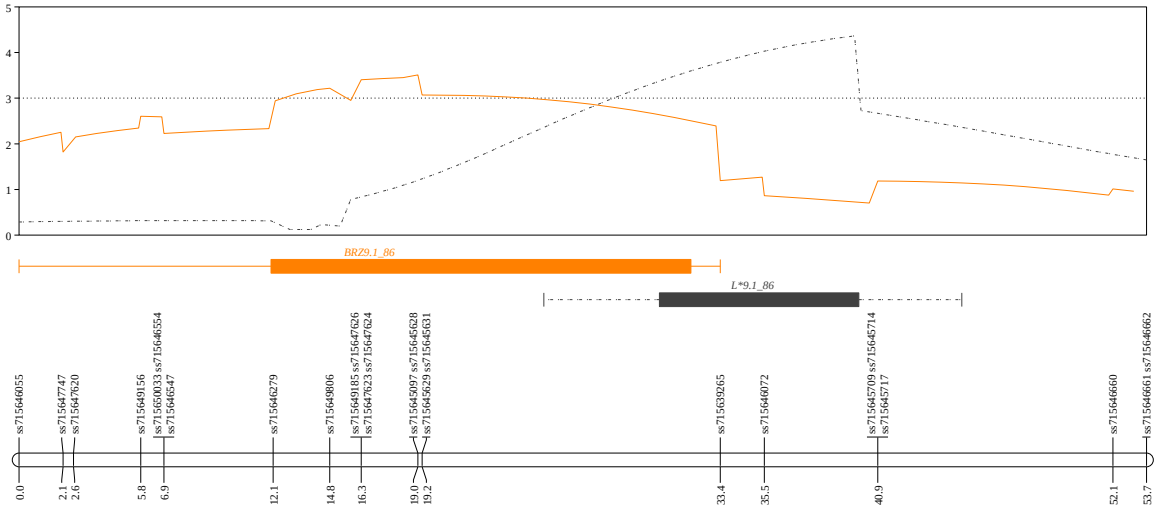

J: Pop. 86 Pv10

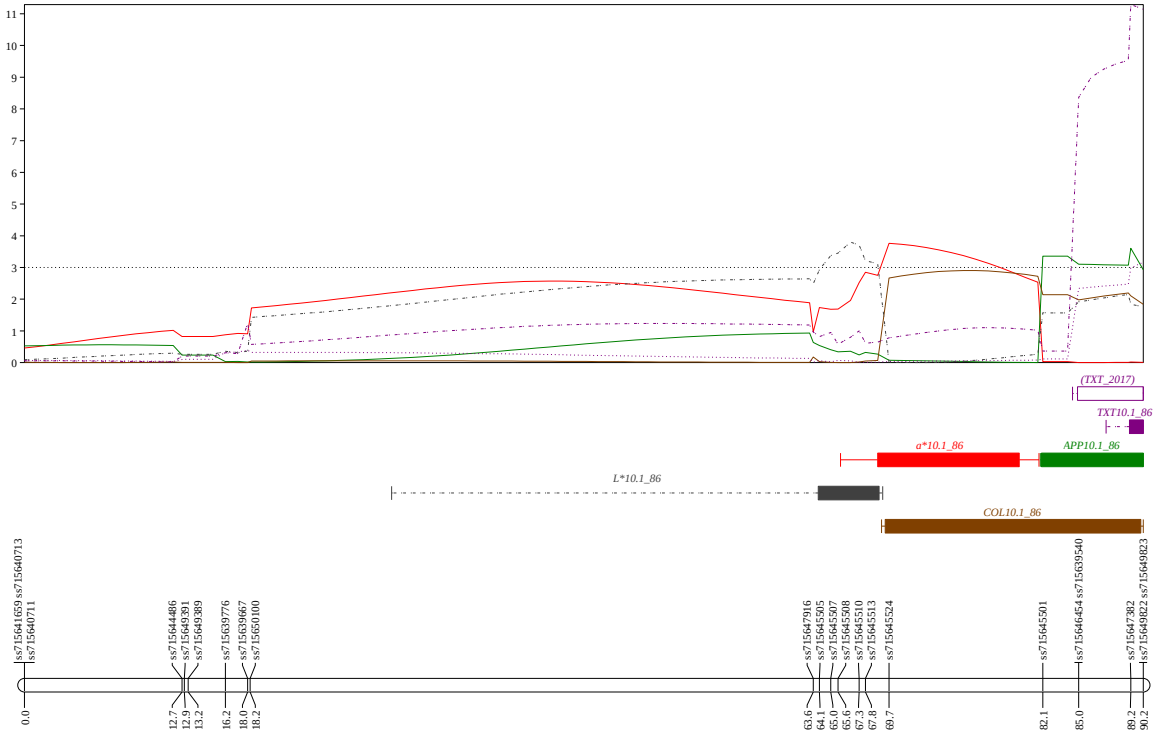

Figure 13. (cont'd).

K: Pop. 86 Pv11

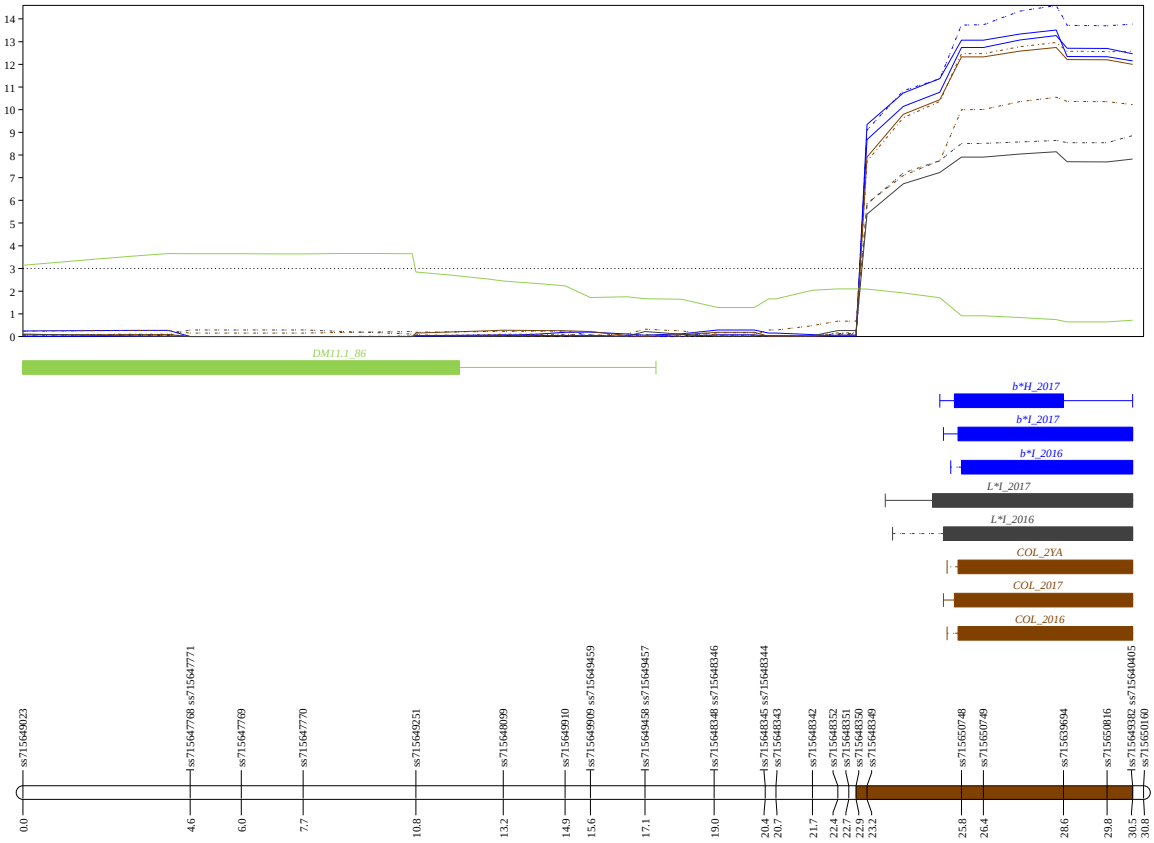

SNP markers and their genetic positions in centimorgans (cM) are shown on linkage maps. Abbreviations: COL: canned color rating, APP: canned appearance rating, TXT: texture; WDW: washed and drained weight; SY: seed yield, SW: 100-seed weight, DF: days to flowering, DM: days to maturity, HT: canopy height, DS: desirability score, BRZ: ozone bronzing, CBB: common bacterial blight resistance

Figure 14. Screening parents of Populations 76 and 86 with NDSU InDel markers near major color retention QTL on Pv08 and Pv11.

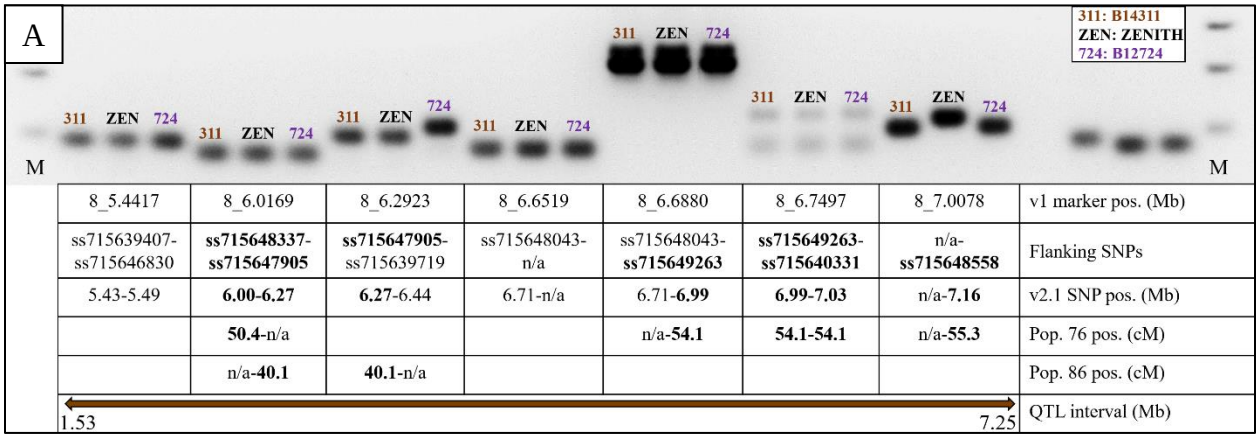

8_5.4417	8_6.0169	8_6.2923	8_6.6519	8_6.6880	8_6.7497	8_7.0078	v1 marker pos. (Mb)
ss715639407-ss715646830	**ss715648337-ss715647905**	**ss715647905**-ss715639719	ss715648043-n/a	ss715648043-**ss715649263**	**ss715649263-ss715640331**	n/a-**ss715648558**	Flanking SNPs
5.43-5.49	**6.00-6.27**	**6.27**-6.44	6.71-n/a	6.71-**6.99**	**6.99-7.03**	n/a-**7.16**	v2.1 SNP pos. (Mb)
	50.4-n/a			n/a-**54.1**	**54.1-54.1**	n/a-**55.3**	Pop. 76 pos. (cM)
	n/a-**40.1**	**40.1**-n/a					Pop. 86 pos. (cM)
1.53						7.25	QTL interval (Mb)

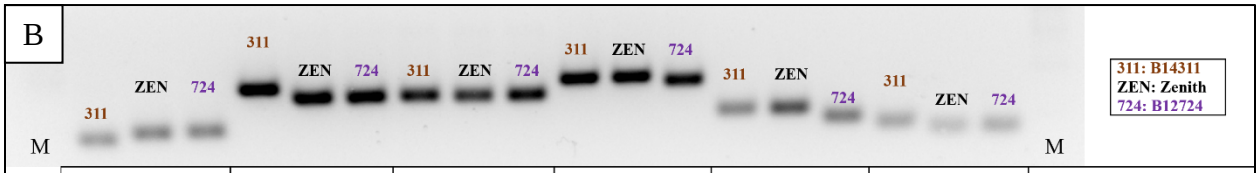

11_47.0739	11_47.7708	11_47.9412	11_48.4937	11_48.7818	11_49.5223	v1 marker pos. (Mb)
ss715647765-ss715647767	ss715648096-ss715648096	ss715648093-ss715648100	ss715649456-**ss715648349**	**ss715650748**-ss715641910	ss715650328-ss715649209	Flanking SNPs
50.68-50.75	51.50-51.53	51.72-51.75	52.23-**52.48**	**52.53**-52.54	52.96-53.17	v2.1 SNP pos. (Mb)
						Pop. 76 pos. (cM)
			n/a-**23.2**	**25.8**-n/a		Pop. 86 pos. (cM)
		52.16		52.84		QTL interval (Mb)

Markers were run on 3% agarose gels according to Moghaddam et al. (2014). InDel marker names correspond to their physical positions in the v1 dry bean genome. Flanking BARCBean6k_3 SNPs and their v2.1 physical positions are given. SNPs that were mapped in at least one mapping population are bolded.

A: InDel markers near COL8.1[76] and COL8.1[86]. COL QTL on Pv08 were significant over a 1.53-7.25 Mb interval estimated by the brown bar.

B: InDel markers near COL11.1[76] and COL11.1[86]. COL QTL on Pv11 were most significant over a 52.16-52.84 Mb interval estimated by the brown bar.

REFERENCES

REFERENCES

Akond, G.M.A., L. Khandaker, J. Berthold, L. Gates, K. Peters, H. Delong, and K. Hossain. 2011. Anthocyanin, total polyphenols and antioxidant activity of common bean. Am. J. Food Technol. 6(5): 385–394.

Ariani, A., J.C. Berny Mier y Teran, and P. Gepts. 2016. Genome-wide identification of SNPs and copy number variation in common bean (*Phaseolus vulgaris* L.) using genotyping-by-sequencing (GBS). Mol. Breed. 36(7): 1–11.

Ariyarathne, H.M., D.P. Coyne, G. Jung, P.W. Skroch, A.K. Vidaver, J.R. Steadman, P.N. Miklas, and M.J. Bassett. 1999. Molecular mapping of disease resistance genes for halo blight, common bacterial blight, and bean common mosaic virus in a segregating population of common bean. J. Am. Soc. Hortic. Sci. 124(6): 654–662.

Arts, I.C.W., and P.C.H. Hollman. 2005. Polyphenols and disease risk in epidemiologic studies. Am. J. Clin. Nutr. 81(January): 317S–325S.

Bassett, M.J. 1994. Tight linkage of purple pod character and the complex C locus in common bean. J. Hered. 85(4): 288–290.

Bassett, M.J. 2007. Genetics of seed coat color and pattern in common bean. p. 239–315. *In* Janick, J. (ed.), Plant Breeding Reviews. John Wiley & Sons, Inc.

Bednar, R.A., and J.R. Hadcock. 1988. Purification and characterization of chalcone isomerase from soybeans. J. Biol. Chem. 263(20): 9582–9588.

Beninger, C.W., and G.L. Hosfield. 2003. Antioxidant activity of extracts, condensed tannin fractions, and pure flavonoids from *Phaseolus vulgaris* L. seed coat color genotypes. J. Agric. Food Chem. 51(27): 7879–7883.

Blair, M.W., F. Pedraza, H.F. Buendía, E. Gaitán-Solís, S.E. Beebe, P. Gepts, and J. Tohme. 2003. Development of a genome-wide anchored microsatellite map for common bean (*Phaseolus vulgaris* L.). Theor. Appl. Genet. 107(8): 1362–1374.

Bonds, J.K. 2017. Pulses production expanding as consumers cultivate a taste for U.S. lentils and chickpeas. United States Department of Agriculture- Economic Research Service.

Brand-Miller, J., S. Hayne, P. Petocz, and S. Colagiuri. 2003. Low–glycemic index diets in the management of diabetes. Diabetes Care 26(8): 2261 LP-2267.

Bravo, L. 1998. Polyphenols: chemistry, dietary sources, metabolism, and nutritional significance. Nutr. Rev. 56(11): 317–333.

Busse, M., and Ä. Bäumer-Schleinkofer. 1996. Ewald Hering und die Gegenfarbtheorie. NTM Int. J. Hist. Ethics Nat. Sci. Technol. Med. 4(1): 159–172.

Cheng, A.-X., X. Zhang, X.-J. Han, Y.-Y. Zhang, S. Gao, C.-J. Liu, and H.-X. Lou. 2018. Identification of chalcone isomerase in the basal land plants reveals an ancient evolution of enzymatic cyclization activity for synthesis of flavonoids. New Phytol. 217(2): 909–924.

Cichy, K.A., A.C. Fernandez, A. Kilian, J.D. Kelly, C.H. Galeano, S. Shaw, M.A. Brick, D. Hodkinson, and E. Troxtell. 2014. QTL analysis of canning quality and color retention in black beans (*Phaseolus vulgaris* L.). Mol. Breed. 33(1): 139–154.

CIE. 2008. ISO 1164-4. Part 4: CIE 1976 *L*a*b** Colour Space. Geneva, Switzerland.

Collard, B.C.Y., M.Z.Z. Jahufer, J.B. Brouwer, and E.C.K. Pang. 2005. An introduction to markers, quantitative trait loci (QTL) mapping and marker-assisted selection for crop improvement: The basic concepts. Euphytica 142(1–2): 169–196.

Corradini, E., P. Foglia, P. Giansanti, R. Gubbiotti, R. Samperi, and A. Lagana. 2011. Flavonoids: chemical properties and analytical methodologies of identification and quantitation in foods and plants. Nat. Prod. Res. 25(5): 469–495.

Diniz, A.L., M.I. Zucchi, L. Santini, L.L. Benchimol-Reis, M.H.P. Fungaro, and M.L.C. Vieira. 2014. Nucleotide diversity based on phaseolin and iron reductase genes in common bean accessions of different geographical origins. Genome 57(2): 69–77.

Doyle, J.., and J.. Doyle. 1991. DNA Isolation from Small Amount of Plant Tissue. Phytochem. Bull. 57: 13–15.

Elshire, R.J., J.C. Glaubitz, Q. Sun, J.A. Poland, K. Kawamoto, E.S. Buckler, and S.E. Mitchell. 2011. A robust, simple genotyping-by-sequencing (GBS) approach for high diversity species. PLoS One 6(5): 1–10.

Feenstra, W.J. 1960. Biochemical aspects of seedcoat colour inheritance in *Phaseolus vulgaris* L.

Fehr, W.R. 1991. Principles of Cultivar Development Vol I: Theory and Technique. 2nd ed. Iowa State University, Ames, IA.

Fourie, D., P.N. Miklas, and H.M. Ariyarathne. 2004. Genes conditioning halo blight resistance to races 1, 7, and 9 occur in a tight cluster. Annu. Rep. Bean Improv. Coop. 47: 103–104.

Foyer, C.H., H.-M. Lam, H.T. Nguyen, K.H.M. Siddique, R.K. Varshney, T.D. Colmer, W. Cowling, H. Bramley, T.A. Mori, J.M. Hodgson, J.W. Cooper, A.J. Miller, K. Kunert, J. Vorster, C. Cullis, J.A. Ozga, M.L. Wahlqvist, Y. Liang, H. Shou, K. Shi, J. Yu, N. Fodor, B.N. Kaiser, F.-L. Wong, B. Valliyodan, and M.J. Considine. 2016. Neglecting legumes has compromised human health and sustainable food production. Nat. Plants 2(8): 16112.

Freyre, R., P.W. Skroch, V. Geffroy, A.-F. Adam-Blondon, A. Shirmohamadali, W.C. Johnson, V. Llaca, R.O. Nodari, P.A. Pereira, S.M. Tsai, J. Tohme, M. Dron, J. Nienhuis, C.E. Vallejos, and P. Gepts. 1998. Toward an integrated linkage map of common bean. 4. Development of a core linkage map and alignment of RFLP maps. Theor. Appl. Genet. 97: 847–856.

Geffroy, V., F. Creusot, J. Falquet, M. Sévignac, A.-F. Adam-Blondon, H. Bannerot, P. Gepts, and M. Dron. 1998. A family of LRR sequences in the vicinity of the Co-2 locus for anthracnose resistance in *Phaseolus vulgaris* and its potential use in marker-assisted selection. Theor. Appl. Genet. 96(3–4): 494–502.

Geffroy, V., M. Sévignac, J.C.F. De Oliveira, G. Fouilloux, P. Skroch, P. Thoquet, P. Gepts, T. Langin, and M. Dron. 2000. Inheritance of partial resistance against *Colletotrichum lindemuthianum* in *Phaseolus vulgaris* and co-localization of quantitative trait loci with genes involved in specific resistance. Mol. Plant-Microbe Interact. 13(3): 287–296.

Gepts, P. 1999. Development of an integrated linkage map. p. 53–91. *In* Singh, S.P. (ed.), Common Bean Improvement in the Twenty-First Century. 1st ed. Developments in Plant Breeding. Springer Netherlands, Dordrecht.

Gerke, V., C.E. Creutz, and S.E. Moss. 2005. Annexins: linking Ca2+ signalling to membrane dynamics. Nat. Rev. Mol. Cell Biol. 6(6): 449–461.

Ghaderi, A., G.L. Hosfield, M.W. Adams, and M.A. Uebersax. 1984. Variability in culinary quality, component interrelationships, and breeding implications in navy and pinto beans. J. Amer. Soc. Hort. Sci. 109(1): 85–90.

Goff, L.M., D.E. Cowland, L. Hooper, and G.S. Frost. 2013. Low glycaemic index diets and blood lipids: A systematic review and meta-analysis of randomised controlled trials. Nutr. Metab. Cardiovasc. Dis. 23(1): 1–10.

Goodstein, D.M., S. Shu, R. Howson, R. Neupane, R.D. Hayes, J. Fazo, T. Mitros, W. Dirks, U. Hellsten, N. Putnam, and D.S. Rokhsar. 2012. Phytozome: a comparative platform for green plant genomics. Nucleic Acids Res. 40 (Database issue): D1178-86.

Grisi, M.C.M., M.W. Blair, P. Gepts, C. Brondani, P.A.A. Pereira, and R.P. V Brondani. 2007. Genetic mapping of a new set of microsatellite markers in a reference common bean (*Phaseolus vulgaris*) population BAT93 x Jalo EEP558. Genet. Mol. Res. 6(3): 691–706.

Hart, J.P., and P.D. Griffiths. 2015. Genotyping-by-sequencing enabled mapping and marker development for the By-2 potyvirus resistance allele in common bean. Plant Genome 8(1): 1–14.

Heller, W., and G. Forkmann. 1988. Biosynthesis. p. 400–425. *In* Harbone, J. (ed.), The Flavonoids: Advances in research since 1980. Chapman and Hall, London.

Hornick, B.A., and L. Weiss. 2011. Comparative nutrient analysis of commonly consumed vegetables. Nutr. Today 46(3): 130–137.

Hosfield, G.L. 2001. Seed coat color in *Phaseolus vulgaris* L.: Its chemistry and associated health related benefits. Annu. Rep. Bean Improv. Coop.

Hosfield, G.L., and M.A. Uebersax. 1980. Variability in physico-chemical properties and nutritional components of tropical and domestic dry bean germplasm. J. Amer. Soc. Hort Sci 105(2): 246–252.

Hosfield, G.L., and M.A. Uebersax. 1990. Culinary quality in dry bean- Can it be improved? Annu. Rep. Bean Improv. Coop. 33: 17–18.

Hosfield, G.L., M.A. Uebersax, and T.G. Isleib. 1984. Seasonal and genotypic effects on yield and physico-chemical seed characteristics related to food quality in dry, edible beans. J. Amer. Soc. Hort. Sci. 109(2): 182–189.

Hoyos-Villegas, V., W. Mkwaila, P.B. Cregan, and J.D. Kelly. 2015. Quantitative trait loci analysis of white mold avoidance in pinto bean. Crop Sci. 55(5): 2116.

Hunter Laboratories. 1996. Insight on Color: Hunter Lab Color Scale. Reston, VA.

Hurtado-Gonzales, O.P., G. Valentini, T.A.S. Gilio, A.M. Martins, Q. Song, and M.A. Pastor-Corrales. 2017. Fine mapping of Ur-3, a historically important rust resistance locus in common bean. G3 7(2): 557–569.

Hyten, D.L., Q. Song, E.W. Fickus, C. V Quigley, J.-S. Lim, I.-Y. Choi, E.-Y. Hwang, M.A. Pastor-Corrales, and P.B. Cregan. 2010. High-throughput SNP discovery and assay development in common bean. BMC Genomics 11(1): 475.

Jung, G., H.M. Ariyarathne, D.P. Coyne, and J. Nienhuis. 2003. Mapping QTL for bacterial brown spot resistance under natural infection in field and seedling stem inoculation in growth chamber in common bean. Crop Sci. 43(1): 350–357.

Jung, G., D.P. Coyne, P.W. Skroch, J. Nienhuis, E. Arnaud-Santana, J. Bokosi, H.M. Ariyarathne, J.R. Steadman, J.S. Beaver, and S.M. Kaeppler. 1996. Molecular markers associated with plant architecture and resistance to common blight, web blight, and rust in common beans. J. Am. Soc. Hortic. Sci. 121(5): 794–803.

Kamfwa, K., K.A. Cichy, and J.D. Kelly. 2015. Genome-wide association study of agronomic traits in common bean. Plant Genome 8(2): 1–12.

Kelly, J.D. 2010. The Story of Bean Breeding. East Lansing, MI.

Kelly, J.D., and K.A. Cichy. 2013. Dry Bean Breeding and Production Technologies. p. 23–54. *In* Siddiq, M., Uebersax, M.A. (eds.), Dry Beans and Pulses Production, Processing and Nutrition. First. John Wiley & Sons, Inc., Oxford, UK.

Kelly, J.D., G. V. Varner, K.A. Cichy, and E.M. Wright. 2015. Registration of ‘Zenith’ Black Bean. J. Plant Regist. 9(1): 15–20.

Kelly, J.D., G. V. Varner, P.D. O’Boyle, and B. Long. 2009. Registration of ‘Zorro’ Black Bean. J. Plant Regist. 3(3): 226.

Konopka-Postupolska, D., G. Clark, and A. Hofmann. 2011. Structure, function and membrane interactions of plant annexins: An update. Plant Sci. 181(3): 230–241.

Lobaton, J.D., T. Miller, J. Gil, D. Ariza, J.F. de la Hoz, A. Soler, S. Beebe, J. Duitama, P. Gepts, and B. Raatz. 2018. Resequencing of common bean identifies regions of inter–gene pool introgression and provides comprehensive resources for molecular breeding. Plant Genome 11(2): 1-21.

Lotito, S.B., and B. Frei. 2006. Consumption of flavonoid-rich foods and increased plasma antioxidant capacity in humans: Cause, consequence, or epiphenomenon? Free Radic. Biol. Med. 41(12): 1727–1746.

Lucier, G., L. Biing-Hwan, J. Allshouse, and L.S. Kantor. 2000. Factors affecting dry bean consumption in the United States. Econ. Res. Serv. (April): 26–34.

Luthria, D.L., and M.A. Pastor-Corrales. 2006. Phenolic acids content of fifteen dry edible bean (*Phaseolus vulgaris* L.) varieties. J. Food Compos. Anal. 19(2–3): 205–211.

Ma, Y., and F.A. Bliss. 1978. Seed proteins of common bean. Crop Sci. 18: 431–437.

Marles, M.A.S., P. Balasubramanian, and K.E. Bett. 2010. Differential accumulation of polyphenolics in black bean genotypes grown in four environments. J. Agric. Food Chem. 58(11): 7001–7006.

Martens, S., A. Preuß, and U. Matern. 2010. Multifunctional flavonoid dioxygenases: Flavonol and anthocyanin biosynthesis in *Arabidopsis thaliana* L. Phytochemistry 71(10): 1040–1049.

Martínez-Manrique, E., C. Jacinto-Hernández, R. Garza-García, A. Campos, E. Moreno, and I. Bernal-Lugo. 2011. Enzymatic changes in pectic polysaccharides related to the beneficial effect of soaking on bean cooking time. J. Sci. Food Agric. 91(13): 2394–2398.

Matella, N.J., D.K. Mishra, and K.D. Dolan. 2013. Hydration, Blanching and Thermal Processing of Dry Beans. p. 129–154. *In* Siddiq, M., Uebersax, M.A. (eds.), Dry Beans and Pulses Production, Processing and Nutrition. Blackwell Publishing Ltd., Oxford, UK.

McClean, P.E., R.K. Lee, C. Otto, P. Gepts, and M.J. Bassett. 2002. Molecular and phenotypic mapping of genes controlling seed coat pattern and color in common bean (*Phaseolus vulgaris* L.). J. Hered. 93(2): 148–52.

Mendoza, F.A., K.A. Cichy, R. Lu, and J.D. Kelly. 2014. Evaluation of canning quality traits in black beans (*Phaseolus vulgaris* L.) by Visible/Near-Infrared Spectroscopy. Food Bioprocess Technol. 7(9): 2666–2678.

Mendoza, F.A., K.A. Cichy, C. Sprague, A. Goffnett, R. Lu, and J.D. Kelly. 2018. Prediction of canned black bean texture (*Phaseolus vulgaris* L.) from intact dry seeds using visible/near infrared spectroscopy and hyperspectral imaging data. J. Sci. Food Agric. 98(1): 283–290.

Mendoza, F.A., J.D. Kelly, and K.A. Cichy. 2017. Automated prediction of sensory scores for color and appearance in canned black beans (*Phaseolus vulgaris* L.) using machine vision. Int. J. Food Prop. 20(1): 83–99.

Messina, V. 2014. Nutritional and health benefits of dried beans. Discovery Service for Endeavour College of Natural Health Library. Am. J. Clin. Nutr. 100(1): 437.

Micha, R., P.J. Rogers, and M. Nelson. 2010. The glycaemic potency of breakfast and cognitive function in school children. Eur. J. Clin. Nutr. 64(9): 948–957.

Miguel, M.G. 2011. Anthocyanins: Antioxidant and/or anti-inflammatory activities. J. Appl. Pharm. Sci. 1(6): 7–15.

Miklas, P.N., D.P. Coyne, K.F. Grafton, N. Mutlu, J. Reiser, D.T. Lindgren, and S.P. Singh. 2003. A major QTL for common bacterial blight resistance derives from the common bean great northern landrace cultivar Montana No.5. Euphytica 131(1): 137–146.

Miklas, P.N., E. Johnson, V. Stone, J.S. Beaver, C. Montoya, and M. Zapata. 1996. Selective mapping of QTL conditioning disease resistance in common bean. Crop Sci. 36(5): 1344.

Miklas, P.N., J.D. Kelly, S.E. Beebe, and M.W. Blair. 2006. Common bean breeding for resistance against biotic and abiotic stresses: From classical to MAS breeding. Euphytica 147(1–2): 105–131.

Miklas, P.N., and T.G. Porch. 2010. Guidelines for common bean QTL nomenclature. Annu. Rep. Bean Improv. Coop. 53: 202–204.

Miklas, P.N., R. Riley, K.F. Grafton, S.P. Singh, G. Jung, and D.P. Coyne. 2000. Marker-assisted breeding for pyramided resistance to common bacterial blight in common bean. Annu. Rep. Bean Improv. Coop. 43(l): 49–40.

Moghaddam, S.M., S. Mamidi, J.M. Osorno, R. Lee, M.A. Brick, J.D. Kelly, P. Miklas, C. Urrea, Q. Song, P.B. Cregan, J. Grimwood, J. Schmutz, and P.E. McClean. 2016. Genome-wide association study identifies candidate loci underlying agronomic traits in a Middle American diversity panel of common bean. Plant Genome 9(3): 1–21.

Moghaddam, S.M., Q. Song, S. Mamidi, J. Schmutz, R. Lee, P.B. Cregan, J.M. Osorno, and P.E. McClean. 2014. Developing market class specific InDel markers from next generation sequence data in *Phaseolus vulgaris* L. Front. Plant Sci. 5(May): 185.

Murphy, M.M., J.S. Douglass, and A. Birkett. 2008. Resistant starch intakes in the United States. J. Am. Diet. Assoc. 108(1): 67–78.

Nodari, R.O., S.M. Tsai, R.L. Gilbertson, and P. Gepts. 1993a. Toward an integrated linkage map of common bean. II. Development of an RFLP-based linkage map. Theor. Appl. Genet. 85(5): 513–520.

Nodari, R.O., S.M. Tsai, P. Guzmán, R.L. Gilbertson, and P. Gepts. 1993b. Toward an Integrated Linkage Map of common bean. III. Mapping genetic factors controlling host-bacteria interactions. Genetics 134(1): 341–50.

Oblessuc, P.R., C. Francisco, and M. Melotto. 2015. The Co-4 locus on chromosome Pv08 contains a unique cluster of 18 COK-4 genes and is regulated by immune response in common bean. Theor. Appl. Genet. 128(6): 1193–1208.

Van Ooijen, J.W. 2011. Multipoint maximum likelihood mapping in a full-sib family of an outbreeding species. Genet. Res. (Camb). 93(5): 343–349.

Oomah, B.D., A. Cardador-Martínez, and G. Loarca-Piña. 2005. Phenolics and antioxidative activities in common beans (*Phaseolus vulgaris* L). J. Sci. Food Agric. 85(6): 935–942.

Parr, B., J.K. Bond, and T. Minor. 2018. Vegetables and Pulses Outlook.

Pedraza García, F., G.J. Gallego, S.E. Beebe, and J.M. Tohme. 1997. Marcadores SCAR y RAPD para la resistancia a la Bacteriosis Común (CBB) del frijol. p. 130–134. *In* Singh, S.P., Voysesy, O. (eds.), Taller de mejoramiento de frijol para el Siglo XXI: Bases para una estrategia para América Latina. CIAT, Cali, Colombia.

Van Der Poel, A.F.B. 1990. Effect of processing on antinutritional factors and protein nutritional value of dry beans (*Phaseolus vulgaris* L.): A review. Anim. Feed Sci. Technol. 29(3–4): 179–208.

Posa-Macalincag, M.C.T., G.L. Hosfield, K.F. Grafton, M.A. Uebersax, and J.D. Kelly. 2002. Quantitative trait loci (QTL) analysis of canning quality traits in kidney bean (*Phaseolus vulgaris* L.). J. Amer. Soc. Hort. Sci. 127(4): 608–615.

Prakken, R. 1974. Inheritance of colours in *Phaseolus vulgaris* L.: IV recombination within the "complex locus C." Meded. Landbouwhogesch. 24: 1–36.

Reinprecht, Y., Z. Yadegari, G.E. Perry, M. Siddiqua, L.C. Wright, P.E. McClean, and K.P. Pauls. 2013. *In silico* comparison of genomic regions containing genes coding for enzymes and transcription factors for the phenylpropanoid pathway in *Phaseolus vulgaris* L. and *Glycine max* L. Merr. Front. Plant Sci. 4(September): 317.

Schmutz, J., P.E. McClean, S. Mamidi, G.A. Wu, S.B. Cannon, J. Grimwood, J. Jenkins, S. Shu, Q. Song, C. Chavarro, M. Torres-Torres, V. Geffroy, S.M. Moghaddam, D. Gao, B. Abernathy, K. Barry, M. Blair, M.A. Brick, M. Chovatia, P. Gepts, D.M. Goodstein, M. Gonzales, U. Hellsten, D.L. Hyten, G. Jia, J.D. Kelly, D. Kudrna, R. Lee, M.M.S. Richard, P.N. Miklas, J.M. Osorno, J. Rodrigues, V. Thareau, C.A. Urrea, M. Wang, Y. Yu, M. Zhang, R.A. Wing, P.B. Cregan, D.S. Rokhsar, and S.A. Jackson. 2014. A reference genome for common bean and genome-wide analysis of dual domestications. Nat. Genet. 46(7): 707–713.

Schneider, C.A., W.S. Rasband, and K.W. Eliceiri. 2012. NIH Image to ImageJ: 25 years of image analysis. Nat. Methods 9(7): 671–5.

Schröder, S., S. Mamidi, R. Lee, M.R. McKain, P.E. McClean, and J.M. Osorno. 2016. Optimization of genotyping by sequencing (GBS) data in common bean (*Phaseolus vulgaris* L.). Mol. Breed. 36(1): 1–9.

Shi, C., K. Yu, W. Xie, G.E. Perry, A. Navabi, K.P. Pauls, P.N. Miklas, and D. Fourie. 2012. Development of candidate gene markers associated to common bacterial blight resistance in common bean. Theor. Appl. Genet. 125(7): 1525–1537.

Simões, I., and C. Faro. 2004. Structure and function of plant aspartic proteinases. Eur. J. Biochem. 271(11): 2067–2075.

Song, Q., G. Jia, D.L. Hyten, J. Jenkins, E.-Y. Hwang, S.G. Schroeder, J.M. Osorno, J. Schmutz, S.A. Jackson, P.E. McClean, and P.B. Cregan. 2015. SNP assay development for linkage map construction, anchoring whole genome sequence and other genetic and genomic applications in common bean. G3 Genes|Genomes|Genetics 5(11): 2285–2290.

Takeoka, G.R., L.T. Dao, G.H. Full, R.Y. Wong, L.A. Harden, R.H. Edwards, and J.D.J. Berrios. 1997. Characterization of black bean (*Phaseolus vulgaris* L.) anthocyanins. J. Agric. Food Chem. 45(97): 3395–3400.

Thompson, M.D., M.A. Brick, J.N. McGinley, and H.J. Thompson. 2009. Chemical composition and mammary cancer inhibitory activity of dry bean. Crop Sci. 49(1): 179–186.

USDA- Agricultural Research Service. 2018. Nutrient search. Natl. Nutr. Database Stand. Ref. Leg. Release. Available at https://ndb.nal.usda.gov/ndb/nutrients/index.

USDA- NASS. 2016. Crop Production 2015 Summary.

USDA- NASS. 2018. Crop Production 2017 Summary.

Vlasova, A., S. Capella-Gutiérrez, M. Rendón-Anaya, M. Hernández-Oñate, A.E. Minoche, I. Erb, F. Câmara, P. Prieto-Barja, A. Corvelo, W. Sanseverino, G. Westergaard, J.C. Dohm, G.J. Pappas, S. Saburido-Alvarez, D. Kedra, I. Gonzalez, L. Cozzuto, J. Gómez-Garrido, M.A. Aguilar-Morón, N. Andreu, O.M. Aguilar, J. Garcia-Mas, M. Zehnsdorf, M.P. Vázquez, A. Delgado-Salinas, L. Delaye, E. Lowy, A. Mentaberry, R.P. Vianello-Brondani, J.L. García, T. Alioto, F. Sánchez, H. Himmelbauer, M. Santalla, C. Notredame, T. Gabaldón, A. Herrera-Estrella, R. Guigó, P. Graham, C. Vance, J. Kami, V. Velásquez, D. Debouck, P. Gepts, M. Kwak, E. Bitocchi, L. Nanni, E. Bellucci, M. Rossi, A. Giardini, P. Zeuli, S. Mamidi, S. Moghaddam, D. Annam, R. Lee, R. Papa, J. Schmutz, P. McClean, G. Wu, S.B. Cannon, J. Grimwood, S. Moghaddam, S. Chacón, B. Pickersgill, A. Delgado-Salinas, R. Bibler, M. Lavin, D. Rau, M. Rodriguez, E. Biagetti, J.A. Acosta-Gallegos, M.W. Blair, A. Soler, A.J. Cortés, B. Gaut, X. Huang, Q. Feng, Q. Qian, Q. Zhao, L. Wang, A. Wang, K. Arumuganathan, E. Earle, M. Bennett, J. Smith, G. Parra, K. Bradnam, I. Korf, G. Arimura, R. Ozawa, S. Kugimiya, J. Takabayashi, J. Bohlmann, J.D. Kelly, P. Miklas, D.P. Coyne, V. Geffroy, M. Sévignac, J. Oliveira, G. Fouilloux, P. Skroch, P. Thoquet, U. Ørom, T. Derrien, M. Beringer, K. Gumireddy, A. Gardini, G. Bussotti, J. Huerta-Cepas, L. Pryszcz, M. Marcet-Houben, T. Gabaldón, I. Denisov, D. Kormes, Y. Jiao, N. Wickett, S. Ayyampalayam, A. Chanderbali, L. Landherr, P. Ralph, Y. Yang, M. Moore, S. Brockington, D. Soltis, G. Wong, L. Sterck, S. Rombauts, S. Sato, F. Cheung, J. Gouzy, J. Schlueter, J. Ma, T. Mitros, W. Nelson, A. Ferrarini, A. Benazzo, S. Klie, J. O'Rourke, L. Iniguez, F. Fu, B. Bucciarelli, S. Miller, S.A. Jackson, A. Severin, J. Woody, Y.-T. Bolon, B. Joseph, B. Diers, A.D. Farmer, L. Mao, J. Hemert, S. Dash, J. Dickerson, J. Huerta-cepas, J. Dopazo, M. Huynen, T. Padawer, R. Leighty, D. Wang, M.

McConnell, S. Chikara, M. Ramírez, M. Graham, L. Blanco-lo, S. Silvente, A. Medrano-soto, M. Melotto, C. Monteiro-Vitorello, A. Bruschi, L. Camargo, F. Belzile, J. Tian, P. Venkatachalam, H. Liao, X. Yan, K. Raghothama, V. Kalavacharla, Z. Liu, B. Meyers, J. Thimmapuram, K. Melmaiee, B. Le, J. Wagmaister, T. Kawashima, A. Bui, J. Harada, R. Goldberg, V. Singh, R. Garg, M. Jain, J. Verdier, I. Torres-Jerez, M. Wang, A. Andriankaja, S. Allen, J. He, R. Johnson, A. Tanzer, S. Djebali, H. Tilgner, J. Sun, Y. Lin, J. Wu, C. Kutter, S. Watt, K. Stefflova, M. Wilson, A. Goncalves, C. Ponting, M. Mutwil, B. Usadel, M. Schütte, A. Loraine, O. Ebenhöh, S. Persson, K. Aoki, Y. Ogata, D. Shibata, S. Ma, S. Shah, H. Bohnert, M. Snyder, S. Dinesh-Kumar, M. Lynch, A. Force, V. Prince, F. Pickett, S. Renny-Byfield, J. Gallagher, C. Grover, E. Szadkowski, J. Page, J. Udall, J. Duarte, L. Cui, P. Wall, Q. Zhang, X. Zhang, J. Leebens-Mack, R. Ferreira, P. Ramos, E. Franco, C. Ricardo, A. Teixeira, D. Sicard, S. Cohen, S. Chisholm, G. Coaker, B. Day, B. Staskawicz, D. Cook, T. Lee, X. Guo, S. Melito, K. Wang, A. Bayless, M.C.M. Grisi, C. Brondani, P. Pereira, R. Brondani, T. Flutre, E. Duprat, C. Feuillet, H. Quesneville, D. Ellinghaus, S. Kurtz, U. Willhoeft, S. Steinbiss, G. Gremme, J. Jurka, V. Kapitonov, A. Pavlicek, P. Klonowski, O. Kohany, J. Walichiewicz, S. EMBL, P. Agarwal, J. Abril, T. Wiehe, J. Fickett, R. Guigo, M. Stanke, O. Keller, I. Gunduz, A. Hayes, S. Waack, B. Morgenstern, W. Majoros, M. Pertea, S. Salzberg, B. Haas, W. Zhu, J. Allen, J. Orvis, S. Hunter, P. Jones, A. Mitchell, R. Apweiler, T. Attwood, A. Bateman, M. Kanehisa, S. Goto, Y. Sato, M. Furumichi, M. Tanabe, D. Croft, A. Mundo, R. Haw, M. Milacic, J. Weiser, G. Wu, T. Petersen, S. Brunak, G. Heijne, H. Nielsen, S. Götz, J. García-Gómez, J. Terol, T. Williams, S. Nagaraj, M. Nueda, W. Sanseverino, A. Hermoso, R. D'Alessandro, A. Vlasova, G. Andolfo, L. Frusciante, S. Altschul, W. Gish, W. Miller, E. Myers, D. Lipman, G. Slater, E. Birney, C. Notredame, D. Higgins, J. Heringa, C. Trapnell, B. Williams, G. Pertea, A. Mortazavi, G. Kwan, M. Baren, E. Nawrocki, D. Kolbe, S.R. Eddy, K. McCue, L. Schaeffer, B. Wold, M. Robinson, D. McCarthy, G. Smyth, J. Friedman, T. Hastie, R. Tibshirani, T. Fruchterman, M. Reingold, A. Clauset, M. Newman, C. Moore, R. Edgar, K. Katoh, H. Toh, T. Lassmann, O. Frings, E. Sonnhammer, I. Wallace, O. O'Sullivan, J. Silla-Martínez, O. Gascuel, S. Guindon, J. Dufayard, V. Lefort, M. Anisimova, W. Hordijk, D.M. Goodstein, S. Shu, R. Howson, R. Neupane, R. Hayes, J. Fazo, H. Li, and R. Durbin. 2016. Genome and transcriptome analysis of the Mesoamerican common bean and the role of gene duplications in establishing tissue and temporal specialization of genes. Genome Biol. 17(1): 32.

Voorrips, R.E. 2002. MapChart: software for the graphical presentation of linkage maps and QTLs. J. Hered. 93(1): 77–8.

Walters, K.J., G.L. Hosfield, M.A. Uebersax, and J.D. Kelly. 1997. Navy bean canning quality: Correlations, heritability estimates, and randomly amplified polymorphic DNA markers associated with component traits. J. Amer. Soc. Hort. Sci. 122(3): 338–343.

Wang, S., C.J. Basten, and Z.-B. Zeng. 2012. Windows QTL Cartographer.

Wang, L.-S., and G.D. Stoner. 2008. Anthocyanins and their role in cancer prevention. Cancer Lett. 269(2): 281–290.

Wassimi, N.N., G.L. Hosfield, and M.A. Uebersax. 1990. Inheritance of physico-chemical seed characters related to culinary quality in dry bean. J. Amer. Soc. Hort Sci 115(3): 492–499.

Wright, E.M., and J.D. Kelly. 2011. Mapping QTL for seed yield and canning quality following processing of black bean (*Phaseolus vulgaris* L.). Euphytica 179(3): 471–484.

Xia, Y., H. Suzuki, J. Borevitz, J. Blount, Z. Guo, K. Patel, R.A. Dixon, and C. Lamb. 2004. An extracellular aspartic protease functions in *Arabidopsis* disease resistance signaling. EMBO J. 23(4): 980–988.

Xu, B., and S.K.C. Chang. 2009. Total phenolic, phenolic acid, anthocyanin, flavan-3-ol, and flavonol profiles and antioxidant properties of pinto and black beans (*Phaseolus vulgaris* L.) as affected by thermal processing. J. Agric. Food Chem. 57(11): 4754–4764.

Zou, X., C. Shi, R.S. Austin, D. Merico, S. Munholland, F. Marsolais, A. Navabi, W.L. Crosby, K.P. Pauls, K. Yu, and Y. Cui. 2014. Genome-wide single nucleotide polymorphism and Insertion-Deletion discovery through next-generation sequencing of reduced representation libraries in common bean. Mol. Breed. 33(4): 769–778.

Zuiderveen, G.H., B.A. Padder, K. Kamfwa, Q. Song, and J.D. Kelly. 2016. Genome-Wide association study of anthracnose resistance in Andean beans (*Phaseolus vulgaris*). PLoS One 11(6): 1–17.